THE ROLE OF THE NUCLEUS ACCUMBENS CORE IN SCALING FEAR TO DEGREE OF THREAT

MADELYN H. RAY

A dissertation

submitted to the Faculty of

the department of Psychology and Neuroscience

in partial fulfillment

of the requirements for the degree of

Doctor of Philosophy

Boston College
Morrissey College of Arts and Sciences
Graduate School

March 2021

Title: The Role of the Nucleus Accumbens Core in Scaling Fear to Degree of Threat

By: Madelyn H. Ray

Advisor: Michael A. McDannald, Ph.D.

Abstract: Identifying the neural circuits underlying adaptive fear is fundamental to understanding and developing more effective treatments for anxiety disorders. Adaptive behavior requires fear to scale to the level of threat and dysfunction in this capacity is a hallmark of fear-related anxiety disorders. Identifying the neural circuits underlying adaptive fear is fundamental to understanding anxiety disorders and propelling more effective treatments for patients. Fear is adaptive when the level of the response rapidly scales to degree of threat. Using a discrimination procedure consisting of danger, uncertainty, and safety cues, our laboratory has found rapid fear scaling (within 2 s of cue presentation). However, the neural underpinnings of this behavior are unknown. The overarching goal of this dissertation is to examine a role for the nucleus accumbens core (NAcc) in scaling fear to degree of threat. In three experiments I used neurotoxic lesions, optogenetic inhibition, and *in vivo* electrophysiology combined with an intricate fear learning procedure to elucidate a role for the

NAcc in both general and rapid scaling of fear. Permanent NAcc dysfunction, via neurotoxic lesion, generally disrupted the ability to scale fear to degree of threat and specifically impaired one component of scaling: rapid discrimination of uncertain threat and safety. Reversible NAcc dysfunction, via optogenetic inhibition, specifically impaired rapid discrimination of uncertain threat and safety. Further, I demonstrated that NAcc activity is threat responsive and exhibits heterogeneity in the timing and specific nature of threat firing. The results reveal that the NAcc is essential to scale fear to degree of threat and responds to threat cues across both rapid and general timescales. Taken together, the results reveal a novel role for the NAcc in scaling fear and identify it as a plausible source of dysfunction in stress and anxiety disorders. Identifying the brain regions underlying adaptive fear is fundamental to understanding and developing more effective treatments for anxiety disorders.

TABLE OF CONTENTS

LIST OF TABLES

LIST OF FIGURES

LIST OF ABBREVIATIONS

ANOVA	Analysis of Variance
BLA	Basolateral Amygdala
CeA	Central Amygdala
CR	Conditioned Response
CS	Conditioned Stimulus
DA	Dopamine
dHPC	Dorsal Hippocampus
D1	Dopamine Receptor 1
D2	Dopamine Receptor 2
eNpHR	Enhanced Natronomonas Halorhodopsin
FPS	Fear Potentiated Startle
FSI	Fast-Spiking Interneuron
GABA	Gamma-Aminobutyric Acid
Halo	Halorhodopsin
IEG	Immediate Early Gene
IL	Infralimbic Cortex
ITI	Inter-trial Interval
LA	Lateral Amygdala
mPFC	Medial Prefrontal Cortex
MSN	Medium Spiny Neuron
NAcc	Nucleus Accumbens Core

NAcS	Nucleus Accumbens Shell
NMDA	N-Methyl-D-Aspartic Acid
NS	Neutral Stimulus
PBS	Phosphate Buffered Saline
PL	Prelimbic Cortex
PTSD	Post-Traumatic Stress Disorder
UR	Unconditioned Response
US	Unconditioned Stimulus
vHPC	Ventral Hippocampus
VI-30	Variable Interval, 30 s
VI-60	Variable Interval, 60 s
VP	Ventral Pallidum
YFP	Yellow Fluorescent Protein

ACKNOWLEDGMENTS

First and most importantly, I give immense thanks to my advisor, Dr. Michael McDannald, without whom this dissertation would not exist. From day one of arriving at Boston College, you have been an outstanding mentor, teacher, and role model. You have taught me so much about both science and life and I am without a doubt a better scientist and a better person because of it. Your kindness, humor, patience, and understanding are just a few of the things I am exceptionally grateful for. You have always believed in me even when I didn't believe in myself and you've encouraged me to be the best version of myself. Thank you for everything. Next, I would like to thank the additional committee members: Drs. Gorica Petrovich, Maureen Ritchey, and Ziv Williams. Gorica, thank you for always making me feel welcome and supported regardless of the question or concern. You have been a strong force of encouragement that I desperately needed at times and have helped me navigate decisions in both science and life. Additionally, you fostered my incredible appreciation for neuroanatomy and histology that I will take with me throughout my scientific career. Maureen, I will never forget the first day in your Hippocampus classroom when I barely knew what an fMRI was, let alone how it worked. Thank you for always taking extra time to explain things, entertaining my endless questions and thoughts, and always making me feel welcome, even when I felt out of my element. Ziv, thank you for believing in me and my research and supporting my work in both official and unofficial capacities. You have provided a source of encouragement and guidance outside of Boston College that I am very grateful

for. Each of you has been crucial to my advancement through this degree process and I am incredibly thankful for your mentorship and guidance throughout this journey.

I would also like to thank all of the past and present members of the McDannald laboratory: Dr. Mahsa Moaddab, Dr. Jasmin Strickland, Dr. Rachel Walker, Kristina Wright, and Amanda Chu, who have all helped out and supported me along the way. I would especially like to thank Dr. Mahsa Moaddab. Mahsa has served as a mentor to me throughout the past several years and I feel extremely lucky to have worked with her. Thank you for putting up with my endless questions and fostering my passion for electrophysiology. You have been an invaluable resource to me. I would also like to thank the numerous undergraduate assistants who have helped with this work including Alyssa, Andrew, Alexa, Mackenzie, Rebecca, Kevin, Euna, and Emma, whose contributions and dedication made this work possible. I would also like to thank Bret Judson and the Boston College Imaging Core for infrastructure and support. Bret has been an exceptional teacher and mentor, thank you. This work would not have been possible without the exceptional animal care staff at Boston College, especially Nancy and Todd.

Getting to this point would not have happened without the support of two very important people from my undergraduate training, Dr. Chip Pickens and Dr. Mary Cain. Chip, thank you for taking a chance on me as a 19-year-old college student with a resume full of babysitting experience and letting me set up your laboratory. Looking back, I'm not sure you should have trusted me with all of that

expensive equipment but I'm so thankful you did. Your mentorship didn't stop when I left KSU and I look forward to it continuing throughout my career. To quote you, "We are on our way to success". Mary, your class on drugs and behavior sparked my curiosity in neuroscience and led me to this career path. Thank you for your unwavering support over the past 8 years. You've been a mentor, a teacher, and a friend and I can't thank you enough for all of your support and encouragement.

I would be remiss if I didn't thank my dear friends for their support and encouragement along the way. In particular, Dr. Britt Jeye, Dr. Lauren Anderson, Emily Jorgensen, Danielle Lafferty, Eliza Greiner, and Amanda Chu. Your friendship and support throughout this process have been nothing short of incredible and I cannot thank you all enough for your constant encouragement, particularly in this last year. Though it may seem unconventional, I would also like to thank my two cats, Emerson and Basal Ganglia. Graduate school is an incredibly tough, and at times, isolating experience. I can't thank my cats enough for always greeting me at the door and giving me friendly faces to come home to after long days in the Higgins basement. Last but not least, I would like to thank my family back in Oklahoma. My deepest thanks go out to my parents, siblings, and grandparents. Angie and Todd, thank you for always believing in me and supporting me throughout my endeavors. I wouldn't be where I am today without your unconditional love and support. Sharon and Victor, thank you for all of the facetime calls, Starbucks gift cards, and handwritten cards. Though these things may have seemed small at the time, they meant more to me than you know. I

cannot thank my family enough for their unwavering support, hard work, sacrifices, and encouragement through the toughest of times. I am truly fortunate to have each one of you in my life.

Chapter 1: Introduction to the nucleus accumbens and threat learning

1.1. Threat Learning

1.1.1 Behavioral Paradigms

The ability to discriminate danger from safety is critical to survival. Individuals with stress and anxiety disorders are commonly impaired in discrimination, showing excessive fear-related responses to safety (Jovanovic et al., 2010, 2012; Lissek et al., 2014; Duits et al., 2015). Danger and safety represent extremes of a threat continuum, with most real-world threats involving uncertainty. Ideally, one's level of fear should scale to the degree of threat. A scaled fear response would be most adaptive if it was rapidly organized following an encounter with a potential threat. The importance of distinguishing danger and safety is clear, but how do we study learned fear behavior in a laboratory?

One way to study learned fear behavior is through Pavlovian conditioning, a form of associative learning. In Pavlovian conditioning, pairing a neutral cue with a biologically salient event, such as food results in the formation of a cue-food association. This association is evident in the subject's behavior. A cue paired with food will acquire the ability to elicit behaviors previously only elicited by food (Pavlov, 1928). In Pavlov's example using dogs, a bell would initially produce no food-related behavior, while food would elicit salivation. Repeated bell-food pairings result in the formation of a bell-food association. Following conditioning, the bell alone is sufficient to produce salivation.

The principles governing cue-food learning are readily applied to threat learning, which is most commonly termed Pavlovian fear conditioning. In the cued version of Pavlovian fear conditioning, a discrete cue such as a tone, light,

or odor, is paired with an aversive foot shock (LeDoux, 2000; Maren, 2001). Cued fear conditioning most commonly involves one cue that predicts foot shock with absolute certainty (100% of trials). Though less common, some paradigms include an additional cue that predicts the absence of shock (i.e., safety), with absolute certainty (0% of trials). In these paradigms, rats are trained to distinguish cues signaling absolute danger and absolute safety. However, these approaches do not examine fear to intermediate cues falling between the extremes of danger and safety. This is problematic because uncertainty is an inherent feature of many real world threats.

1.1.2 Measuring Fear

There are many methods to study fear in rats, but how do we measure fear? In Pavlovian fear conditioning, fear is most commonly measured by freezing. Freezing is a species-specific defensive behavior in rats in which the animal exhibits a rigid “crouching” posture and withholds bodily movement (Blanchard, 1969; Fanselow, 1980). Freezing is an adaptive defensive behavior because predators are less likely to detect immobile prey. For example, a cat is much less likely to detect an immobile rodent (Hirsch, 1977). Freezing is a universal defensive behavior in rats that generalizes from predators to other imminent threats, including those found in a laboratory setting (Hagenaars et al., 2014). Freezing has been well documented in response to cues signaling an aversive outcome, making it a useful index of fear (Fanselow, 1980, 1993; LeDoux et al., 1988; Maren et al., 1996; Maren, 2001; Sierra-Mercado et al.,

2011). When measuring freezing, low freezing is interpreted as low fear and high freezing is interpreted as high fear.

Another measure of fear is conditioned suppression. In a standard conditioned suppression procedure, rats are moderately food-deprived and trained to perform an instrumental response (i.e., lever press or nose poke) to obtain rewards. Following response-food training, rats go through cued fear conditioning. After repeated cue-shock pairings, presentation of the cue results in suppression of instrumental responding for food, termed conditioned suppression (Estes and Skinner, 1941; Kamin et al., 1963; Anglada-Figueroa and Quirk, 2005; McDannald, 2009; Pickens et al., 2009; Arico and McNally, 2014). Conditioned suppression is observed due to the competition of responding between conditioned freezing and the instrumental responding for reward, as well as the competition between appetitive and aversive states (McDannald, 2009). Similar to the suppression of movement, animals will also suppress food-seeking during a threat encounter. If an animal is freezing, it cannot simultaneously be reward-seeking, and freezing is correlated with the conditioned suppression of lever pressing and licking (Bouton and Bolles, 1980). Thus, conditioned suppression and freezing are not synonymous, but rather independent behavioral consequences of threat learning. Critically, these processes also rely on separate neural circuits (Killcross et al., 1997; Amorapanth et al., 1999; Lee et al., 2005; McDannald, 2010; McDannald and Galarce, 2011; Shumake and Monfils, 2015).

One pitfall of using freezing to measure fear is the sex differences in this measure. The majority of fear studies have only used male rats (Lebron-Milad

and Milad, 2012). However, more recent studies using both males and females have reported lower freezing rates in females (Maren et al., 1994; Gupta et al., 2001; Gruene et al., 2015a). Recent investigations into this sex difference revealed that females exhibit more active fear responses, known as darting, which is reflected in a reduction in freezing, when in fact, females may display fear in a more active manner compared to males (Gruene et al., 2015a, 2015b; Colom-Lapetina et al., 2019; Greiner et al., 2019). There is a clear need for additional fear research across sexes.

Another measure of fear, fear-potentiated startle (FPS), involves using the acoustic startle reflex as a behavioral measure. In FPS, a short-lived neutral stimulus (i.e., a light) is paired with a foot shock. Later, subjects are tested by presenting a series of startle-eliciting noise bursts, some of which are paired with the stimulus that had previously been paired with foot shock, while others in the absence. FPS examines the increase in startle in the presence versus absence of the conditioned fear stimulus (Davis, 1986, 1992; Walker and Davis, 2002). FPS is a widely used fear learning paradigm because of its translatability to humans (Grillon and Davis, 1997). Additionally, the startle response can be reliably measured up to one month after training, allowing for the examination of long-term fear memories (Campeau et al., 1990). However, a major drawback of FPS is that it focuses on examining how threat cues modulate behavior to neutral cues. Though this is important in its own regards, this paradigm does not examine adaptive fear responses to cues themselves and instead focuses on threat cue modulation of a neutral cue. To understand how adaptive fear

responses are organized, cue examination should compare cue presentation to a baseline period, similar to cued fear conditioning. Additionally, for fear responses to accurately portray real-life threat encounters, fear learning should include not just absolute signals of danger and safety, but also uncertainty.

1.1.3 Updated Paradigms from Learning Theory

Associative learning has been instrumental in shaping the fear learning literature. One of the most prominent learning theory models is the Rescorla-Wagner model of Pavlovian conditioning which describes the associative strength between a CS (cue) and US (shock) (Rescorla, 1968; Rescorla and Wagner, 1972). This model builds on Rescorla's independent work from 1968 examining the shock contingency of a cue using different probabilities of foot shock. In this renowned paper, Rescorla demonstrates that increasing the shock contingency of a cue increases conditioned suppression. Such that, as the probability of shock associated with the cue increases, conditioned suppression also increases (Rescorla, 1968). This finding was remarkable, yet it was heavily ignored until recent years. The overwhelming majority of fear conditioning procedures have used simplistic cue-shock paradigms, severely limiting our understanding of the neural circuits underlying fear learning and behavior. Associative learning has the ability to propel fear research to go beyond the basic Pavlovian cue-outcome conditioning, to better study the different neural and behavioral mechanisms of learning by using more complex behavioral procedures, that better imitate real life encounters.

Danger and safety represent extremes of a threat continuum, with most real world threats involving uncertainty. Ideally, one's level of fear should scale to degree of threat. Drawing from learning theory and Rescorla's pivotal paper (Rescorla, 1968), our laboratory has devised a discrimination procedure in which distinct auditory cues predict unique foot shock probabilities: danger (p=1.00), uncertainty (p=0.25), and safety (p=0.00) (Berg et al., 2014). Fear conditioning takes place over a baseline of rewarded nose poking. Importantly, the schedules for cue and shock delivery are independent of the schedule for rewarded nose poking. 'Fear' is measured by the cue-induced suppression of poking (Estes and Skinner, 1941). Using this paradigm, we observe scaled fear responses across the 10 s cue presentation with rats showing highest fear to danger, moderate fear to uncertainty, and low or no fear to safety (Berg et al., 2014; DiLeo et al., 2016; Ray et al., 2018). Such that, the degree of suppression observed to each cue roughly approximates the foot shock probability associated with each cue.

A scaled fear response would be most adaptive if it was rapidly organized following a threatening encounter. Few studies have examined temporally specific threat responses. One such study from our laboratory has found that fear level scales to shock probability within two seconds of cue presentation (DiLeo et al., 2016). The concept of rapid encoding and responding to stimuli is not new (Quirk et al., 1995; Setlow et al., 2003; Josselyn et al., 2005; Uchida et al., 2006). Neurons in the lateral amygdala (LA) respond to a fear conditioned cue at a latency of ~20 msec (Quirk et al., 1995). In olfaction and vision, rapid perceptual decisions can be consistently observed in ~200-300 msec latencies (Uchida et

al., 2006), while in FPS, behavior is observed in the ~200 msec period following the onset of the startle stimulus (Josselyn et al., 2005). This demonstrates that perceptual, neural, and behavioral responses to stimuli occur on a rapid timescale. However, this research has focused on either simplistic cue-shock paradigms or in FPS, behavior in response to another (neutral) stimulus. Our laboratory was the first to demonstrate the rapid behavioral emergence of scaled fear responses (DiLeo et al., 2016), yet the brain regions underlying rapid fear scaling are still unknown.

1.2. Anatomical Substrates of Threat Learning

1.2.1 Amygdala

The neural underpinnings of fear have been widely studied over the years and implicated a variety of brain regions including, but not limited to, the amygdala, nucleus accumbens, medial prefrontal cortex (mPFC), and hippocampus.

The primary theory of amygdalar function suggests that the basolateral amygdala (BLA) encodes and maintains cue-shock associations (LeDoux et al., 1990; Maren et al., 1996; Amorapanth et al., 2000; LeDoux, 2000; Goosens and Maren, 2001; Koo et al., 2004), and sends this information to the central amygdala (CeA), which mediates the behavioral expression of fear responses (LeDoux et al., 1988). Amygdala lesions have long been associated with a reduction in fear (Weiskrantz, 1956). The BLA is divided into the lateral (LA), basolateral nucleus (BA) and basomedial nucleus (BM). The BLA is comprised

mostly of glutamatergic pyramidal neurons, which are primarily projection neurons, and some GABAergic interneurons, which form local circuits within the BLA (McDonald, 1982, 1992; McDonald and Mascagni, 2001). BLA neurons exhibit increased responding to cue presentation (Quirk et al., 1995, 1997; Rogan et al., 1997; Repa et al., 2001), with neurons in the LA responding at a latency of ~20 msec (Quirk et al., 1995). Interestingly, BLA activity is greater for uncertain or ambiguous cues (Belova et al., 2007; Dunsmoor et al., 2008).

The BLA projects both directly and indirectly to the CeA and this pathway is associated with negative valence (Goosens and Maren, 2001; Ciocchi et al., 2010; Beyeler et al., 2016, 2018). Disconnections between the BLA and CeA abolish cue elicited freezing (Jimenez and Maren, 2009). The CeA is divided into the dorsolateral, mediolateral, and ventrolateral regions and is primarily comprised of GABAergic interneurons. The CeA is involved in the acquisition and expression of conditioned fear memories (Goosens and Maren, 2003; Maren and Quirk, 2004; Wilensky et al., 2006; Ciocchi et al., 2010; Fadok et al., 2018), mediating the behavioral expression of fear responses (LeDoux et al., 1988).

1.2.2 Nucleus Accumbens

In order to identify brain regions necessary for fear scaling and its rapid emergence, I must identify candidate regions. Candidate regions should be able to process valence and receive amygdalar input (Quirk et al., 1995; Goosens and Maren, 2001; Koo et al., 2004; McDannald and Galarce, 2011). The nucleus accumbens is a ventral striatal region comprised of two main subregions: the

core (NAcc) and shell (NAcS). The NAcc is anatomically positioned to receive threat-related input based on its strong innervation from the BLA, though it's more widely known for its role in reward settings. The NAcc and NAcS have reciprocal connections, forming an intrastriatal projection pattern both between and within these subregions (van Dongen et al., 2005). The NAcc receives monosynaptic inputs from the ventral pallidum (VP), basolateral and basomedial subregions of the BLA, multiple cortical regions (agranular insular cortex, orbitofrontal cortex, prelimbic cortex, etc.), and several other regions (Li et al., 2018). Most critical to my hypothesis, are the glutamatergic inputs from the BLA (Kita and Kitai, 1990; Brog et al., 1993; Wright and Groenewegen, 1996). The prevailing view is that the BLA preferentially routes information regarding negative valence to the CeA, whereas positive valence is routed to the NAcc (Beyeler et al., 2016, 2018).

The NAcc is primarily comprised of GABAergic medium spiny neurons (MSNs) which are typically dichotomized based on their expression of either D1 or D2 dopamine receptors. D1 and D2 MSNs comprise >95% of all NAcc neurons. Some MSNs express both D1 and D2 receptors, however, this is estimated to only account for about 5% of MSNs in the core (Bertran-Gonzalez et al., 2008; Perreault et al., 2011; Gangarossa et al., 2013; Gagnon et al., 2017). The majority of inputs to the NAcc do not differ based on MSN cell type and show an extremely high correlation between inputs. Both D1 and D2 MSNs receive projections from the orbitofrontal cortex, cingulate cortex, prelimbic cortex, agranular insular cortex, and several other regions (Li et al., 2018).

1.2.3 Medial Prefrontal Cortex

One of these NAcc-innervation regions, the mPFC, has been widely studied in fear learning and extinction. The mPFC has close functional and anatomical connections with both the NAcc and amygdala (Krettek and Price, 1977; Kita and Kitai, 1990; Garcia et al., 1999; Gabbott et al., 2005; Li et al., 2018). The mPFC is involved in Pavlovian fear conditioning, particularly in fear extinction. Fear extinction involves the presentation of a cue in the absence of shock. Manipulating mPFC activity impairs cued fear extinction (Morgan et al., 1993; Quirk et al., 2000). The mPFC is divided into two subregions: prelimbic (PL) and infralimbic (IL). The PL and IL play differential roles in threat learning (Marek and Sah, 2018). The PL has been implicated in acquisition, consolidation, and expression of fear memory. In cued fear conditioning, PL stimulation increases freezing while inhibition of PL activity decreases freezing (Quirk et al., 2000; Vidal-Gonzalez et al., 2006; Sierra-Mercado et al., 2011). In fear extinction, PL activity promotes the expression of conditioned fear (Vidal-Gonzalez et al., 2006; Corcoran and Quirk, 2007; Burgos-Robles et al., 2009; Sierra-Mercado et al., 2011). The IL does not appear to have a significant role in the acquisition of extinction but is required for consolidation, and perhaps expression, of extinction memory. Silencing the IL increases freezing and impairs extinction while stimulation decreases conditioned freezing and enhances extinction (Vidal-Gonzalez et al., 2006; Sierra-Mercado et al., 2011; Bukalo et al., 2015). Additionally, the amygdala modulates mPFC activity related to conditioned fear

(Garcia et al., 1999) and stimulation of the IL – BLA pathway facilitates extinction (Bukalo et al., 2021). Together, these studies demonstrate dissociable roles for the PL and IL in threat learning.

1.2.4 Hippocampus

The hippocampus is another threat learning region with anatomical and functional connections with the NAcc, amygdala, and mPFC. The hippocampus is the primary region underlying the storage and retrieval of explicit memory, including threat-related information. Hippocampal neural activity responds to cues and contexts associated with foot shock (Moita et al., 2003; Moita, 2004). The hippocampus is comprised of multiple subregions including the dorsal (dHPC) and ventral (vHPC) subregions. The dHPC and vHPC are functionally distinguished, with the dHPC normally linked to cognitive functions and spatial navigation while the vHPC is linked to the regulation of emotional states such as fear and anxiety (Moser and Moser, 1998; Fanselow and Dong, 2010), yet both regions have been associated with fear learning. Optogenetic inhibition of the dorsal hippocampus (dHPC) has shown a role for the dHPC in encoding ambiguous outcomes to enhance fear memory (Amadi et al., 2017). While pharmacological inactivation of dHPC neurons impairs remote auditory fear memory formation (Oh and Han, 2020). The vHPC CA3 subregion is necessary for the retrieval of cued fear conditioning (Hunsaker and Kesner, 2008) and stimulation of the vHPC blocks cued fear conditioning (Zhang et al., 2001). The BLA evenly routes positive and negative valence to the vHPC (Beyeler et al.,

2016) and stimulation of the BLA – vHPC pathway modulates anxiety-related behaviors (Felix-Ortiz et al., 2013). Similar to the prevailing view of the BLA, the vHPC CA1 subregion preferentially routes behavior-contingent information to distinct target regions. Specifically, the vCA1 preferentially routes anxiety-related information to the mPFC while goal-related information is routed to the mPFC, NAcc, and amygdala (Ciocchi et al., 2015). However, it's important to note that although this paper was pivotal, the data was only collected from four animals. Taken together, the hippocampus plays a subregion and pathway specific role in threat and anxiety behaviors and sends threat-related responses to its anatomical connections, including the nucleus accumbens.

The current threat learning network discussed here includes the amygdala, accumbens, mPFC, and hippocampus. The BLA encodes and maintains cue-shock associations (LeDoux et al., 1990; Maren et al., 1996; Amorapanth et al., 2000; LeDoux, 2000; Goosens and Maren, 2001; Koo et al., 2004) and sends this information to the central amygdala (CeA), which mediates the behavioral expression of fear responses (LeDoux et al., 1988). The BLA sends strong glutamatergic projections to the NAcc, which is a top candidate region for fear scaling. The mPFC has close anatomical and functional connections with both the BLA and the NAcc, as well as the hippocampus, both of which are involved in threat learning. Though each region has been studied individually, the complex pathways and interactions between these regions to coordinate threat responses are still unclear. In this dissertation, I will be focusing on the NAcc and its involvement in threat learning.

1.3 The Nucleus Accumbens in Reward Learning

The NAcc's ability to rapidly signal relative reward value, as well as its anatomical connectivity with the amygdala, make it a likely candidate for signaling relative threat. The nucleus accumbens has long been studied in reward settings. The prevailing view of NAcc function is that it processes information regarding the relative value of rewards. Relative reward value is the estimated value of a reward compared to other previous or current rewards, with the goal of obtaining the highest valued reward. Neurotoxic lesions of the NAcc have been shown to alter discrimination between rewards of different magnitude (Galtress and Kirkpatrick, 2010; Steele et al., 2018). Optogenetic inhibition of accumbens fast-spiking interneurons (FSIs) promotes impulsive reward choices (Pisansky et al., 2019). NAcc neuron activity has been shown to discriminate rewards of different values, showing differential firing to reward discrimination. When NAcc neurons are recorded during a risk-reward task, NAcc neuron activity differentially scales to animals' preferred option when animals must weigh the cost-benefit of value and risk and differentially encodes reward omissions based on risk preference (Sugam et al., 2014). In non-human primates, single-unit NAcc recordings have shown that some NAcc neurons show rapid increases in firing during cues signaling reward availability (i.e., go-cue), reward feedback, and reward delivery, while other neurons show responses to trial outcomes, during reward periods (Gale et al., 2014). In rats, NAcc single-units respond to relative value and palatability of rewards (Taha, 2005). NAcc activity to reward-

predictive cues and reward delivery is modulated by reward size (Roesch et al., 2009; Goldstein et al., 2012; Bissonette et al., 2013; Cooch et al., 2015) and concentration (Taha, 2005; Wheeler et al., 2005; Villavicencio et al., 2018). The NAcc plays a clear role in appetitive learning, but the critical question is whether or not the NAcc is involved in threat learning.

1.4 The Nucleus Accumbens in Threat Learning

The prevailing view is that the BLA preferentially routes information regarding negative valence to the CeA, whereas positive valence is routed to the NAcc (Beyeler et al., 2016, 2018). While considerable research supports the view, few studies have examined the routing of negative valence information from the BLA to the NAcc. One of the few studies that has examined the NAcc in negative valence demonstrated that the NAcc is an essential component of the fear network (Ray et al., 2020). These data suggest that the NAcc is essential for adaptive fear, revising the prevailing view that this region is exclusive to reward. A role for the NAcc in threat learning would be expected based on immediate early gene (IEG) studies. Shock-associated cues and contexts reliably upregulate NAcc c-fos and zif268 (Beck and Fibiger, 1995; Campeau et al., 1997; Thomas et al., 2002). Although the NAcc contains information about shock-associated cues and contexts, specifying the role of the NAcc in fear has presented a considerable challenge. Parkinson and colleagues found that NAcc lesions impaired cued fear, but enhanced contextual fear (Parkinson et al., 1999). Taking a similar experimental approach, Levita and colleagues found that

NAcc lesions had no impact on the acquisition or expression of cued fear, but impaired retention of contextual fear (Levita et al., 2002). Contemporary work by Haralambous and Westbrook found that inhibiting accumbens activity (core + shell) specifically impaired the acquisition, but not the expression of contextual fear, and had no effect on cued fear (Haralambous and Westbrook, 1999). Even considering slightly different methodologies, it is difficult to reconcile these disparate results.

These are not the only conflicts in the literature. Schwienbacher and colleagues found that blocking NAcc activity with tetrodotoxin abolished acquisition, and impaired expression, of fear-potentiated startle (Schwienbacher et al., 2004). The very next year Josselyn and colleagues utilized a variety of methods to manipulate the NAcc during fear-potentiated startle: lesion, agonizing dopamine, and blocking glutamate. NAcc manipulation did not impact any aspect of fear-potentiated startle (Josselyn et al., 2005). Since these initial studies, the NAcc has been implicated in a variety of fear-related processes. For example, the NAcc can modulate salience, regulating the ability of cues to enter into associations with shock (Iordanova et al., 2006b, 2006b; Iordanova, 2009) and is necessary for the expression of fear (Dutta et al., 2020). More recent research into the accumbens has shown that inactivation of the NacS reduces expression of conditioned suppression, while inactivation of the NAcc does not affect fear expression. This study utilized a fear learning task with discrete cues for danger and safety (Piantadosi, 2017; Piantadosi et al., 2020). Thus, it is likely that the

NAcc plays a more prominent role when there are multiple cues signaling different probabilities of threat.

1.5 Dissertation Aims and Synopsis

The central aim of this dissertation is to examine the role of the NAcc in scaling fear to different degrees of threat. To do this, I employed a behavioral procedure where rats were trained to discriminate three auditory cues predicting unique foot shock probabilities: danger (p=1.00), uncertainty (p=0.25), and safety (p=0.00). To measure fear, I utilized conditioned suppression of rewarded nose poking which permitted unbiased and temporally precise measurement of fear to each of the three cues. This behavioral paradigm was combined with neurotoxic lesions, optogenetic inhibition, and single-unit recordings to determine a role for the NAcc in fear scaling.

In three experiments, I explicitly tested the following research questions:

1. Is the NAcc is necessary for the acquisition of both rapid and general fear scaling?
2. Is the NAcc is necessary for the expression of rapid fear scaling?
3. Do NAcc single units show firing changes to threat cues? If so, what specific patterns of threat responding are observed?

In chapter 2, I permanently ablated NAcc neurons in male rats via neurotoxic lesions. Following recovery, rats received fear discrimination in which auditory cues predicted unique foot shock probabilities. To isolate the rapid scaling of fear, I broke the 10-s cues into five, 2-s cue intervals. This permitted

analysis of rapid scaling of fear, focusing on the first 2-s cue interval, as well as overall scaling across all intervals. Neurotoxic lesions revealed a general role for the NAcc in the acquisition of fear scaling, as well as a specific role in acquiring rapid uncertainty-safety discrimination. The results reveal that the NAcc is an essential component of a neural circuit permitting the acquisition of rapid and overall fear scaling, as well as a more specific role in acquiring rapid uncertainty-safety discrimination. However, the permanent ablation of NAcc neurons leaves the question of whether the NAcc is involved in the expression of fear scaling.

In chapter 3, I used a within-subjects optogenetic approach which allowed for the precise and controlled examination of the NAcc's role in the expression of fear scaling. Male rats acquired general fear scaling and once stable, NAcc neural activity was optogenetically inhibited at the time of cue presentation or a control period. Optogenetic inhibition impaired rapid uncertainty-safety discrimination, demonstrating that NAcc cue activity is necessary for the expression of rapid uncertainty-safety discrimination. Taken together with chapter 2, the results demonstrate that NAcc activity is necessary for the acquisition of general fear scaling across cue presentation, as well as the acquisition and expression of rapid uncertainty-safety discrimination at cue onset. However, the NAcc activity requirement for fear scaling does not necessitate that NAcc neurons respond to threat.

In chapter 4, NAcc single-unit activity was recorded in female rats during fear discrimination taking place over a baseline of reward-seeking. NAcc cue responsive neurons showed threat responses, but specific threat responding

differed between populations, specifically, units showing phasic activity at cue onset and tonic activity across cue presentation. Phasic units showed threat-responsive firing (i.e., greatest changes in firing to danger and uncertainty, lesser changes to safety) while tonic units showed danger-responsive firing (i.e., greatest changes in firing to danger, lesser changes to uncertainty and safety). NAcc single-unit activity demonstrates that NAcc neurons are threat responsive and exhibit heterogeneity in the timing and specific nature of threat firing.

The current aims are independent yet complementary and demonstrate a novel role for the NAcc in adaptive fear behavior, specifically scaling fear to the level of threat. Together, the three experiments demonstrate that the NAcc is not just necessary for fear scaling, but also responds to threat cues across both rapid and persistent time periods. Identifying the brain regions underlying adaptive fear is fundamental to understanding and developing more effective treatments for anxiety disorders.

Chapter 2: The Nucleus Accumbens Core is Necessary for General and Rapid Threat Estimation

Portions of this chapter have been published in the following research article:

Ray, M.H., Russ, A.N., Walker, R.A., and McDannald, M.A. (2020). The nucleus accumbens core is necessary to scale fear to degree of threat. *Journal of Neuroscience, 40 (24),* 4750-4760.

2.1 Introduction

A role for the NAcc in rapid fear scaling is supported by its ability to rapidly process reward-predictive cues (Cromwell and Schultz, 2003; Setlow et al., 2003; Ambroggi et al., 2011; McGinty et al., 2013; Saddoris and Carelli, 2014; Sugam et al., 2014; Ottenheimer et al., 2018), as well as its anatomical connectivity with the amygdala (Kita and Kitai, 1990; Petrovich et al., 1996; Wright and Groenewegen, 1996). Additionally, the NAcc is implicated in a variety of fear-related processes (Haralambous and Westbrook, 1999; Thomas et al., 2002; Schwienbacher et al., 2004; Iordanova et al., 2006a, 2006b; Fadok et al., 2010; Badrinarayan et al., 2012; Li and McNally, 2015; Correia et al., 2016).

In the current chapter, I examined a role for the NAcc in acquisition of fear scaling by permanently ablating NAcc neurons via neurotoxic lesion. Following recovery, rats received fear discrimination consisting of danger, uncertainty, and safety cues. Fear was measured with suppression of rewarded nose poking (Estes and Skinner, 1941; Bouton and Bolles, 1980). Examining suppression over the entire 10-s cue permitted analysis of overall fear scaling. To examine the temporal emergence of scaling, I divided the 10-s cues into five, 2-s cue intervals. Focusing on suppression during the first 2-s cue interval permitted analysis of rapid fear scaling. The current experiment allowed me to examine a role for the NAcc in the acquisition of both rapid and general fear scaling.

2.2 Materials and Methods

2.2.1 Animals

Subjects were forty-five male Long Evans rats weighing 275-300 g upon arrival (Charles River Laboratories; RGD Cat# 2308852, RRID:RGD_2308852). Rats were individually housed and maintained on a 12-h dark-light cycle (lights off at 6:00 PM) with water *ad libitum*. Procedures adhered to the NIH Guide for the Care and Use of Laboratory Animals and were approved by the Boston College Institutional Animal Care and Use Committee.

2.2.2 Behavioral Apparatus

Eight sound-attenuated enclosures each housed a behavior chamber with aluminum front and back walls, clear acrylic sides and top, and a metal grid floor. Grid floors were electrically connected to a shock generator. A single external food cup and central nose poke opening equipped with infrared photocells were present on one wall. Auditory stimuli were presented through two speakers mounted on the ceiling of each behavior chamber.

2.2.3 Surgical Procedures

Stereotaxic surgery was performed under isoflurane anesthesia (2-5%) using aseptic technique. Twenty-four rats received bilateral infusions of N-Methyl-D-aspartic acid (15 µg/µl in Dulbecco's PBS) aimed at the NAcc (0.40 µl, +1.90 AP, ±1.80 ML, -6.60 DV from skull). Infusions were delivered via 2 µl syringe (Hamilton, Neuros) controlled by a microsyringe pump (World Precision

Instruments, UMP3-2). Infusion rate was ~0.11 µl/min. Thirty seconds after the completion of each infusion, the syringe was raised 0.1 mm then left in place for five minutes to encourage delivery to the target site. The remaining twenty-one rats received identical surgical treatment without infusions. Rats received carprofen (5 mg/kg) for post-operative analgesia.

2.2.4 Nose Poke Acquisition

Following recovery from surgery, rats were food restricted to 85% of their initial free-feeding body weight, then fed (2 - 20 g/day) to increase their target body weight by 1 g/day for the remainder of testing. Rats were shaped to nose poke for pellet (BioServ F0021 – protein/fat/carbohydrate blend) delivery using a fixed ratio 1 schedule: one nose poke yielded one pellet. Shaping sessions lasted 30 min or approximately 50 nose pokes. Over the next 3, 60-min sessions, rats were placed on variable interval (VI) schedules in which nose pokes were reinforced on average every 30 s (session 1), or 60 s (sessions 2 and 3). For the remainder of testing, nose pokes were reinforced on a VI-60 schedule independent of all Pavlovian contingencies.

2.2.5 Pre-exposure

In two separate sessions, each rat was pre-exposed to the three cues to be used in Pavlovian fear discrimination. Cues were auditory stimuli, 10-s in duration and consisted of repeating motifs of a broadband click, phaser, or trumpet. Previous studies have found these stimuli to be equally salient, yet highly discriminable (Berg et al., 2014; DiLeo et al., 2016; Ray et al., 2018). The

42-min pre-exposure sessions consisted of four presentations of each cue (12 total presentations) with a mean inter-trial interval (ITI) of 3.5 min. The order of trial type presentation was randomly determined by the behavioral program and differed for each rat during each session throughout behavioral testing.

For all sessions, fear to each auditory cue was measured using a suppression ratio based on nose poke rates during the 20-s baseline period immediately preceding the 10-s cue period: suppression ratio = (baseline nose poke rate – cue nose poke rate) / (baseline nose poke rate + cue nose poke rate). A ratio of 1 indicated complete suppression of nose poking during the cue and a high level of fear; 0, no suppression and no fear. Intermediate suppression ratios reflected intermediate fear levels. The same suppression ratio formula was used to calculate fear in 2-s cue intervals.

2.2.6 Fear Discrimination

Each rat received sixteen, 54-min Pavlovian fear discrimination sessions. Sessions began with a ~5-min warm-up period during which no cues or shock were presented. The three cues were associated with a unique foot shock (0.5 mA, 0.5-s) probability: danger (p=1.00), uncertainty (p=0.25), and safety (p=0.00). Foot shock was administered 1-s following cue offset. A single session consisted of four danger, six uncertainty omission, two uncertainty shock, and four safety trials. Auditory stimulus identity was counterbalanced across rats. Mean ITI was 3.5 min.

2.2.7 Histology

Upon the conclusion of behavior, rats were anesthetized with an overdose of isoflurane and perfused intracardially with 0.9% biological saline. Brains were extracted and stored in 4% (v/v) formalin and 10% (w/v) sucrose. Forty-micrometer sections were collected on a sliding microtome. Tissue was then washed with Phosphate Buffered Solution (PBS), incubated in NeuroTrace (Thermo Fisher, N21479) at a 1:200 concentration, washed again, mounted, dried, and coverslipped with Vectashield Hardset mounting media (Vector Labs, H-1400). Slides were imaged within 3 weeks of processing.

2.2.8 Statistical analysis

Behavioral data were acquired using Med Associates Med-PC IV software (MED PC, RRID:SCR_012156). Raw data were processed in Matlab (MATLAB, RRID:SCR_001622) to extract timestamps for nose poke and cue onset. Suppression ratios were calculated as: (baseline poke rate – cue poke rate) / (baseline poke rake + cue poke rate) and were analyzed with repeated measures ANOVA in SPSS (RRID:SCR_002865). Repeated measures ANOVA was performed with factors of group, cue, and time. Partial eta squared (η_p^2) and observed power (op) are reported for ANOVA results for indicators of effect size. For all analyses, $p<0.05$ (or an appropriate Bonferroni correction) was considered significant.

2.3 Summary of Experiments and Results

2.3.1 Histological Results

Rats received bilateral sham or neurotoxic NAcc lesions. Neurotoxic damage (cell loss and gliosis) was quantified. Twenty-four NAcc rats showed damage primarily in the NAcc (>85%) with minor damage (~10% or less) in the neighboring accumbens shell. Shams showed no evidence of neurotoxic damage. Representative sham (Figure 2.1A, left), and NAcc lesion (Figure 2.1A, right) sections are shown. Each subject's lesion was drawn, made transparent, and stacked (Figure 2.1B). Darker areas indicate regions of greater overlap and more consistent damage. Rats fully recovered from surgery before receiving fear discrimination (Figure 2.1C).

2.3.2 Baseline Nose Poking

NAcc lesions altered the progression of nose poking over discrimination sessions, but did not grossly reduce nose poke rates (Figure 2.1D). Analysis of variance (ANOVA) for baseline nose poke rate with session (16) and group (sham vs. NAcc) as factors found a main effect of session ($F_{15,645}$ = 47.14, p=3.77 x 10^{-93}, η_p^2 = 0.52, op = 1.00), a session x group interaction ($F_{15,645}$ = 2.10, p=0.008, η_p^2 = 0.05, op = 0.97) but no main effect of group ($F_{1,43}$ = 0.16, p=0.69, η_p^2 = 0.004, op = 0.07). Dividing the 16 sessions into 2, 8-session blocks; ANOVA found a block x group interaction ($F_{1,43}$ = 4.81, p=0.034, η_p^2 = 0.10, op = 0.57). While sham (t_{20} = 7.69, p=2.13 x 10^{-7}) and NAcc rats (t_{23} = 5.63, p=1.00 x 10^{-5}) both increased poking from the first to second half of discrimination, sham

rats showed greater increases (Figure 2.1E). Mean ± SEM baseline nose pokes rates for sessions 1-8: sham (28.44 ± 2.96) and NAcc (28.83 ± 1.97); sessions 9-16: sham (38.80 ± 3.62) and NAcc (35.33 ± 2.46; Figure 2.1E).

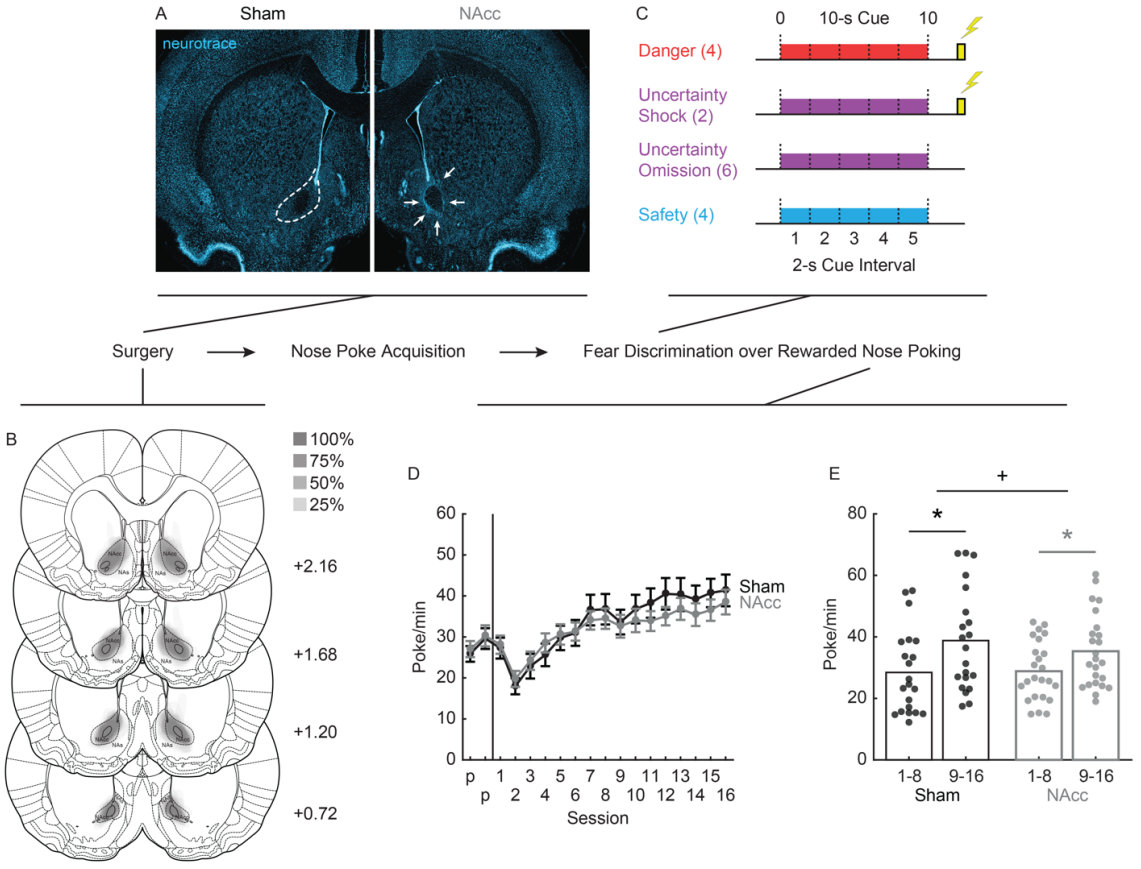

Figure 2.1 NAcc lesion experimental outline. (A) Representative sham with NAcc intact (left) and lesion with NAcc damage (right) is shown. Dotted lines (left) show approximate NAcc location. Arrows (right) indicate gliosis and damage restricted to the NAcc. **(B)** The extent of neurotoxic NAcc lesions across four coronal planes is shown, and the anterior distance from bregma (millimeters) indicated. **(C)** Pavlovian fear discrimination consisted of three, 10-s cues predicting unique foot shock probabilities: danger (p=1.00), red; uncertainty (p=0.25), purple; and safety (p=0.00), blue. Cues were divided into 5, 2-s intervals (dotted lines) for rapid analyses. **(D)** Mean ± SEM baseline nose poke rates for the sixteen fear discrimination sessions are shown for sham (black) and NAcc (gray) rats. **(E)** Mean baseline nose poke rates for sessions 1-8 and 9-16 for sham and NAcc rats. Data points show individual poke rates. *independent samples t-test, $p<0.025$, $^{+}$block x group interaction $p<0.05$. Abbreviations: NAcc – nucleus accumbens core, NAs – nucleus accumbens shell.

2.3.3 Fear Scaling

Sham rats acquired appropriate scaling of the fear response over the 16 sessions (Figure 2.2A, left). Suppression ratios for the entire 10-s cue were low in pre-exposure and initially increased to all cues. As discrimination proceeded, the suppression ratio for each cue diverged: high to danger, intermediate to uncertainty, and low to safety. NAcc rats showed a similar progression, but poorer overall scaling (Figure 2.2A, right). In support of the general emergence of scaling, ANOVA [between factor: group (sham vs. NAcc); within factors: session (16) and cue (danger, uncertainty and safety)] revealed a main effect of cue ($F_{2,86}$ = 115.51, p=4.34 x 10^{-25}, η_p^2 = 0.73, op = 1.00) and a cue x session interaction ($F_{30,1290}$ = 14.05, p=6.30 x 10^{-60}, η_p^2 = 0.25, op = 1.00). Revealing impaired scaling in NAcc rats, ANOVA found a cue x group interaction ($F_{2,86}$ = 5.76, p=0.004, η_p^2 = 0.12, op = 0.86). The cue x group interaction was also observed when only the last six sessions were analyzed ($F_{2,86}$ = 4.50, p=0.014, η_p^2 = 0.10, op = 0.76), the period by which scaling patterns were stable.

To further reveal the deficit in NAcc rats, I focused on suppression ratios from the final six sessions. Difference scores were calculated for the two components of scaling: (danger – uncertainty) and (uncertainty – safety). Sham (Figure 2.2B, left) and NAcc rats (Figure 2.2B, right) discriminated each cue pair. One-sample t-tests found that difference scores exceeded zero for each comparison: sham, danger vs. uncertainty (t_{20} = 10.25, p=2.07 x 10^{-9}), uncertainty vs. safety (t_{20} = 6.11, p=4.17 x 10^{-8}); NAcc, danger vs. uncertainty (t_{23} = 8.01, p=0.001), uncertainty vs. safety (t_{23} = 3.65, p=0.002). However, NAcc rats

showed poorer overall discrimination. ANOVA [between factor: group (sham vs. NAcc); within factor: discrimination (danger – uncertainty) and (uncertainty – safety)] revealed a main effect of group ($F_{1,43}$ = 5.68, p=0.022, η_p^2 = 0.12, op = 0.64). Difference scores were reduced across both components in NAcc rats. These results reveal a general role for the NAcc in fear scaling.

2.3.4 Rapid Fear Scaling

I was interested in revealing a possible role for the NAcc in the rapid emergence of fear scaling. To do this, I examined mean suppression ratios from the last six sessions. Each cue was divided into 5, 2-s cue intervals and suppression ratios were calculated for each cue/interval. Sham rats showed scaling of the fear response in the first 2-s cue interval and in all subsequent intervals (Figure 2.2C, left). Scaling was reduced across all 2-s cue intervals in NAcc rats (Figure 2.2C, right). ANOVA [between factor: group (sham vs. NAcc); within factors: interval (5, 2-s cue intervals) and cue (danger, uncertainty and safety)] found a group x cue interaction ($F_{2,86}$ = 3.88, p=0.024, η_p^2 = 0.08, op = 0.69). Supporting a specific role for the NAcc in rapid fear scaling, NAcc rats showed impaired scaling even when only the first 2-s cue interval was analyzed (cue x group interaction; $F_{2,86}$ = 5.08, p=0.0008, η_p^2 = 0.11, op = 0.81). No cue x group interaction was observed when the last 2-s cue interval was analyzed ($F_{2,86}$ = 1.90, p=0.16, η_p^2 = 0.04, op = 0.39).

To specify the nature of the deficit in NAcc rats, I reduced scaling into its component parts: (danger – uncertainty) and (uncertainty – safety) and

calculated difference scores for the first and last 2-s cue intervals. Sham rats showed positive difference scores for each cue pair at each interval (Figure 2.2D, left). Difference scores exceeded zero, as revealed by one-sample t-tests: first 2-s cue interval: danger vs. uncertainty (t_{20} = 10.95, p=6.7 x 10^{-4}), uncertainty vs. safety (t_{20} = 3.55, p=0.002); last 2-s cue interval: danger vs. uncertainty (t_{23} = 4.60, p=1.76 x 10^{-4}), uncertainty vs. safety (t_{23} = 5.73, p=1.30 x 10^{-5}) for shams. NAcc rats were generally impaired at rapid scaling. ANOVA for the first 2-s cue interval differences revealed a main effect of group ($F_{1,43}$ = 6.50, p=0.014, η_p^2 = 0.01, op = 0.70), while ANOVA for the last 2-s cue interval differences scores found no main effect ($F_{1,43}$ = 2.49, p=0.12, η_p^2 = 0.05, op = 0.34). Difference scores also suggest that NAcc rats were more specifically impaired in rapid uncertainty-safety discrimination (Figure 2.2D, right). One-sample tests found that only the NAcc uncertainty-safety difference score from the first 2-s cue interval failed to differ from zero: first interval: danger vs. uncertainty (t_{23} = 4.20, p=3.38 x 10^{-4}), uncertainty vs. safety (t_{23} = 1.31, p=0.20); last interval: danger vs. uncertainty (t_{20} = 5.22, p=2.70 x 10^{-5}), uncertainty vs. safety (t_{20} = 4.19, p=3.53 x 10^{-4}). All significant, one-sample t tests survive Bonferroni correction (0.05/8, p<0.00625). Altogether, these results reveal a general role for the NAcc in the acquisition of rapid and overall fear scaling, as well as a more specific role in rapid uncertainty-safety discrimination.

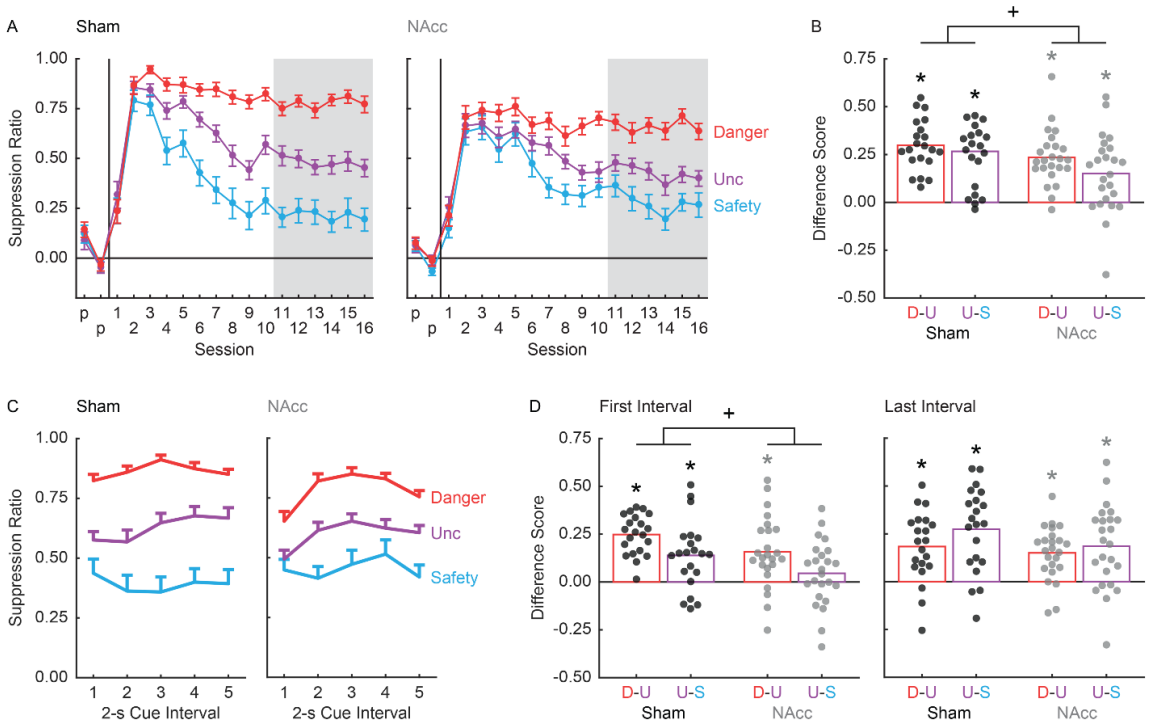

Figure 2.2 NAcc lesions and fear scaling. (A) Mean ± SEM suppression ratio for danger (red), uncertainty (purple), and safety (blue) are shown for sham (left) and NAcc (right) rats. The vertical lines separate the two pre-exposure and sixteen fear discrimination sessions. The last six discrimination sessions are shaded. **(B)** Mean difference score for danger vs. uncertainty (D-U, red bar) and uncertainty vs. safety (U-S, purple bar) across the entire 10-s cue is shown for sham (left) and NAcc (right) rats. Data points show individual difference scores. *One-sample t-test compared to zero, $p<0.0125$; $^{+}$main effect of group, $p<0.05$. **(C)** Mean + SEM suppression ratios for the 5, 2-s cue intervals are shown for sham (left) and NAcc (right) rats. Cue color scheme maintained from A. **(D)** Mean difference score for danger vs. uncertainty (D-U, red bar) and uncertainty vs. safety (U-S, purple bar) is shown for the first 2-s cue interval (left) and last 2-s cue interval (right) for sham and NAcc rats. Data points show individual difference scores. *One-sample t-test compared to zero, $p<0.00625$; $^{+}$main effect of group, $p<0.05$.

2.4 Discussion

In this chapter, I set out to examine a role for the NAcc in the acquisition of fear scaling. Neurotoxic lesions revealed a general role for the NAcc in the acquisition of fear scaling, as well as a specific role in acquiring rapid uncertainty-safety discrimination. The results reveal that the NAcc is an essential component

of a neural circuit permitting the acquisition of rapid and overall fear scaling, as well as a more specific role in acquiring rapid uncertainty-safety discrimination.

Before considering the implications of these findings, we must first consider the limitations of the present experiment. Our experiment only used male rats. Several studies have reported sex differences in danger-safety discrimination (Day et al., 2016; Foilb et al., 2018; Greiner et al., 2019) while other cued-fear studies report no sex differences (Maren et al., 1994; Markus and Zecevic, 1997; Maes, 2002; Baker-Andresen et al., 2013; Fenton et al., 2014; Clark et al., 2019). We find only modest sex differences in our discrimination procedure (Walker et al., 2018, 2019), suggesting similar neural circuits may be used across sexes. Another important consideration is that our dependent measure of fear is derived from the rate of rewarded nose poking. Conditioned suppression is a strength because it provides an objective measure of fear on multiple time scales (Estes and Skinner, 1941; Bouton and Bolles, 1980). It is a potential weakness because the NAcc plays a well-established role in reward-seeking. Disrupting NAcc function can attenuate reward-related behavior in many settings (Corbit et al., 2001; Hall et al., 2001; Ito et al., 2004; Blaiss and Janak, 2009; Ambroggi et al., 2011; McDannald et al., 2011, 2013), though this finding is not universal (Ramirez and Savage, 2007; Corbit and Balleine, 2011). In the current experiment, NAcc lesions slowed the increase of baseline nose poking over discrimination sessions and also impaired fear scaling. However, the temporal emergence of the deficits in reward-seeking and acquisition of fear

scaling did not align. The fear scaling deficit was apparent across all sessions while the nose poking deficit only emerged in the later sessions.

The current experiment demonstrates the NAcc is generally necessary for the acquisition of fear scaling throughout the duration of an encounter, in this case for the entirety of cue presentation. At the same time, the NAcc is specifically necessary for one specific component of fear scaling: acquiring rapid discrimination of uncertain threat and safety. However, the neurotoxic lesions permanently ablated NAcc neurons which leaves the question of the NAcc's role in post-acquisition expression of fear scaling. Chapter 3 will focus on determining a specific role for the NAcc in the expression of fear scaling.

Chapter 3: The Nucleus Accumbens Core is Necessary for Rapid Discrimination of Uncertainty and Safety

Portions of this chapter have been published in the following research article:

Ray, M.H., Russ, A.N., Walker, R.A., and McDannald, M.A. (2020). The nucleus accumbens core is necessary to scale fear to degree of threat. *Journal of Neuroscience, 40 (24),* 4750-4760.

3.1 Introduction

In chapter 2, I demonstrated that NAcc activity is necessary for the acquisition of both general fear scaling across cue presentation and rapid uncertainty-safety discrimination at the time of cue onset. However, the permanent ablation of NAcc neurons leaves the question of whether the NAcc is involved in the expression of fear scaling.

In the current chapter, I designed an experiment to determine a role for the NAcc in the expression of fear scaling. To isolate a specific role for NAcc cue activity in the expression of fear scaling, I utilized a within-subjects optogenetic approach. Rats were NAcc-transducted with halorhodopsin or a control fluorophore and bilaterally implanted with ferrules above the NAcc. Following recovery, rats received fear discrimination to danger, uncertainty, and safety, until fear scaling was stable. Once scaling was established, rats received eight sessions in which the NAcc was green-light illuminated during cue presentation or a control period, optogenetically inhibiting activity in halorhodopsin rats. This within-subjects design controlled for general effects of illumination by allowing for behavioral comparisons of cue and control illumination periods in the same rat. Thus, if NAcc inhibition generally disrupts behavior, cue and control illumination would produce equivalent results. However, if NAcc inhibition disrupts adaptive fear scaling, deficits would only be observed in halorhodopsin rats receiving cue illumination. The current experiment allowed for the precise and controlled examination of a specific role for the NAcc in the expression of fear scaling.

3.2 Materials and Methods

3.2.1 Animals

Subjects were 25 male Long Evans rats weighing 275-300 g upon arrival (Charles River Laboratories; RGD Cat# 2308852, RRID:RGD_2308852). Rats were individually housed and maintained on a 12-h dark-light cycle (lights off at 6:00 PM) with water *ad libitum*. Procedures adhered to the NIH Guide for the Care and Use of Laboratory Animals and were approved by the Boston College Institutional Animal Care and Use Committee.

3.2.2 Behavioral apparatus `

The behavioral apparatus was identical to chapter 1. In addition to the standard behavior apparatus, green lasers (532 nm, max 500 mW; Shanghai Laser & Optics Century Co., Ltd.; Shanghai, China) were used to illuminate the NAcc. Lasers were connected to the behavior cables via 1X2 fiber optic rotatory joints (Doric; Quebec, Canada). A ceramic sleeve maintained contact between the ferrules on the optogenetic cable and the head cap. The ferrule junction was shielded with black shrink wrap to block light emission into the behavioral chamber. A PM160 light meter (Thorlabs; Newton, NJ) was used to measure light output.

3.2.3: Optogenetic materials

Optical ferrules were constructed using 2.5 mm ceramic zirconia ferrules (Precision Fiber Products; Chula Vista, CA). Behavior cables were custom made for light delivery (Multimode Fiber, 0.22 NA, High-OH, Ø200 µm Core).

3.2.4 Surgical procedures

Stereotaxic surgery was performed under isoflurane anesthesia (2-5%) using aseptic technique. Thirteen rats received bilateral infusions of AAV-hSyn-eNpHR3.0-EYFP (halorhodopsin) aimed at the NAcc (0.50 µl, +1.90 AP, ±1.80 ML, -6.60 DV at a 0° angle) and bilateral optical ferrules (+1.70 AP, ±2.80 ML, -6.00 DV at a 10° angle). Infusions were delivered via 2 µl syringe (Hamilton, Neuros) controlled by a microsyringe pump (World Precision Instruments, UMP3-2). Infusion rate was ~0.11 µl/min. The syringe was raised 0.1 mm after each infusion, then left in place for five min to encourage delivery to the target site. The remaining 12 rats received identical surgical treatment but were infused with a control fluorophore (AAV-hSyn-EYFP). Implants were secured with dental cement surrounded by a modified, 50 mL centrifuge tube. Post-surgery, rats received 2 weeks of undisturbed recovery with prophylactic antibiotic treatment (cephalexin; Henry Schein 049167) before beginning nose poke acquisition. All rats received carprofen (5 mg/kg) for post-operative analgesia.

3.2.5 Pre-illumination training and cable habituation

Nose poke acquisition, pre-exposure and initial fear discrimination (10 sessions) were identical to chapter 1. I increased the delay between cue offset and shock onset to 2 s to ensure that neural activity would not be inhibited during shock delivery. Cable habituation was provided in two consecutive sessions by plugging rats into optogenetic cables and administering fear discrimination

without illumination. In total, rats received twelve fear discrimination sessions before receiving light illumination.

3.2.6 NAcc illumination

Rats received eight sessions of fear discrimination plus NAcc illumination. The NAcc was illuminated via bilateral delivery of 12.5 mW of 532 nm 'green' light: DPSS laser → optogenetic cables → implanted ferrules. There were two types of illumination sessions: cue and ITI. For cue sessions, light illumination began 0.5 s prior to cue onset and ended 0.5 s following cue offset, resulting in a total illumination time of 11 s. Light illumination was given for all trial types (danger, uncertainty, and safety) for a total of 16 illumination events per session. For ITI sessions, illumination occurred during the inter-trial intervals between cue presentations. Illumination was roughly equidistant from the previous cue offset and subsequent cue onset (~90 s from each). Sixteen ITI illumination events were administered, each lasting 11 s, equating total illumination time for cue and ITI sessions. The within-subjects design meant that each rat received four cue illumination sessions and four ITI illumination sessions. Illumination was given in two-session blocks, with half of the subjects starting with cue illumination.

3.2.7 Histology

After behavioral testing ended, rats were anesthetized with an overdose of isoflurane and perfused intracardially with 0.9% biological saline and 4% paraformaldehyde in a 0.2 M PBS. Brains were extracted and stored in 4% (v/v)

formalin and 10% (w/v) sucrose. Forty-micrometer sections were collected on a sliding microtome. Tissue was rinsed, incubated in NeuroTrace (Thermo Fisher, N21479) at a 1:200 concentration, rinsed again, mounted, dried, and coverslipped with Vectashield Hardset (Vector Labs, H-1400). Slides were imaged within 3 weeks of processing.

3.2.8 Statistical analysis

Behavioral data were acquired using Med Associates Med-PC IV software (MED PC, RRID:SCR_012156). Raw data were processed in Matlab (MATLAB, RRID:SCR_001622) to extract timestamps for nose poke and cue onset. Suppression ratios were calculated as: (baseline poke rate – cue poke rate) / (baseline poke rake + cue poke rate) and were analyzed with repeated measures ANOVA in SPSS (RRID:SCR_002865). Repeated measures ANOVA was performed with factors of group, cue, time, and illumination. Partial eta squared (η_p^2) and observed power (op) are reported for ANOVA results for indicators of effect size. For all analyses, $p<0.05$ (or an appropriate Bonferroni correction) was considered significant.

3.3 Summary of Experiments and Results

3.3.1 Introduction to results

The current results aim to determine a temporally specific role for the NAcc in the expression of fear scaling. The current experiment utilized a within-subjects, optogenetic approach. Rats were NAcc-transducted with halorhodopsin

or a control fluorophore, recovered, then acquired a scaled fear response to danger, uncertainty and safety. Once scaling was established, rats received sessions in which the NAcc was illuminated during cue presentation or during the inter-trial interval. If the NAcc plays identical roles in the acquisition and expression of fear scaling, I would expect to observe a three-way interaction (group x illumination x cue) with only halorhodopsin rats showing impaired overall scaling during cue illumination sessions. If the NAcc plays a more selective role in the expression of rapid fear scaling, I would anticipate a four-way interaction (group x interval x illumination x cue) with only halorhodopsin rats showing impaired rapid uncertainty-safety discrimination during cue illumination sessions.

3.3.2 Histological results

Rats received bilateral NAcc transduction with halorhodopsin (Halo) or a control fluorophore (YFP) and bilateral optical ferrule implantation just above the NAcc. Representative transduction is shown (Figure 3.1A). Each subject's total transduction area was drawn, made transparent, and stacked (Figure 3.1B). Darker areas indicate regions of greater overlap and more consistent transduction. Transduction centered around and above the anterior commissure, the precise NAcc location.

3.3.3 Baseline nose poking

YFP and Halo rats showed equivalent baseline nose poking rates throughout pre-exposure, discrimination, cable habituation, and light illumination

(Figure 3.2A). ANOVA for baseline nose poke rate [factors: session (20) and group (YFP vs. Halo)] demonstrated a main effect of session ($F_{19,437}$ = 12.60, p=4.19 x 10^{-31}, η_p^2 = 0.35, op = 1.00), but no main effect or interaction with group (Fs < 0.93, ps>0.55). Equivalent performance lessens the concern that differences in suppression ratios between groups result from differences in baseline nose poke rates.

3.3.4 Initial fear scaling

YFP and Halo rats acquired reliable fear scaling over the 10 sessions (Figure 3.1C). Suppression ratios were low in pre-exposure and initially increased to all cues. As discrimination proceeded, the suppression ratio for each cue diverged: high to danger, intermediate to uncertainty, and low to safety. Demonstrating overall scaling, ANOVA [within factors: session (10) and 10-s cue (danger, uncertainty and safety); between factor: group (YFP vs. Halo)] revealed a main effect of cue ($F_{2,46}$ = 36.21, p=3.58 x 10^{-10}, η_p^2 = 0.61, op = 1.00), session ($F_{9,207}$ = 25.74, p=2.04 x 10^{-29}, η_p^2 = 0.53, op = 1.00) and a cue x session interaction ($F_{18,414}$ = 6.26, p=1.14 x 10^{-13}, η_p^2 = 0.21, op = 1.00). ANOVA found no main effect or interaction with group (Fs < 3.42, ps>0.08). Thus, YFP and Halo entered the light illumination phase (Figure 3.1D, E) showing equivalent fear scaling.

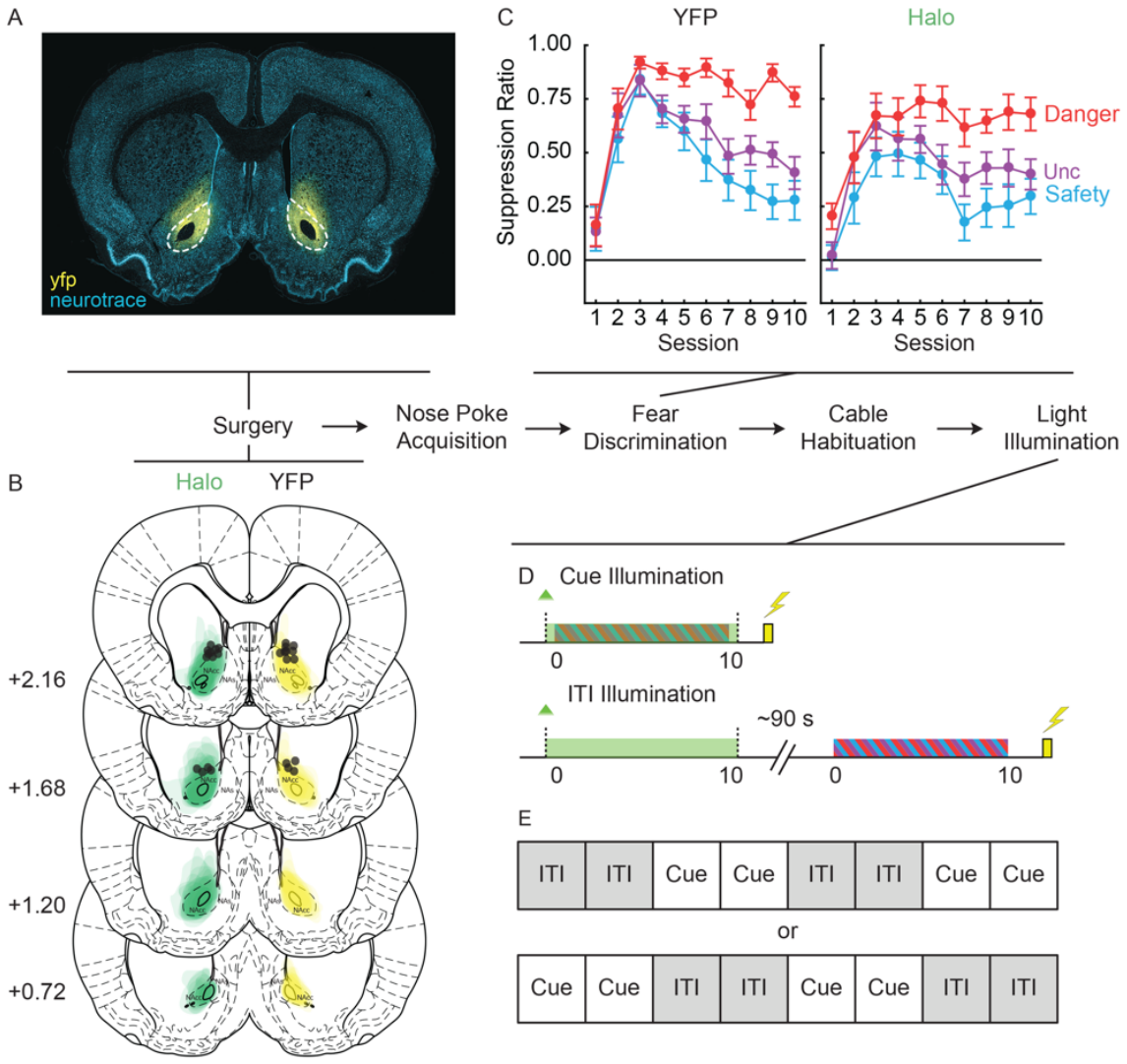

Figure 3.1 NAcc illumination experimental outline. (A) Representative NAcc transduction is shown with YFP expression (yellow fluorescent protein; yellow) and NeuroTrace (blue). Dotted lines approximate NAcc location. **(B)** The extent of viral transduction across four coronal planes is shown for Halo (green, left) and YFP rats (yellow, right), and the anterior distance from bregma (millimeters) indicated. Individual ferrule placement indicated in black circles. **(C)** Mean ± SEM suppression ratios for danger (red), uncertainty (purple), and safety (blue) are shown for YFP (left) and Halo rats (right) during the ten initial fear discrimination sessions. **(D)** In the final eight sessions, rats received NAcc light illumination during cue presentation (top) or during the inter-trial interval (ITI, bottom). Green indicates light illumination, yellow indicates shock delivery and candy-striped indicates cue presentation. **(E)** Cue and ITI illumination were given in alternating, two-session blocks. Block order was counterbalanced with roughly half of the subjects first receiving ITI illumination (top). Abbreviations: NAcc – nucleus accumbens core, NAs – nucleus accumbens shell.

3.3.5 Overall fear scaling during light illumination

When suppression ratios were calculated for the entire 10-s cue, YFP and Halo rats showed scaling of the fear response over the 10 sessions of cable habituation, cue illumination and ITI illumination (Figure 3.2). ANOVA [between factor: group (YFP vs. Halo); within factors: session (10) and cue (danger, uncertainty and safety)] was separately performed for rats receiving ITI-cue illumination order (YFP, n = 5; Halo, n = 5; Figure 3.2B) and cue-ITI illumination order (YFP, n = 7; Halo, n = 8; Figure 3.2C). Each ANOVA returned a main effect of cue (Fs > 29, *p*s<2 x 10^{-7}), but neither returned a main effect of group, group x cue interaction or a group x cue x session interaction (Fs < 2.5, *p*s>0.1). Complete ANOVA results provided in Table 3.1. Next, I calculated difference scores for the two components of scaling: (danger – uncertainty) and (uncertainty – safety) (Figure 3.2D). ANOVA [between factors: group (YFP vs. Halo) and order (ITI-cue vs. cue-ITI); within factors: illumination (hab/ITI vs. cue) and discrimination (danger – uncertainty vs. uncertainty – safety)] found main effects of illumination ($F_{1,21}$ = 8.90, *p*=0.007, η_p^2 = 0.30, op = 0.81) and discrimination ($F_{1,21}$ = 14.29, *p*=0.001, η_p^2 = 0.41, op = 0.95), as well as a group x illumination interaction ($F_{1,21}$ = 4.75, *p*=0.041, η_p^2 = 0.19, op = 0.55). The interaction resulted from YFP rats showing poorer overall discrimination in cue illumination sessions compared to ITI illumination, whereas Halo rats showed equivalent discrimination in each session type. No main effect of group ($F_{1,21}$ = 0.19, *p*=0.67, η_p^2 = 0.009, op = 0.07) or any group interaction was detected (Fs < 1.2, *p*s>0.3). These

results reveal that NAcc activity is not necessary for the expression of fear scaling when suppression is measured for the duration of cues.

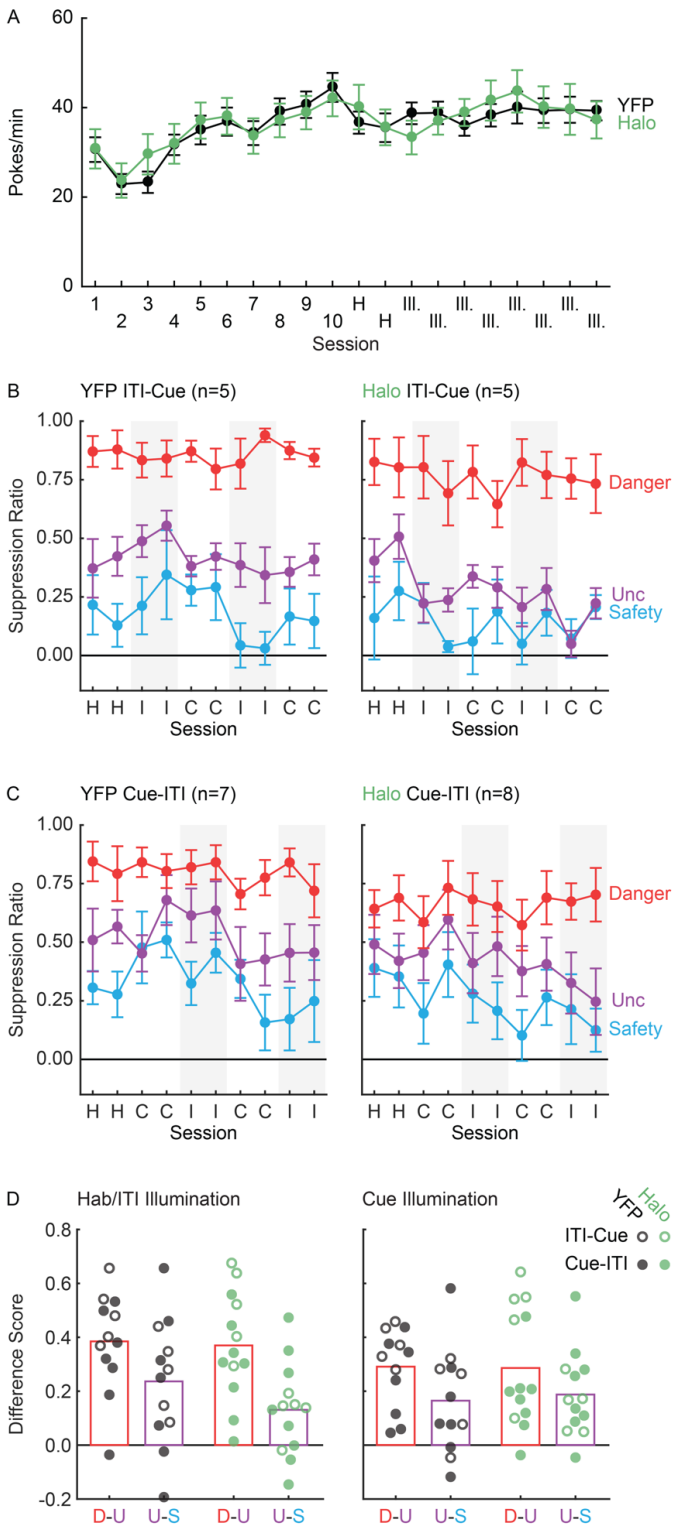

Figure 3.2 NAcc illumination and overall fear scaling. (A) Mean ± SEM nose poke rate is shown for YFP (black) and Halo rats (green) during the 10 pre-illumination (1-10), 2 cable habituation (H) and 8 illumination (III.) sessions. **(B)** Mean ± SEM suppression ratios over the entire 10-s cue are plotted for danger

(red), uncertainty (purple), and safety (blue). Data are plotted for cable habituation (H), ITI illumination (I) and cue illumination (C) for YFP (n=5) and Halo rats (n=5) receiving ITI-cue illumination. ITI illumination sessions shaded. **(C)** YFP (n=7) and Halo rats (n=8) receiving cue-ITI illumination plotted as in A. **(D)** Difference scores for danger vs. uncertainty (D-U, red bar) and uncertainty vs. safety (U-S, purple bar) are shown for YFP (black) and Halo rats (green) during cable habituation/ITI illumination (left) and cue illumination (right). ITI-cue rats are indicated by open circles, cue-ITI rats by closed circles.

ITI-Cue				
Term	F	p	η_p^2	op
cue	**103.37**	**7.09×10^{-10}**	**0.93**	**1.00**
cue x group	0.55	0.59	0.06	0.13
session	**1.55**	**0.15**	**0.16**	**0.68**
session x group	2.04	0.047	0.2	0.82
cue x session	1.21	0.26	0.13	0.79
cue x session x group	1.18	0.29	0.13	0.78
group	2.51	0.15	0.24	0.29
Cue-ITI				
cue	**29.23**	**2.23×10^{-7}**	**0.69**	**1.00**
cue x group	0.15	0.86	0.01	0.07
session	**3.46**	**0.001**	**0.21**	**0.98**
session x group	0.77	0.65	0.06	0.37
cue x session	1.07	0.39	0.08	0.74
cue x session x group	1.47	0.10	0.10	0.90
group	1.19	0.30	0.08	0.17

Table 3.1 Complete ANOVA results for NAcc illumination and overall fear scaling. ANOVA was performed for suppression ratio over the 10-s cue with factors of group, session and cue for: (top) rats receiving the ITI-Cue illumination order and (bottom) rats receiving the Cue-ITI illumination order. F-statistic, *p*-value, partial eta squared (ηp^2) and observed power (op) are reported for every main effect and interaction. Significant main effects and interactions are bolded.

3.3.6 Rapid fear scaling during light illumination

To examine rapid fear scaling, I divided the 10-s cue into 5, 2-s intervals. Suppression ratios are shown for each cue/interval during habituation/ITI illumination sessions [YFP rats (Figure 3.3A, left) and Halo rats (Figure 3.3B, left)] and for cue illumination sessions [YFP rats (Figure 3.3A, right) and Halo rats (Figure 3.3B, right)]. To examine a possible role for the NAcc in rapid fear scaling, I performed ANOVA with all factors [within factors: session-type (cable habituation, ITI illumination and cue illumination), cue (danger, uncertainty and safety), and interval (5, 2-s cue intervals); between factor: group (YFP vs. Halo)]. The complete ANOVA output is reported in Table 3.2. Consistent with general scaling across groups, ANOVA revealed a main effect of cue ($F_{2,46}$ = 89.04, p=1.53 x 10^{-16}, η_p^2 = 0.80, op = 1.00), as well as a cue x interval interaction ($F_{8,184}$ = 6.14, p=5.16 x 10^{-7}, η_p^2 = 0.21, op = 1.00). Indicative of a selective role for the NAcc in rapid fear scaling, ANOVA revealed a significant 4-way interaction [session-type x cue x interval x group ($F_{16,368}$ = 1.80, p=0.029, η_p^2 = 0.07, op = 0.95)], but not a significant 3-way interaction [session-type x cue x group ($F_{4,92}$ = 1.35, p=0.26, η_p^2 = 0.06, op = 0.41)].

The 4-way interaction indicates that YFP and Halo rats showed differing temporal scaling patterns across the different session types. To begin to clarify the differing patterns, I split YFP and Halo rats and performed identical ANOVAs [within factors: session-type (habituation, ITI illumination and cue illumination), cue (danger, uncertainty and safety), and interval (5, 2-s cue intervals)]. Indicative of reliable scaling, ANOVA for YFP rats found a main effect of cue

($F_{2,22}$ = 47.71, p=1.0 x 10^{-10}, η_p^2 = 0.81, op = 1.00) and a cue x interval interaction ($F_{8,88}$ = 2.76, p=0.009, η_p^2 = 0.20, op = 0.92). Revealing no effect of illumination on the temporal pattern of fear scaling, the 3-way interaction (session-type x cue x interval) was not significant ($F_{16,176}$ = 0.59, p=0.89, η_p^2 = 0.05, op = 0.39). ANOVA for Halo rats also found a main effect of cue ($F_{2,24}$ = 41.39, p=1.66 x 10^{-8}, η_p^2 = 0.78, op = 1.00), and a cue x interval interaction ($F_{8,96}$ = 4.07, p=3.36 x 10^{-4}, η_p^2 = 0.25, op = 0.99). Only now, ANOVA revealed a significant 3-way interaction (session-type x cue x interval; $F_{16,192}$ = 1.92, p=0.021, η_p^2 = 0.14, op = 0.95). NAcc illumination only disrupted the temporal scaling pattern for Halo rats. It appears that, similar to the NAcc lesioned rats in chapter 2, Halo rats receiving NAcc optogenetic inhibition during cue presentation were specifically impaired in rapid uncertainty-safety discrimination (Figure 3.3B, right). If this were the case, then Halo rats should show poorer uncertainty-safety discrimination in the first 2-s cue interval during cue illumination sessions compared to ITI illumination sessions. YFP rats show would equivalent performance during each type of illumination, with no changes between cue illumination and control periods. Further, this deficit should not be observed in the last 2-s cue interval.

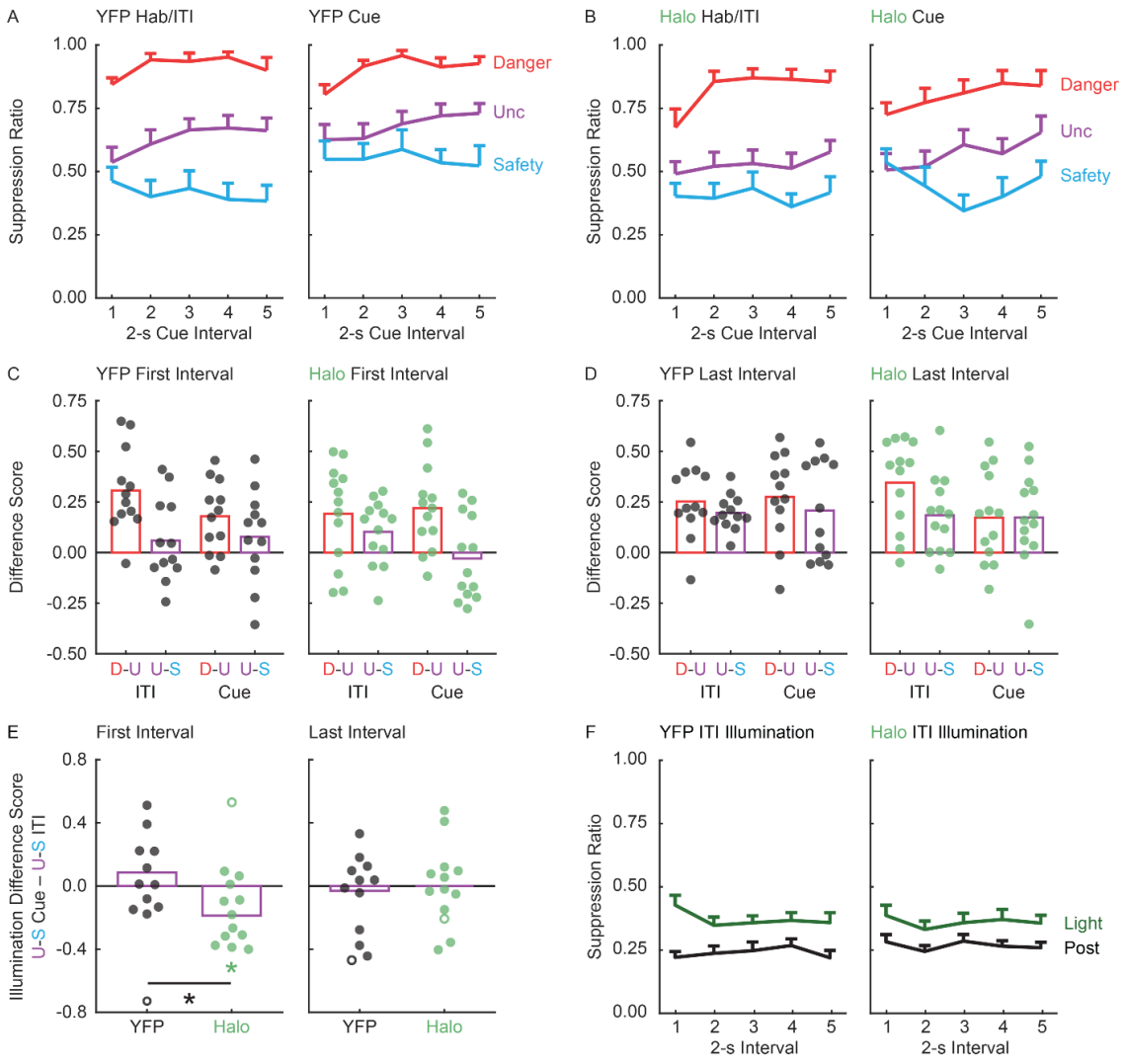

Figure 3.3 NAcc illumination and rapid fear scaling. Mean + SEM suppression ratio is plotted for the 5, 2-s cue intervals for danger (red), uncertainty (purple), and safety (blue), for **(A)** YFP and **(B)** Halo rats during cable habituation/ITI illumination (left), and cue illumination (right). **(C)** Mean difference score for danger vs. uncertainty (D-U, red bar) and uncertainty vs. safety (U-S, purple bar) for the first 2-s cue interval is shown for YFP (left, black circles) and Halo rats (right, black circles). Data points show individual difference scores. **(D)** Difference score data for the last 2-s cue interval shown as in C. **(E)** Difference scores were separately calculated for ITI and cue illumination, then an illumination difference was calculated (cue difference score – ITI difference score). Mean and individual illumination difference scores are plotted for the first 2-s cue interval (left) and last 2-s cue interval (right), for YFP (black) and Halo rats (green). Open circles are outliers. *(green) one-sample t-test compared to zero, p=0.0038. *(black) independent samples t-test, p=0.0041. **(F)** Mean + SEM suppression ratios are plotted for the 5, 2-s intervals during ITI illumination (dark green) and for the 5, 2-s intervals during the post-illumination period (black) (YFP, left; Halo, right).

I calculated (uncertainty – safety) difference scores for the first (Figure 3.3C) and last 2-s cue intervals (Figure 3.3D). Separate scores were calculated for cue and ITI illumination sessions. I then calculated a difference score for the two session-illumination-types (cue difference score – ITI difference score). This approach capitalized on our within-subject design; each rat was tested during cue and ITI illumination. The approach is consistent with our ANOVA results, which found a differential effect of cue and ITI illumination for Halo rats, but not for YFP rats. A difference score of difference scores has the added benefit of reducing the differential illumination effects to a single value. Values around zero would indicate equivalent uncertainty-safety discrimination during cue and ITI illumination sessions. Negative values would indicate worse uncertainty-safety discrimination during cue illumination sessions. Two individuals (1 YFP and 1 Halo) had first interval difference scores ±2 standard deviations beyond the group mean. The data for these individuals is shown (Figure 3.3E, open circles), but were not included in t-test analyses.

In the first 2-s cue interval, Halo rats showed worse uncertainty-safety discrimination during cue illumination sessions compared to ITI illumination sessions (Figure 3.3E, left). This was supported by significant, negative shift of differences scores away from zero (one-sample t-test, $t_{11} = -3.65$, $p=0.004$). YFP rats showed equivalent uncertainty-safety discrimination during cue and ITI illumination sessions; difference scores hovered around zero ($t_{10} = 1.22$, $p=0.25$). Further, YFP and Halo difference scores differed from one another (independent samples t-test, $t_{21} = 3.22$, $p=0.004$). Impaired uncertainty-safety discrimination in

Halo rats receiving cue illumination was restricted to the first 2-s cue interval. Identical analysis of the last 2-s cue interval found that difference scores did not differ from zero for YFP (one-sample t-test, t_{10} = -0.41, p=0.69) and Halo rats (one-sample t-test, t_{11} = 0.27, p=0.80) (Figure 3.3E, right). Difference scores were similar between the two groups (independent samples t-test, t_{21} = 0.48, p=0.64). Altogether, the results reveal that NAcc activity at the time of cue presentation is necessary to rapidly discriminate uncertainty and safety.

Of course, it is possible that NAcc optogenetic inhibition simply suppressed rewarded nose poking. In this case, impaired rapid fear scaling would be the byproduct of a general reduction in poking. To rule out this possibility, I examined nose poke suppression during light illumination in ITI sessions (Figure 3.3F). No cues were present during this period, allowing us to determine the effect of light illumination alone to suppress nose poking. The middle 10 s of the 11-s light illumination was divided into 5, 2-s cue intervals – exactly as was done for the cue illumination analyses. For comparison, I also sampled 10 s of nose poking 30-s following illumination offset. This post-illumination served as a control period to which light illumination could be compared. ANOVA [within factors: period (light and post) and interval (5, 2-s cue intervals); between factor: group (YFP vs. Halo)] revealed main effects of period ($F_{1,23}$ = 34.53, p=5 x 10^{-6}, η_p^2 = 0.60, op = 1.00) and interval ($F_{4,92}$ = 2.49, p=0.049, η_p^2 = 0.10, op = 0.69). Critically, ANOVA found no main effect or interaction with group (Fs < 1.10, ps>0.31). So, while suppression ratios were

higher during light illumination, this did not differ between YFP and Halo rats and was therefore not due to inhibition of NAcc activity.

Term	F	p	η_p^2	op
group	1.94	0.18	0.08	0.27
session-type	**10.64**	**1.59×10^{-4}**	**0.32**	**0.99**
session-type x group	2.22	0.12	0.09	0.43
cue	**89.04**	**1.53×10^{-16}**	**0.80**	**1.00**
cue x group	0.57	0.57	0.02	0.14
interval	**6.00**	**2.46×10^{-4}**	**0.21**	**0.98**
interval x group	1.37	0.25	0.06	0.41
session-type x cue	**4.21**	**0.004**	**0.16**	**0.91**
session-type x cue x group	1.35	0.26	0.06	0.41
session-type x interval	0.71	0.68	0.03	0.32
session-type x interval x group	1.46	0.17	0.06	0.65
cue x interval	**6.14**	**5.16×10^{-7}**	**0.21**	**1.00**
cue x interval x group	0.64	0.74	0.03	0.29
session-type x cue x interval	0.78	0.71	0.03	0.54
session-type x cue x interval x group	**1.80**	**0.029**	**0.07**	**0.95**

Table 3.2 Complete ANOVA results for NAcc illumination and rapid fear scaling. ANOVA was performed for suppression ratio over the 5, 2-s cue intervals with factors of group, session-type, cue and interval. F-statistic, *p*-value, partial eta squared and observed power are reported for every main effect and interaction. Significant main effects and interactions are bolded.

3.4 Discussion

In the current chapter, optogenetic inhibition revealed a role for NAcc cue activity in the expression of rapid, uncertainty-safety discrimination. Light illumination during the cue period impaired rapid uncertainty-safety discrimination in NAcc-halorhodopsin rats, but not NAcc-YFP rats. By contrast, light illumination during the inter-trial interval produced equivalent and modest reductions in nose poking for both groups. Thus, optogenetic inhibition of the NAcc was insufficient to reduce rewarded nose poking.

My experimental design and analysis approach allowed me to examine two possible roles for the NAcc in the expression of adaptive fear scaling. One role in which NAcc cue activity is generally necessary for scaling fear across all cues for the entirety of their duration. Another role in which NAcc cue activity is specifically necessary to rapidly discriminate uncertainty and safety. The results clearly point to a more specific role for NAcc cue activity in the expression of fear scaling.

The current results, taken together with chapter 2, reveal the NAcc is necessary for the acquisition of general fear scaling, and more specifically, the acquisition and expression of rapid uncertainty-safety discrimination at cue onset. NAcc activity is necessary to scale fear to degree of threat. However, these results do not demonstrate that NAcc single units show specific responding to threat cues. Although perhaps unlikely, it is possible that NAcc single units do not specifically respond to threat cues, but rather to the effects of threat cues on reward-seeking. To answer this question, Chapter 4 will focus on recording NAcc single-unit activity while rats undergo fear discrimination.

Chapter 4: Distinct Threat and General Value Signals in the Nucleus Accumbens Core

The work presented in this chapter is currently in preparation:

Ray, M.H., Moaddab, M., and McDannald, M.A. (In Preparation). Distinct threat and valence signals in rodent nucleus accumbens core.

4.1 Introduction

In chapters 2 and 3, I demonstrated that NAcc activity is necessary for the acquisition of general fear scaling across cue presentation, as well as the acquisition and expression of rapid uncertainty-safety discrimination at cue onset. However, the NAcc activity requirement for adaptive fear scaling does not necessitate that NAcc neurons signal relative threat. Why might NAcc single-unit activity differentiate threat and safety? Evidence for the NAcc signaling relative value can be found extensively in reward settings. For example, Setlow et al. recorded NAcc single-unit activity while rats discriminated odors predicting either a rewarding (sucrose) or aversive (quinine) liquid. NAcc single units showed robust discriminative firing of rewarding versus aversive odors (Setlow et al., 2003). Roitman et al. also recorded NAcc single-unit activity and found that accumbens neurons not only discriminated between cues signaling rewarding (sucrose) and aversive (quinine) liquid but did so in opposing manners. NAcc neurons tended to show inhibitory responses to sucrose and excitatory responses to quinine (Roitman et al., 2005).

This evidence for NAcc signaling of relative value in reward settings combined with our previous research showing NAcc activity is necessary to adaptively respond to relative threat value suggests that NAcc activity may show differential firing to threatening versus safe cues. However, it's important to note that aversion and threat are likely processed differently. Aversive stimuli like quinine fall within taste/reward systems while foot shock, and cues predicting foot shock, produce species-specific defensive behaviors (Bolles, 1970; Bolles and

Collier, 1976; Bouton and Bolles, 1980). It is not known if or how NAcc neurons show firing changes to shock-predictive cues, much less whether they will show differential firing to uncertain and absolute predictors of shock.

I designed the current experiment to test two hypotheses. First, do NAcc single units show firing changes to threat cues? If so, what specific patterns of threat responding are observed? Looking back at chapters 2 and 3, we know that the NAcc seems to play two separate roles in fear scaling. First, the NAcc is necessary for the acquisition of fear scaling across cue presentation. Second, the NAcc is necessary for the acquisition and expression of rapid discrimination of uncertainty-safety, specifically at cue onset. Based on these findings, I predict that NAcc activity consists of two signals: tonic activity across the duration of cue presentation and phasic activity specific to cue onset. NAcc-lesioned rats were unable to acquire general fear scaling across cue presentation (see chapter 2). Thus, NAcc tonic activity would likely consist of neurons showing changes in firing to threat that is sustained for the duration of cue presentation, supporting the general fear scaling that NAcc-lesioned rats were unable to acquire. The NAcc phasic activity may consist of changes in cue firing specific to cue onset, supporting the rapid fear scaling that requires NAcc activity (see chapters 2 and 3). Given that the impairment in rapid scaling is specific to uncertainty-safety discrimination, it is plausible that phasic neurons show a different pattern of threat firing compared to the tonic population(s), specifically supporting uncertainty-safety discrimination.

It is important to note that a substantive limitation of chapters 2 and 3 was the exclusive use of only male rats. Our laboratory has previously shown only moderate sex differences in our behavioral paradigm (Walker et al., 2018, 2019), and I predict that NAcc threat signaling is conserved across males and females. Thus, I took my behavioral and neural predictions derived from males and tested whether these hypothesized neuron populations exist in females. Observing threat responding in NAcc in female rats consistent with behavioral observations from male rats would support my interpretation that NAcc threat signaling is conserved across sexes.

I recorded NAcc single-unit activity from female rats undergoing fear discrimination consisting of cues predicting unique foot shock probabilities: danger (p = 1.00), uncertainty (p = 0.25), and safety (p = 0.00). Fear discrimination took place over a baseline of reward-seeking. The approach allowed for recording single-unit activity during cue presentation, as well as during reward-seeking (through nose pokes), and reward delivery. This approach is especially powerful because it allows for each event to be analyzed separately, as well as compared.

4.2 Materials and Methods

4.2.1 Animals

A total of 7 adult female Long Evans rats, weighing 215–300 g were obtained from Long Evans breeders maintained in the Boston College Animal Care Facility. The rats were single-housed on a 12 h light/dark cycle (lights on at

6:00 a.m.) with free access to water. Rats were maintained at 85% of their free-feeding body weight with standard laboratory chow (18% Protein Rodent Diet #2018, Harlan Teklad Global Diets, Madison, WI), except during surgery and post-surgery recovery. The Boston College Animal Care and Use Committee approved all protocols and all experiments were carried out in accordance with the NIH guidelines regarding the care and use of rats for experimental procedures.

4.2.2 Electrode assembly

Microelectrodes consisted of a drivable bundle of sixteen 25.4 μm diameter Formvar-Insulated Nichrome wires (761500, A-M Systems, Carlsborg, WA) within a 27-gauge cannula (B000FN3M7K, Amazon Supply) and two 127 μm diameter PFA-coated, annealed strength stainless-steel ground wires (791400, A-M Systems, Carlsborg, WA). All wires were electrically connected to a nano-strip Omnetics connector (A79042-001, Omnetics Connector Corp., Minneapolis, MN) on a custom 24-contact, individually routed and gold immersed circuit board (San Francisco Circuits, San Mateo, CA). Sixteen individual recording wires were soldered to individual channels of an Omnetics connector. The sixteen wire bundle was integrated into a microdrive permitting advancement in ~42 μm increments.

4.2.3 Surgical procedures

Stereotaxic surgery was performed aseptic conditions under isoflurane anesthesia (1-5% in oxygen). Carprofen (5 mg/kg, s.c.) and lactated ringer's solution (10 mL, s.c.) were administered preoperatively. The skull was scoured in a crosshatch pattern with a scalpel blade to increase the efficacy of implant adhesion. Six screws were installed in the skull to further stabilize the connection between the skull, electrode assembly and a protective head cap. A 1.4 mm diameter craniotomy was performed to remove a circular skull section centered on the implant site and the underlying dura was removed to expose the cortex. Nichrome recording wires were freshly cut with surgical scissors to extend ~2.0 mm beyond the cannula. Just before implant, current was delivered to each recording wire in a saline bath, stripping each tip of its formvar insulation. The current was supplied by a 12 V lantern battery and each Omnetics connector contact was stimulated for 2 s using a lead. Machine grease was placed by the cannula and on the microdrive. For implantation dorsal to the NAcc, the electrode assembly was slowly advanced (~100 μm/min) to the following coordinates: +1.44 mm from bregma, -1.40 mm lateral from midline, and -6.00 mm ventral from the cortex. Once in place, stripped ends of both ground wires were wrapped around two screws in order to ground the electrode. The microdrive base and a protective head cap were cemented on top of the skull using orthodontic resin (C 22-05-98, Pearson Dental Supply, Sylmar, CA), and the Omnetics connector was affixed to the head cap.

4.2.4 Behavioral apparatus

All experiments were conducted in two, identical sound-attenuated enclosures that each housed a Pavlovian fear discrimination chamber with aluminum front and back walls retrofitted with clear plastic covers, clear acrylic sides and top, and a stainless steel grid floor. Each grid floor bar was electrically connected to an aversive shock generator (Med Associates, St. Albans, VT) through a grounding device. This permitted the floor to be grounded at all times except during shock delivery. An external food cup and a central nose poke opening, equipped with infrared photocells were present on one wall. Auditory stimuli were presented through two speakers mounted on the ceiling of the enclosure. Behavior chambers were modified to allow for free movement of the electrophysiology cable during behavior; plastic funnels were epoxied to the top of the behavior chambers with the larger end facing down, and the tops of the chambers were cut to the opening of the funnel.

4.2.5 Nose poke acquisition

The experimental procedure started with two days of pre-exposure in the home cage where rats received the pellets (Bio-Serv, Flemington, NJ) used for rewarded nose poking. Rats were then shaped to nose poke for pellet delivery in the behavior chamber using a fixed ratio schedule in which one nose poke yielded one pellet until they reached at least 50 nose pokes. Over the next 5 days, rats were placed on variable interval (VI) schedules in which nose pokes were reinforced on average every 30 s (VI-30, day 1), or 60 s (VI-60, days 2

through 5). For fear discrimination sessions, nose pokes were reinforced on a VI-60 schedule independent of auditory cue or foot shock presentation.

4.2.6 Fear discrimination

Prior to surgery, each rat received eight 54-minutes Pavlovian fear discrimination sessions. Each session consisted of 16 trials, with a mean inter-trial interval of 3.5 min. Auditory cues were 10 s in duration and consisted of repeating motifs of either a broadband beep, click, phaser, or trumpet. Each cue was associated with a unique probability of foot shock (0.5 mA, 0.5 s): danger, p=1.00; uncertainty, p=0.25; and safety, p=0.00. Auditory identity was counterbalanced across rats. For danger and uncertainty shock trials, foot shock was administered 2 s following the termination of the auditory cue. A single session consisted of four danger trials, two uncertainty shock trials, six uncertainty omission trials, and four safety trials. The order of trial type presentation was randomly determined by the behavioral program and differed for each rat, each session. After the eighth discrimination session, rats were given full food and implanted with drivable microelectrode bundles. Following surgical recovery, discrimination resumed with single-unit recording. The microelectrode bundles were advanced in ~42-84 μm steps every other day to record from new units during the following session.

4.2.7 Single-unit data acquisition

During recording sessions, a 1x amplifying headstage connected the Omnetics connector to the commutator via a shielded recording cable (Headstage: 40684-020 & Cable: 91809-017, Plexon Inc., Dallas TX). Analog neural activity was digitized and high-pass filtered via an amplifier to remove low-frequency artifacts and sent to the Omniplex D acquisition system (Plexon Inc., Dallas TX). Behavioral events (cues, shocks, nose pokes) were controlled and recorded by a computer running Med Associates software. Timestamped events from Med Associates were sent to Omniplex D acquisition system via a dedicated interface module (DIG-716B). The result was a single file (.pl2) containing all timestamps for recording and behavior. Single units were sorted offline using principal components analysis and a template-based spike-sorting algorithm (Offline Sorter V3, Plexon Inc., Dallas TX). Timestamped spikes and events (cues, shocks, nose pokes) were extracted and analyzed with statistical routines in Matlab (Natick, MA).

4.2.8 Histology

Rats were deeply anesthetized using isoflurane and final electrode coordinates were marked by passing current from a 6 V battery through 4 of the 16 nichrome electrode wires. Rats were transcardially perfused with 0.9% biological saline and 4% paraformaldehyde in a 0.2 M Potassium Phosphate Buffered solution. Brains were extracted and post-fixed in a 10% neutral-buffered formalin solution for 24 h, stored in 10% sucrose/formalin, frozen at -80°C and

sectioned via sliding microtome. Nissl staining was performed in order to identify NAcc boundaries. Sections were mounted on coated glass slides, Nissl-stained, and coverslipped with Omnimount mounting medium (Fisher Scientific, Waltham, MA), and imaged using a light microscope (Axio Imager Z2, Zeiss, Thornwood, NY). Electrode placements were reconstructed by subtracting the distance driven between recording sessions from the final recording site. All recording sites within the boundaries of NAcc were included in analyses (Paxinos & Watson, 2007).

4.2.9 Statistical analysis

4.2.9.1 95% bootstrap confidence intervals

95% bootstrap confidence intervals were constructed for suppression ratios and differential firing using the bootci function in Matlab. For each bootstrap, a distribution was created by sampling the data 1,000 times with replacement. Studentized confidence intervals were constructed with the final outputs being the mean, lower bound and upper bound of the 95% bootstrap confidence interval. Differential suppression ratios and firing were said to be observed when the 95% confidence interval did not include zero.

4.2.9.2 Calculating suppression ratios

Fear was measured by suppression of rewarded nose poking, calculated as a ratio: [(baseline poke rate - cue poke rate) / (baseline poke rate + cue poke rate)]. The baseline nose poke rate was taken from the 20 s prior to cue onset and the

cue poke rate from the 10 s cue period. Suppression ratios were calculated for each trial using only that trial's baseline. A ratio of '1' indicated high fear, '0' low fear, and gradations between intermediate levels of fear. Suppression ratios were analyzed using ANOVA with cue (danger, uncertainty, and safety) as a factor. F statistic, *p* value, partial eta squared (η_p^2), and observed power (op) are reported for significant main effects and interactions. The distribution of suppression ratios was visualized using the plotSpread function.

4.2.9.3 Identifying cue-responsive neurons

Single units were screened for cue responsiveness by comparing raw firing rate (Hz) during the 10 s baseline period just prior to cue onset to firing rate during the first 1 s and last 5 s of danger, uncertainty, and safety using a paired, two-tailed t-test ($p<0.05$). A neuron was considered cue-responsive if it showed a significant increase or decrease in firing to any cue in either period. Bonferroni correction (0.5/6) was not performed because this criterion was too stringent, resulting in many cue-responsive neurons being omitted from analysis.

4.2.9.4 Firing and waveform characteristics

The following characteristics were determined for each cue-responsive neuron: baseline firing rate and waveform half duration. Baseline firing rate was mean firing rate (Hz) during the 10 s baseline period just prior to cue onset. Waveform half-duration was calculated by [D/2)], in which D was the x-axis distance between the valley of depolarization and the peak of after-

hyperpolarization and smaller values indicate narrower waveforms (Roesch et al., 2007; Wright and McDannald, 2019). To determine if the waveform half-durations were bimodally distributed, I used Hartigan's Dip statistic to compare the maximum difference between the empirical distribution function and unimodal distribution. This statistic was calculated using the HartigansDipSignifTest function in Matlab.

4.2.9.5 K-means clustering

Clustering was performed using the Matlab kmeans function using normalized firing rate to each cue during the onset (first 1 s) and late cue (last 5 s periods) for six total periods. Cluster number was optimized to produce the fewest number of clusters and the smallest mean Euclidean distance of each cluster member from its centroid.

4.2.9.6 Z-score normalization

For each neuron, and each trial type, firing rate (Hz) was calculated in 250 ms bins from 20 s prior to cue onset to 20 s following cue offset, for a total of 200 bins. Mean firing rate over the 200 bins was calculated by averaging all trials for each trial type. Mean differential firing was calculated for each of the 200 bins by subtracting mean baseline firing rate (10 s prior to cue onset), specific to that trial type, from each bin. Mean differential firing was Z-score normalized across all trial types within a single neuron, such that mean firing = 0, and standard deviation in firing = 1. The Z-score normalization was applied to firing across the

entirety of the recording epoch, as opposed to only the baseline period, in case neurons showed little/no baseline activity. As a result, periods of phasic, excitatory and inhibitory firing contributed to normalized mean firing rate (0). For this reason, Z-score normalized baseline activity can differ from zero. Z-score normalized firing was analyzed with ANOVA using cue, and bin as factors. F and *p* values are reported, as well as partial eta squared (η_p^2) and observed power (op). For reward firing, the firing rate (Hz) was calculated in 250 ms bins from 2 s prior to reward delivery to 2 s following reward delivery, for a total of 16 bins. Mean differential firing was calculated for each of the 16 bins by subtracting pre-reward firing rate (mean of 1 s prior to reward delivery).

4.2.9.7 Heat plot and color maps

Heat plots were constructed from normalized firing rate using the imagesc function in Matlab. Perceptually uniform color maps were used to prevent visual distortion of the data (Crameri, 2018).

4.2.9.8 Population and single-unit firing analyses

Population firing was analyzed using ANOVA with cue (danger, uncertainty, and safety) and bin (250 ms bins from 2 s prior to cue onset to cue offset) as factors. Uncertainty trial types were collapsed because they did not differ firing analysis. This was expected, during cue presentation rats did not know the current uncertainty trial type. F statistic, *p* value, partial eta squared (η_p^2) and observed power (op) are reported for main effects and interactions. The

95% bootstrap confidence intervals were reconstructed for normalized firing to each cue (compared to zero), as well as for differential firing (danger vs. uncertainty) and (uncertainty vs. safety), during cue onset (first 1 s cue interval) and late cue (last 5 s cue interval). The distribution of single-unit firing was visualized using a plotSpread function for Matlab.

Population reward firing was analyzed using repeated measures ANOVA with bin (250 ms bins from 2 s prior to reward delivery to 2 s following reward delivery) as factor. The 95% bootstrap confidence intervals were reconstructed for normalized firing to reward during pre (250 ms prior to reward delivery), and post (first 250 ms following reward delivery) (compared to zero), as well as for differential firing (pre vs. post).

4.2.9.9 Single-unit firing correlations

Single-unit, normalized firing rate was determined for the first 2 s interval of cue presentation (onset) for all safety cue presentations (4), the entire 10 s cue presentation for all danger cue presentations (4), and the 2 s surrounding reward delivery. Each neuron's firing relationship for safety onset was compared to danger and safety onset and danger to reward delivery. R^2 and *p* value were calculated for the Pearson's correlation coefficient.

4.2.9.10 Pitman-Morgan testing

To compare variance in normalized firing rates, the Pitman-Morgan test was used for within-cluster comparisons. Pitman-Morgan was used to compare

variability in normalized firing rates within each cluster for each of the three cues. Associated *p* values are reported for each test.

4.2.9.11 Temporal correlations

Mean normalized firing rates were calculated for the 10, 1-s bins of each cue (30 total bins). A 30 x n matrix was created for each cluster, where n equals the number of cluster single units. A correlation matrix was constructed for each cluster, resulting in a R value for each bin comparison. The bin comparisons of greatest interest were those between cues, on the matrix diagonal. That is, comparing danger firing in cue bin 1 to uncertainty firing in cue bin 1, danger firing in bin 2 to uncertainty firing in bin 2, through bin 10. Clusters showing temporally correlated firing between cues will show high R values, while clusters showing no correlated firing will show R values around zero. The positive or negative R value signifies the direction of the correlations, positive or negative. Between cluster differences in temporal correlations were determined using independent samples t-tests for R values.

4.3 Summary of Experiments and Results

4.3.1 Summary

Female, Long Evans rats (n = 7) were moderately food-deprived and trained to nose poke in a central port to receive a food reward. Nose poking was reinforced throughout fear discrimination, but poke-reward contingencies were independent of cue-shock contingencies. During fear discrimination (Figure 4.1A,

B), three auditory cues predicted unique foot shock probabilities: danger (p=1.00), uncertainty (p=0.25), and safety (p=0.00). After eight discrimination sessions, rats were implanted with drivable, 16-wire microelectrode bundles dorsal to the NAcc. Following recovery, single-unit activity was recorded while rats underwent fear discrimination. At the conclusion of recording, rats were perfused, brains sectioned, and electrode placement confirmed with Nissl staining (Figure 4.1C). Only placements within the NAcc, defined by a tear-shaped region surrounding the anterior commissure, were accepted (Figure 4.1D).

Rats showed complete discrimination during the 82 sessions in which cue-responsive neurons were recorded (Figure 4.1E). Suppression ratios were high to danger, intermediate to uncertainty, and low to safety. ANOVA for mean individual suppression ratio to each cue revealed a main effect of cue ($F_{2,26}$ = 75.34, p=1.52 x 10^{-11}, η_p^2 = 0.85, op = 1.00). Suppression ratios differed for each cue pair. The 95% bootstrap confidence interval for differential suppression ratio did not contain zero for danger vs. uncertainty (mean = 0.21, 95% CI [(lower bound) 0.16, (upper bound) 0.29]), uncertainty vs. safety (M = 0.47, 95% CI [0.35, 1.03]), and danger vs. safety (M = 0.69, 95% CI [0.50, 1.25]). Observing complete fear discrimination permits a meaningful examination of threat-related NAcc firing.

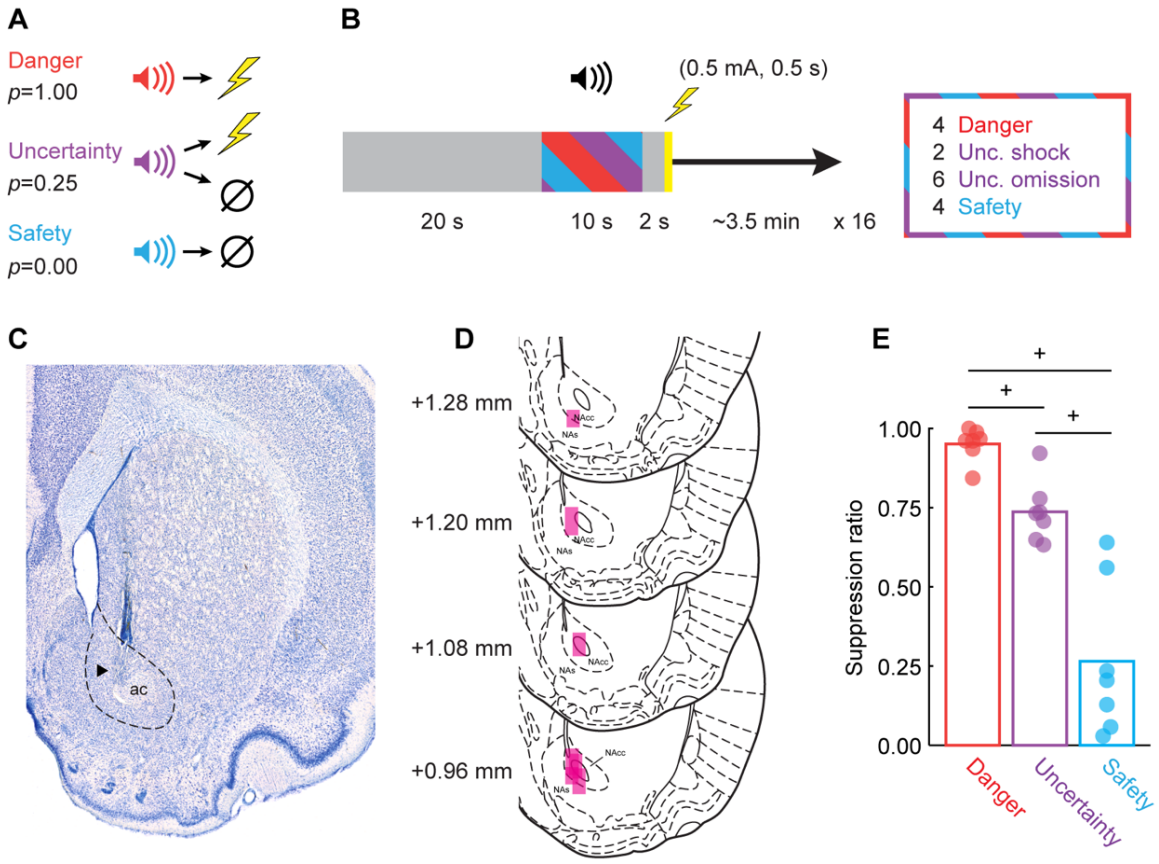

Figure 4.1 Fear discrimination, histology and behavior. (A) Pavlovian fear discrimination consisted of three auditory cues, each associated with a unique probability of foot shock: danger (p=1.00, red), uncertainty (p=0.25, purple) and safety (p=0.00, blue). **(B)** Each trial started with a 20 s baseline period followed by 10 s cue period. Foot shock (0.5 mA, 0.5 s) was administered 2 s following the cue offset in shock and uncertainty shock trials. Each session consisted of 16 trials: four danger trials, two uncertainty shock trials, six uncertainty omission trials and four safety trials with an average inter-trial interval (ITI) of 3.5 min. **(C)** Example of a Nissl stained NAcc (outlined in black) section showing the location of the recording site within the boundaries of the NAcc. **(D)** Histological reconstruction of microelectrode bundle placements (n = 7) in the NAcc are represented by pink bars, bregma levels indicated. **(E)** Mean (bar) and individual subject (data points; n = 7) suppression ratio for each cue (Danger, red; Uncertainty, purple; Safety, blue) is shown. $^{+}$95% bootstrap confidence interval for differential suppression ratio does not contain zero.

A total of 368 NAcc neurons were recorded from 7 rats over 95 fear discrimination sessions. To identify cue-responsive neurons in an unbiased manner, I compared mean baseline firing rate (Hz) to mean firing rate during the first 1 s and last 5 s of cue presentation. A neuron was considered cue-responsive if it showed a significant change (increase or decrease) in firing from baseline to danger, uncertainty, or safety during either the first 1 s or the last 5 s interval (paired, two-tailed t-test, $p<0.05$). This screen identified 193 cue-responsive neurons (~53% of all recorded neurons) from 82 sessions, with at least seven cue-responsive neurons identified in each rat (Figure 4.2). All remaining analyses focus on cue-responsive NAcc neurons (n = 193) and the fear discrimination sessions (n = 82) in which they were recorded.

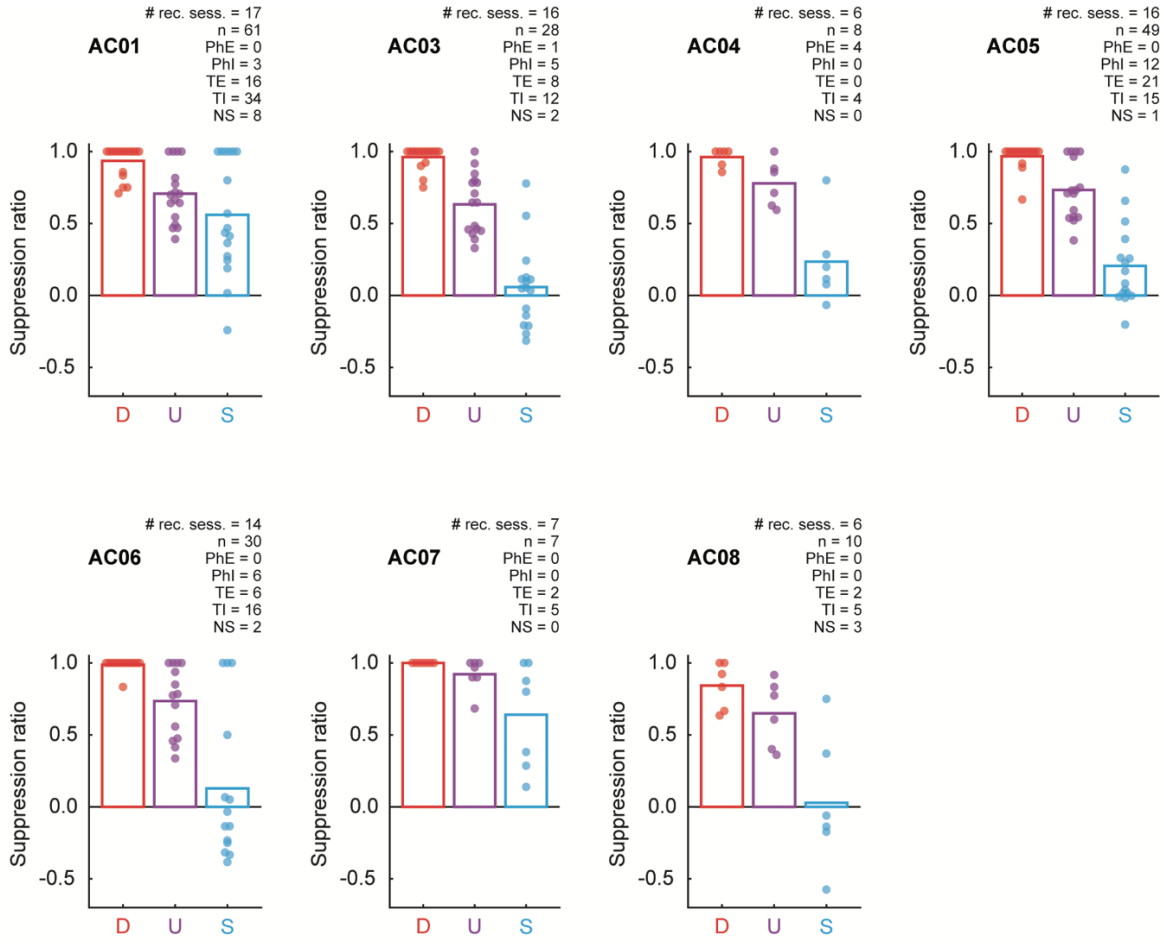

Figure 4.2. Fear discrimination levels of all individuals. Mean (bar) and individual session (data points) suppression ratio for each cue (D, danger, red; U, uncertainty, purple; S, safety, blue) is shown for each individual for all recording sessions with cue-responsive neurons. Animal identity is shown in the top left. For each individual, the number of recording sessions with cue-responsive neurons, the number of cue-responsive neurons, and the number of neurons in each population (PhE, Phasic Excited; PhI, Phasic Inhibited; TE, Tonic Excited; TI, Tonic Inhibited; NS, Non-Selective) are provided.

4.3.2 NAcc neurons show heterogeneous cue responding

The firing pattern of cue-responsive NAcc neurons varied considerably, as did the direction and magnitude of their response. Heterogeneity of firing indicated that NAcc neurons could be divided into discrete, functional populations. To identify these populations, I summarized firing in a 193 single

unit x 6 epoch matrix. The six epochs were taken from the first 1 s and last 5 s for each cue. I applied k-means clustering to the matrix and found that five clusters grouped similar functional types.

To visualize firing patterns, I organized cue-responsive NAcc neurons by cluster and plotted mean single-unit danger, uncertainty, safety, and reward firing (Figure 4.3A). Neurons from two of the clusters showed strong phasic firing to danger and uncertainty, and lesser firing to safety. Phasic Excited neurons demonstrated this pattern through firing increases (PhE, n = 5; Figure 4.3A, Row 1), and Phasic Inhibited neurons through firing decreases (PhI, n = 26; Figure 4.3A, Row 2). Neurons from another two clusters showed modest tonic firing to danger, but lesser and similar firing to uncertainty and safety. Tonic Excited neurons demonstrated this pattern through firing increases (TE, n = 55; Figure 4.3A, Row 3), and Tonic Inhibited neurons through firing decreases (TI, n = 91; Figure 4.3A, Row 4). The final population showed firing increases that did not differentiate the cues (NS, n = 16; Figure 4.3A, Row 5). This was confirmed by ANOVA for normalized firing rate [factors: cue (danger, uncertainty, and safety) and interval (250 ms bins from 2 s prior to cue onset to cue offset)] which found neither a main effect of cue ($F_{2,55} = 2.60$, p=0.091, $\eta_p^2 = 0.15$, op = 0.48) nor a cue x interval interaction ($F_{110,1650} = 1.81$, p=0.098, $\eta_p^2 = 0.07$, op = 1.00).

NAcc waveform width has been tied to neuron type identity. Narrow waveforms are most common in fast-spiking interneurons (FSIs) and wide waveforms are most common in medium spiny neurons (MSNs) (Berke, 2008; Sosa et al., 2020). Phasic inhibited neurons showed wider waveforms, indicative

of MSNs but waveform half duration was distributed bimodally (Hartigan's Dip Statistic $p = 0.036$; Figure 4.3B). Tonic Excited neurons had narrower waveforms, typical of FSIs and waveform half duration and was not distributed bimodally (Hartigan's Dip Statistic $p = 0.17$; Figure 4.3C). Tonic Inhibited neurons showed the greatest mix of narrow and wide waveforms with a bimodal distribution (Hartigan's Dip Statistic, test could not provide specific *p*-values, instead returned 0.00; Figure 4.3D). I return to these observations in the discussion.

Few neurons showed phasic firing increases upon cue presentation (n = 5). Closer inspection revealed that 4 of these units came from one individual. Thus, I am not confident that these neurons are representative of the NAcc. By contrast, Phasic Inhibited units were obtained from 4 of 7 subjects, Tonic Inhibited from all 7 subjects and Tonic Excited units from 6 of 7 subjects. The remaining analyses focused on NAcc-representative populations showing differential cue firing: Phasic Inhibited, Tonic Inhibited, and Tonic Excited neurons.

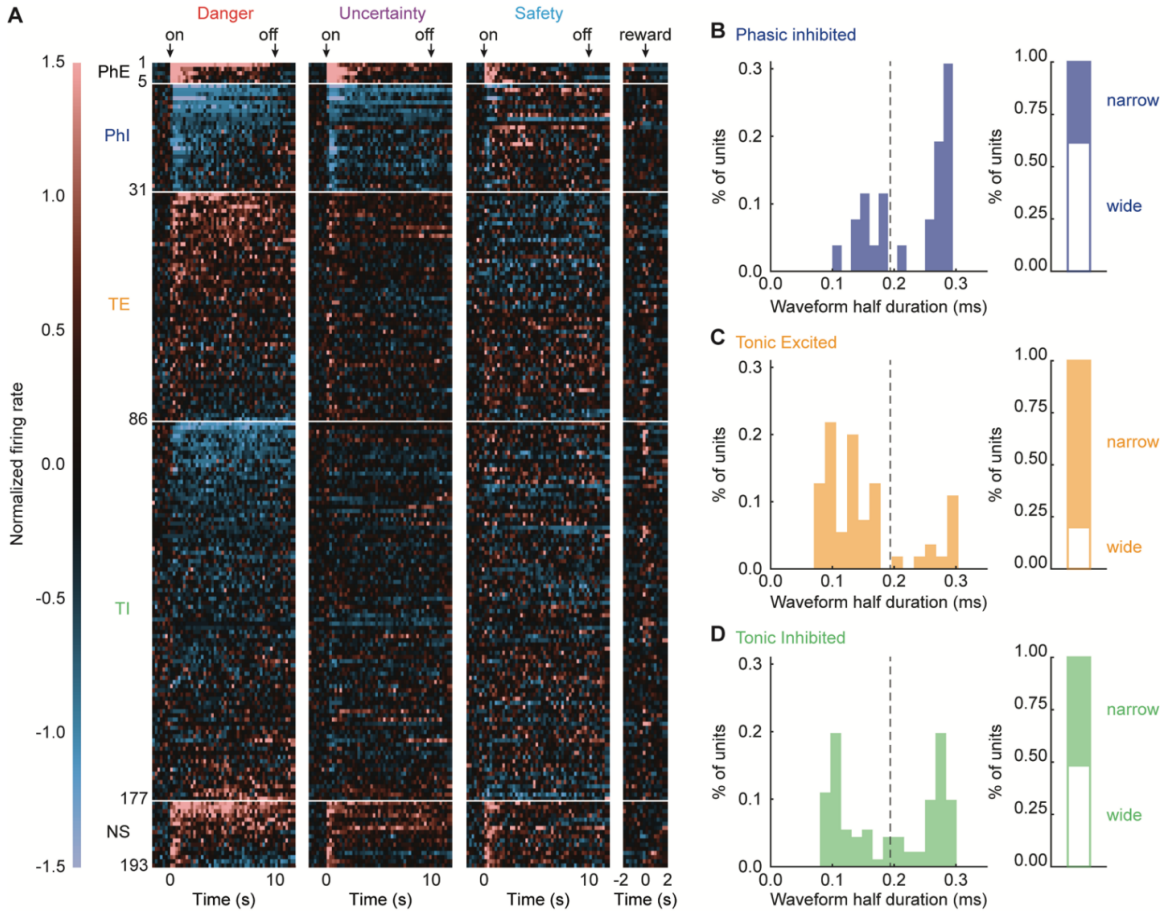

Figure 4.3 Heat plot of cue-responsive neurons. (A) Mean normalized firing rate for each cue-responsive neuron (n = 193) for each of the three trial types danger, uncertainty, and safety (2 s prior to cue onset to cue offset, in 250 ms bins), as well as reward (2 s prior to 2 s following reward delivery). Cue onset (On), offset (Off), and reward are indicated by black arrows. All cue-responsive neurons are sorted by their cue-responsiveness (Phasic Excited, PhE, n = 5; Phasic Inhibited, PhI, n = 26; Tonic Excited, TE, n = 55; Tonic Inhibited, TI, n = 91; Non-Specific, NS, n = 16). Color scale for normalized firing rate is shown to the left. A normalized firing rate of zero is indicated by the color black, with greatest increases light red and greatest decreases light blue. Single unit waveform half duration (ms) is shown for Phasic Inhibited **(B, blue),** Tonic Excited **(C, yellow),** and Tonic Inhibited **(D, green)** neurons (left). The dotted line depicts the boundary between narrow and wide waveforms (left). The percentage of units showing narrow (solid) vs. wide (open) waveforms for each cluster is shown (right).

4.3.3 Phasic Inhibited NAcc neurons are threat-responsive

I have previously shown that NAcc activity during cue presentation is necessary to rapidly discriminate uncertain threat and safety (Ray et al., 2020). I was curious whether phasic NAcc firing rapidly discriminated threat from safety. To determine this, I first performed ANOVA for normalized firing rate by Phasic Inhibited neurons (n = 26) [factors: cue (danger, uncertainty, and safety) and interval (250 ms bins from 2 s prior to cue onset to cue offset)]. Confirming phasic and differential firing, ANOVA revealed a main effect of cue ($F_{2,50}$ = 28.61, p=5.21 x 10^{-9}, η_p^2 = 0.53, op = 1.00), interval ($F_{55,1375}$ = 11.17, p=2.12 x 10^{-76}, η_p^2 = 0.31, op = 1.00), and a significant cue x interval interaction ($F_{110,2750}$ = 5.16, p=1.60 x 10^{-55}, η_p^2 = 0.17, op = 1.00). Population activity suggests equivalent firing decreases to danger and uncertainty that surpassed those to safety (Figure 4.4A). In support, Phasic Inhibited neurons showed greater firing to threat cues (danger and uncertainty) compared to safety at onset (M = -0.47, 95% CI [-0.63, -0.32]; Figure 4.4B, left) but now also during late cue (M = -0.44, 95% CI [-0.60, -0.20]; Figure 4.4B, right), albeit with diminished firing magnitudes. Phasic Inhibited neurons rapidly discriminated threat from safety.

4.3.4 Tonic NAcc neurons are predominantly danger-responsive

My previous study also found that pre-training NAcc lesions disrupted fear discrimination across cue presentation (Ray et al., 2020). This was driven in part by reduced fear to danger in NAcc-lesioned rats. Given that Tonic Excited

neurons showed sustained firing over cue presentation (Figure 4.4C) I was curious whether they showed differential cue firing that was more specific to danger. Confirming differential firing for Tonic Excited neurons (n = 55), ANOVA revealed a main effect of cue ($F_{2,106}$ = 11.24, p=3.70 x 10^{-5}, η_p^2 = 0.18, op = 0.99), interval ($F_{55,2915}$ = 6.47, p=1.71 x 10^{-42}, η_p^2 = 0.11, op = 1.00), and a significant cue x interval interaction ($F_{110,5830}$ = 2.01, p=3.27 x 10^{-9}, η_p^2 = 0.04, op = 1.00). Firing was maximal to danger and fully discriminated the three cues at onset (danger vs. uncertainty: M = 0.22, 95% CI [0.11, 0.33]; uncertainty vs. safety (M = 0.21, 95% CI [0.07, 0.33]; Figure 4.4D, left). As cue presentation proceeded, firing increases were selective to danger whereas uncertainty and safety firing were minimal and equivalent. In support, Tonic Excited neurons showed differential firing to danger compared to the mean of uncertainty and safety during late cue presentation (M = 0.17, 95% CI [0.07, 0.27]; Figure 4.4D, right). Tonic Excited neuronal firing initially discriminated all cues before becoming specific to danger.

Tonic Inhibited neurons (n = 91) were the most abundant functional type, accounting for ~47% of cue-responsive NAcc neurons. To reveal if these neurons also showed differential firing that was more specific to danger (Figure 4.4E), I first performed ANOVA. Confirming differential firing, ANOVA revealed a significant main effect of cue ($F_{2,178}$ = 7.37, p=0.01, η_p^2 = 0.08, op = 0.94), interval ($F_{55,4895}$ = 3.70, p=1.91 x 10^{-18}, η_p^2 = 0.04, op = 1.00), and a significant cue x interval interaction ($F_{110,9790}$ = 1.42, p=0.003, η_p^2 = 0.02, op = 1.00). Confirming more selective danger firing, Tonic Inhibited neurons showed danger firing that

exceeded uncertainty and safety at onset (M = -0.10, 95% CI [-0.19, 0.004]; Figure 4.4F, left), as well as late cue (M = -0.09, 95% CI [-0.16, -0.02]; Figure 4.4F, right).

As a population, Tonic Inhibited neurons showed minimal safety firing. However, inspection of the individual units (Figure 4.4F, left) revealed considerable variation in safety onset firing, with some neurons showing large safety firing increases. Supporting this observation, there was greater variability in onset safety firing compared to either danger (Pitman-Morgan test, p=0.0087) or uncertainty (Pitman-Morgan test, p=0.0046). Tonic Inhibited neuronal firing distinguished danger from uncertainty and safety throughout cue presentation, though neurons varied in their safety onset firing.

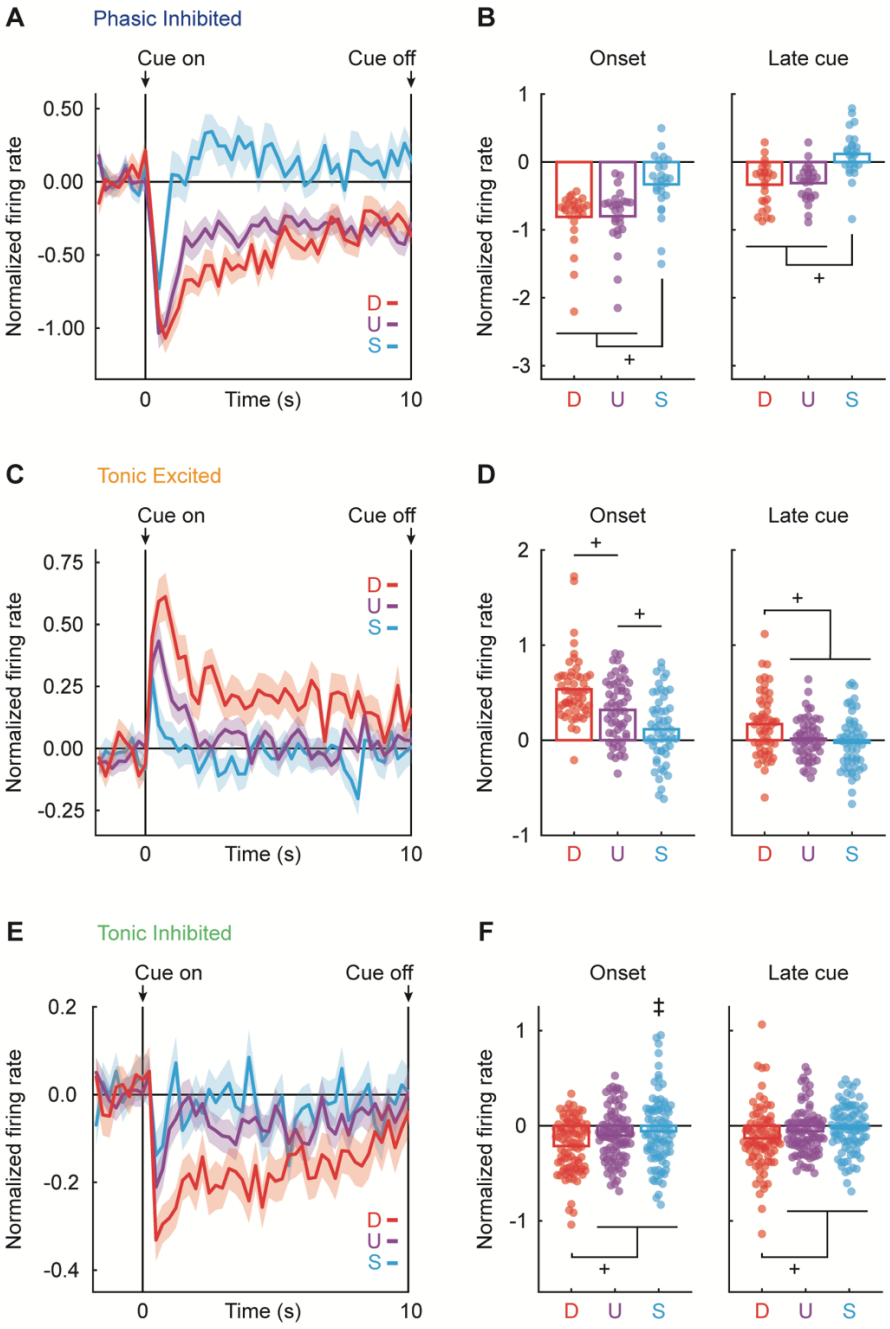

Figure 4.4 NAcc neurons show heterogenous cue responding. (A) Mean normalized firing rate to danger (D, red), uncertainty (U, purple) and safety (S, blue) is shown from 2 s prior to cue onset to cue offset for the Phasic Inhibited neurons (n = 26). Cue onset and offset are indicated by vertical black lines. **(B)** Mean (bar) and individual (data points), normalized firing rate for Phasic Inhibited during the first 1 s cue interval (onset, left), the last 5 s cue interval (late cue, right) are shown for each cue (D, danger, red; U, uncertainty, purple; and S, safety, blue). **(C)** Identical graphs made for **(C, D)** Tonic Excited (n = 55) and **(E, F)** Tonic Inhibited (n = 91) neurons, as in A and B. (+95% bootstrap confidence interval for

differential cue firing does not contain zero; ‡ Pitman-Morgan test for equality of variance, $p<0.05$)

4.3.5 Different temporal firing patterns to danger and uncertainty

Previous analyses reveal that Phasic Inhibited neurons fire similarly to danger and uncertainty, while tonic neurons show dissimilar danger and uncertainty firing. It is possible that despite similar overall levels of activity, Phasic Inhibited neurons showed distinct temporal signatures in their responding to danger and uncertainty over cue presentation. I sought to determine the degree to which the temporal firing pattern for danger predicted the temporal firing pattern for uncertainty and safety, and to determine if stronger temporal relationships between danger and uncertainty were observed in Phasic Inhibited neurons. To do this I divided mean normalized firing for each cue into 10, 1-s intervals. I constructed a correlation matrix for the neurons of each cluster, comparing normalized firing rate for each bin and cue. Of greatest interest were the matrix quadrants comparing danger to uncertainty (Figure 4.5, red top left box) and safety (Figure 4.5, red bottom left box). Cue pairs showing identical, temporal firing patterns would be positively correlated in corresponding 1-s bins (Figure 4.5A), opposing temporal firing patterns would be negatively correlated in corresponding 1-s bins (Figure 4.5B), and independent temporal firing patterns would show zero correlation (Figure 4.5C).

Phasic inhibited neurons showed more consistent temporal firing correlations. The temporal firing pattern for danger positively predicted the temporal firing pattern for uncertainty (Figure 4.5D, red top left box), and this

positive correlation was less apparent for danger and safety (Figure 4.5D, red bottom left box). By contrast, minimal temporal firing correlations were observed for danger and uncertainty for Tonic Excited (Figure 4.5E, red top left) and Tonic Inhibited neurons (Figure 4.5F, red top left). Further, Tonic Excited neurons showed a negative correlation between danger and safety temporal firing patterns (Figure 4.5E, red bottom left), while Tonic Inhibited neurons showed zero correlation (Figure 4.5F, red bottom left).

Revealing stronger temporal firing relationships between danger and uncertainty. Phasic Inhibited neurons showed higher danger-uncertainty correlation coefficients than Tonic Excited (t_{18} = 4.05, p=0.001) and Tonic Inhibited neurons (t_{18} = 4.48, p=0.0003; Figure 4.5G). Owing to negative R values for danger-safety correlations, Phasic Inhibited and Tonic Excited neurons showed differing danger-safety correlation coefficients (t_{18} = 4.59, p=0.0002; Figure 4.5H). The results revealed greater temporal firing relationships between danger and uncertainty for Phasic Inhibited neurons compared to Tonic Excited and Tonic Inhibited neurons.

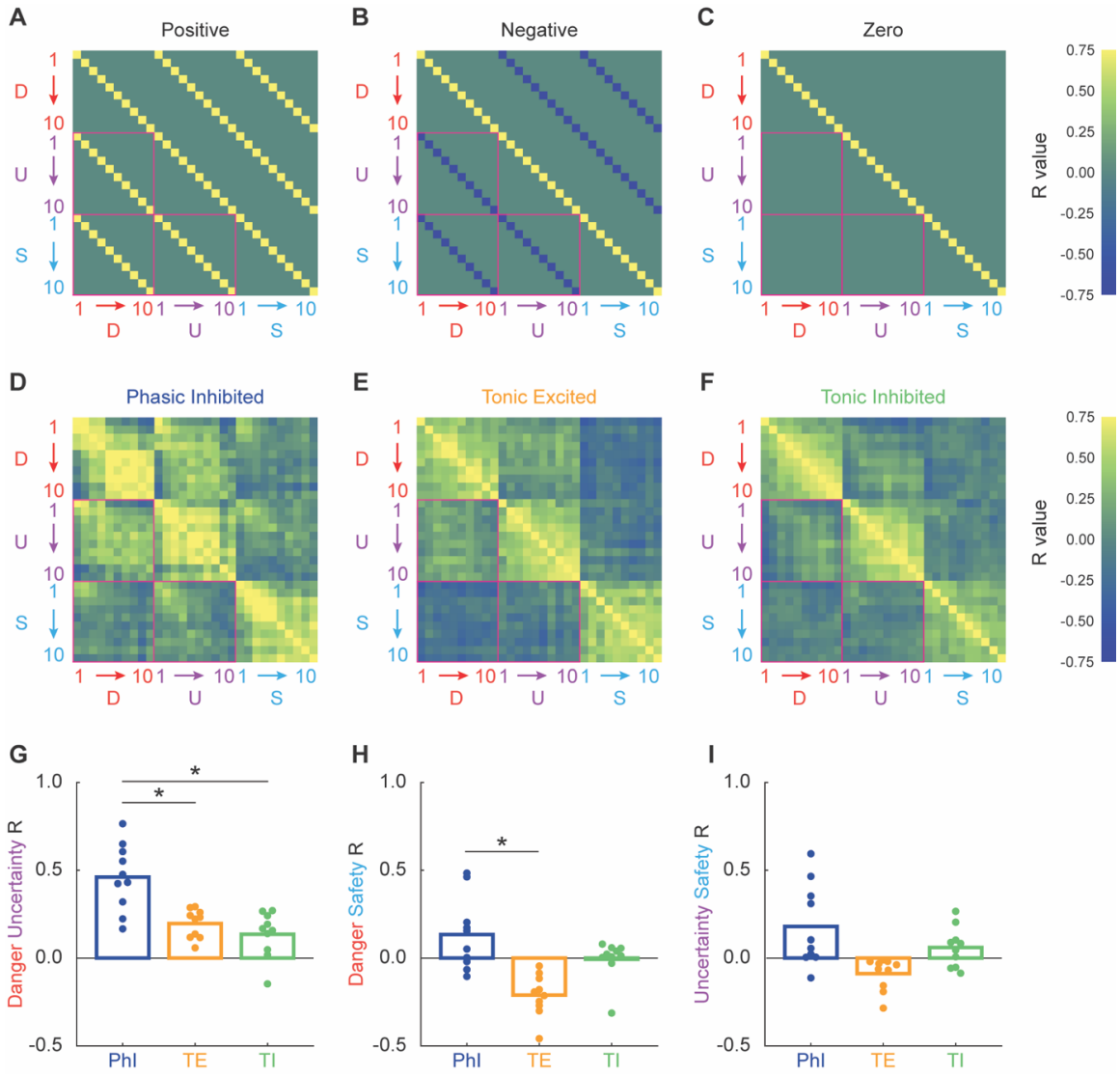

Figure 4.5 Different temporal firing patterns. Correlation matrices were constructed to compare normalized firing rate for each bin (1-10) and cue (D, danger, red; U, uncertainty, purple; S, safety, blue). **(A)** Cue pairs showing identical, temporal firing patterns would be positively correlated, **(B)** opposing temporal firing patterns would be negatively correlated, and **(C)** independent temporal firing patterns would show zero correlation. Correlation matrices were constructed for **(D)** Phasic inhibited, **(E)**Tonic Excited, and **(F)** Tonic Inhibited neurons Mean (bar) and individual (data points) correlation coefficients (R) are shown for each cluster (PhI, Phasic Inhibited, dark blue; TE, Tonic Excited, orange; TI, Tonic Inhibited, green) for **(G)** Danger-Uncertainty, **(H)** Danger-Safety, and **(I)** Uncertainty-Safety. * t-test, $p<0.05$.

4.3.6 Distinct NAcc signals for valence and threat

The goal of the current experiment was to examine NAcc threat-related firing. Of course, the NAcc is best known for its role in reward-related behavior. While our procedure was optimized to assess threat, the use of conditioned suppression permitted us to record activity around reward presentation. To examine if our threat-defined populations showed reward-related responses, I aligned firing of our three main clusters (Phasic Inhibited, Tonic Excited, and Tonic Inhibited) to pellet feeder advance (Figure 4.6A). I performed ANOVA for normalized firing rate [factors: cluster (Tonic Inhibited, Tonic Excited and Phasic Inhibited) and interval (16, 250 ms bins: 2 s prior to and 2 s following pellet feeder advance)]. ANOVA revealed a main effect of interval ($F_{15,2430} = 3.83$, $p=8.49 \times 10^{-7}$, $\eta_p^2 = 0.02$, op = 1.00), but more critically, a cluster x interval interaction ($F_{30,2430} = 1.72$, $p=0.009$, $\eta_p^2 = 0.02$, op = 1.00). The interaction was the result of Tonic Inhibited neurons selectively increasing firing following pellet feeder advance. ANOVA restricted to Tonic Inhibited neurons found a main effect of interval ($F_{15,1290} = 8.78$, $p=1.24 \times 10^{-19}$, $\eta_p^2 = 0.09$, op = 1.00), while separate ANOVA for Tonic Excited and Phasic Inhibited neurons found no main effects of interval ($F < 1.1$, $p>0.4$). Population firing patterns were evident in single units (Figure 4.6B, C, D). Pre and post-reward firing differed neither from zero nor from each other in Tonic Excited and Phasic Inhibited neurons (all 95% CIs contained zero; Figure 4.6B, C). By contrast, Tonic Inhibited neuronal firing around zero prior to reward (M = 0.04, 95% CI [-0.07, 0.13]) gave way to firing increases post

reward (M = 0.47, 95% CI [0.28, 0.62]), and post reward firing exceeding pre reward firing (M = 0.42, 95% CI [0.21, 0.58]; Figure 4.6D).

Reward firing increases by Tonic Inhibited neurons – which sustained firing decreases to danger and showed variable firing increases to safety onset – may indicate more general signaling of valence. If this were the case, positive firing relationships would be observed for safety onset and reward onset (both of which have positive valence); negative firing relationships would be observed for danger and reward (which have opposing valence). Phasic Inhibited neurons (Figure 4.6E) showed a non-significant, negative firing relationship between reward onset firing and safety onset firing (R^2 = 0.07, p=0.18), a significant, negative firing relationship between reward onset firing and danger firing (R^2 = 0.15, p=0.05), and these two correlations did not differ from one another (Z = -0.50, p=0.62). Tonic Excited neurons (Figure 4.6F) showed a non-significant positive firing relationship between reward onset firing and safety onset firing (R^2 = 0.06, p=0.07), a non-significant, negative firing relationship between reward onset firing and danger firing (R^2 = 0.06, p=0.07), but these two correlations differed from one another (Z = -2.10, p=0.035). Tonic Inhibited neurons (Figure 4.6G) showed a significant, positive firing relationship between reward onset firing and safety onset firing (R^2 = 0.08, p=0.006), a significant, negative firing relationship between reward onset firing and danger firing (R^2 = 0.12, p=8.42 x 10^{-4}), and these two correlations significantly differed from one another (Z = -3.96, p=7.70 x 10^{-5}). Finally, if neurons signal valence, opposing firing changes should be observed to safety onset and danger., While zero firing relationship

was observed for Phasic Inhibited neurons (R^2 = 0.06, p=0.24; Figure 4.6H), Tonic Excited (R^2 = 0.25, p=1.17 x 10^{-4}; Figure 4.6I), and Tonic Inhibited (R^2 = 0.06, p=0.015; Figure 4.6J) neurons showed significant positive firing relationships. The results reveal complete valence signaling by Tonic Inhibited neurons, partial valence signaling by Tonic Excited neurons and selective threat signaling by Phasic Inhibited neurons.

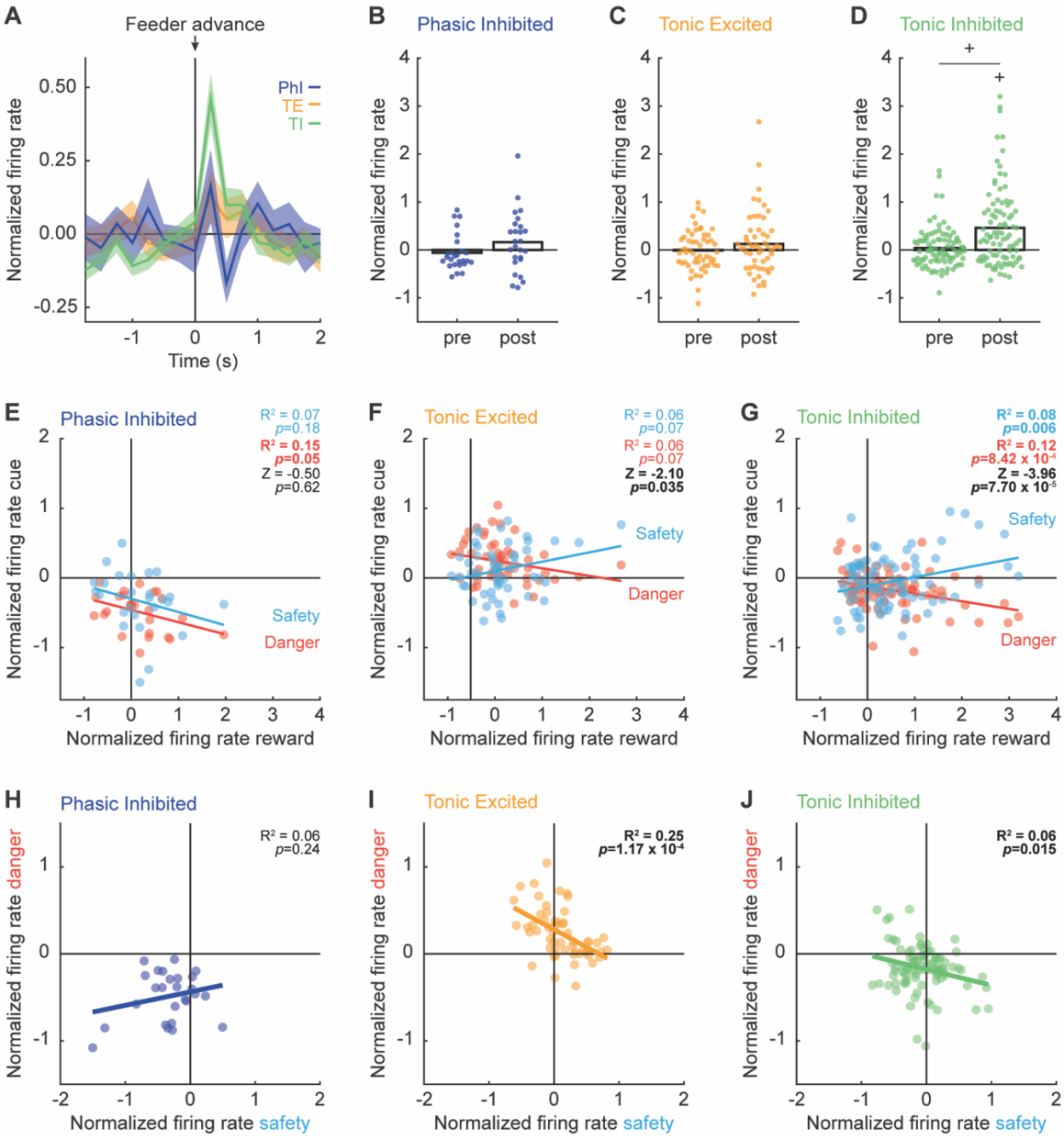

Figure 4.6 Tonic Inhibited neurons show opposing responses to danger and reward. (A) Mean ± SEM normalized firing rate to reward is shown 2 s prior to and 2 s after reward delivery (advancement of feeder) for the Phasic Inhibited (PhI, n = 26, dark blue), Tonic Excited (TE, n = 55, orange), and Tonic Inhibited (TI, n = 91, green) neurons. Reward delivery is indicated by black arrow. SEM is indicated by shading. Mean (bar) and individual (data points), normalized firing rate for **(B)** Phasic Inhibited, **(C)** Tonic Excited, and **(D)** Tonic Inhibited neurons are shown during 500 ms interval prior (pre) to and 500 ms interval after (post) reward delivery. ⁺95% bootstrap confidence interval for differential reward firing does not contain zero. **(E-G)** Mean normalized firing rate to reward vs. cue (danger, red; Safety, blue) is plotted for **(E)** Phasic Inhibited, **(F)** Tonic Excited, and **(G)** Tonic Inhibited neurons. Trendline, the square of the Pearson correlation coefficient (R^2)

and associated *p* value (*p*) are shown. Reward-danger and reward-safety correlations significantly differed for Tonic Excited and Tonic Inhibited, but not Phasic Inhibited neurons. Fisher r-to-z transformation (Z) is shown.

4.4 Discussion

The current experiment used single-unit recording to demonstrate that NAcc neurons respond to threat. Clustering analysis revealed two primary types of NAcc cue-responsive neurons: units showing phasic activity at cue onset and tonic activity across cue presentation. Both phasic and tonic populations consisted of separate populations of inhibitory and excitatory neurons. Interestingly, all NAcc neurons showed responding to threat cues, but specific threat responding differed between populations. Phasic units showed threat-responsive firing (i.e., greatest changes in firing to danger and uncertainty, lesser changes to safety) while tonic units showed danger-responsive firing (i.e., greatest changes in firing to danger, lesser changes to uncertainty and safety).

While the primary objective of the experiment was to examine threat-related activity, the NAcc is primarily known for its role in reward-related behavior. One of the major strengths of our experimental approach is that it allowed not only for the examination of threat-related activity but also reward-related activity and their comparison. Our analyses revealed distinct reward firing patterns for each population. Tonic Inhibited neurons showed a response pattern that suggests bidirectional valence signaling: reward firing increases but danger firing decreases. Danger and reward firing were negatively correlated at the single-unit level. Tonic Inhibited neurons showing greater reward firing increases showed greater danger firing decreases. Even more, Tonic Inhibited neurons

showing stronger phasic, safety firing increases showed greater danger firing decreases. Phasic Inhibited neurons were threat-selective, showing the strongest changes in firing to danger and uncertainty onset and a lesser decrease to safety onset and showed a negative correlation for danger - reward delivery. This finding alone would support valence signaling by Phasic Inhibited neurons, however, there was no relationship between safety-reward firing and danger-reward firing, suggesting that these neurons are instead threat-selective. Tonic Excited neurons exhibited partial valence signaling, showing greatest excitation to danger, lesser excitation to uncertainty and safety, as well as a negative correlation between danger and safety onset. Tonic Excited neurons showed a modest pattern where safety onset and reward delivery were positively related and a negative pattern between danger and reward delivery. Interestingly, though the patterns observed were modest, the difference between these patterns was strong, suggesting that there is a partial valence signal by Tonic Excited neurons. Taken together, the current results reveal complete valence responses by Tonic Inhibited neurons, partial valence responses by Tonic Excited neurons and selective threat responses by Phasic Inhibited neurons.

A strength of this experiment is that it used only female rats while my previous two experiments (see chapters 2 and 3) used only male rats. The decision to switch from males to females allowed for our NAcc findings to better generalize to both sexes. Our laboratory has found only modest sex differences in our paradigm (Walker et al., 2018, 2019), while other cued-fear conditioning studies have found no sex differences (Maren et al., 1994; Markus and Zecevic, 1997;

Maes, 2002; Fenton et al., 2014; Clark et al., 2019), suggesting similar neural circuits may be used across sexes. Additionally, given that the present data demonstrate NAcc activity directly related to our behavioral findings in males, it is likely that NAcc neurons in males and females respond in similar manners during our paradigm. Finally, it is important to look at the field of behavioral neuroscience and acknowledge that the overwhelming majority of behavioral neuroscience research has only used males (Beery and Zucker, 2011; Shansky and Woolley, 2016) while women are more susceptible to many psychiatric illnesses, such as PTSD (Kessler et al., 1996; Breslau et al., 1999, 2004) and experience greater symptom severity (Kessler et al., 1996; Breslau et al., 2004; Tolin and Foa, 2006). The importance of utilizing females in research is critical (Shansky and Woolley, 2016).

A second limitation of the present study is the inability to conclusively link function to genetic cell type. Although the present experiment does not include a method to conclusively identify specific cell types, differences in waveform width (Roesch et al., 2007; Wright and McDannald, 2019) may give us clues. Fast-spiking interneurons have narrower waveforms (Kawaguchi, 1993) and can fire at substantially higher baseline rates while medium-spiny neurons have wider waveforms and lower baseline firing rates (Plenz and Kitai, 1998; Berke, 2011). Phasic Inhibited neurons are likely MSN projection neurons based on their wide waveform. Tonic Excited neurons are likely fast-spiking interneurons based on their narrow waveform whereas Tonic Inhibited, which showed greater variation in waveform half duration, are likely a mix of medium-spiny neurons and fast-

spiking interneurons (Berke et al., 2004; Gage et al., 2010; Lansink et al., 2010; Ahmad et al., 2017). The waveform duration data suggest that Phasic and Tonic Inhibited neurons broadcast threat information to regions outside the NAcc. There are two main types of NAcc MSNs, dopamine receptor 1 (D1) and dopamine receptor 2 (D2). The canonical view of D1 vs D2 MSNs is that D1-MSNs encode positive valence and reward while D2-MSNs encode negative valence and aversive responses (Hikida et al., 2010; Lobo et al., 2010; Kravitz et al., 2012; Tai et al., 2012). However, more recent studies have shown that both D1 and D2 MSNs bidirectionally control reward and aversion (Soares-Cunha et al., 2016, 2018, 2020; Vicente et al., 2016; Natsubori et al., 2017), making it difficult to functionally distinguish these subtypes.

The current study demonstrates that NAcc neurons are threat responsive and exhibit heterogeneity in the timing and specific nature of threat firing. Taken together with chapters 2 and 3, this suggests the NAcc is not just necessary for fear scaling but also processes threat cues on both a rapid and enduring timescale.

Chapter 5: Discussion

5.1 Summary of Findings

The main objective of the current dissertation was to answer the following research questions:

1. Is the NAcc is necessary for the acquisition of both rapid and general fear scaling?
2. Is the NAcc is necessary for the expression of rapid fear scaling?
3. Do NAcc single units show firing changes to threat cues? If so, what specific patterns of threat responding are observed?

Chapter 2 tested the first hypothesis by permanently ablating NAcc neurons in male rats via neurotoxic lesion to determine whether the NAcc is necessary for the acquisition of rapid and general fear scaling. Following recovery from surgery, rats underwent a fear discrimination paradigm consisting of three auditory cues predicting unique foot shock probabilities: danger (p=1.00), uncertainty (p=0.25), and safety (p=0.00). NAcc lesions slowed the progression of baseline nose poking, with sham rats showing greater increases in nose poking across the sixteen sessions. When looking at overall fear scaling, sham rats acquired appropriate scaling of fear showing high fear to danger, intermediate fear to uncertainty, and low fear to safety. NAcc-lesioned rats showed impaired acquisition of fear scaling, showing decreased discrimination between cue pairs compared to sham rats. When looking at rapid fear discrimination at cue onset, sham rats showed fear scaling in the first 2-s interval, while scaling was reduced in NAcc-lesioned rats. Specifically, NAcc-lesioned rats were impaired in rapid uncertainty-safety discrimination. These results

demonstrate that the NAcc is necessary for the acquisition of general fear scaling as well as rapid uncertainty-safety discrimination.

Based on the findings in Chapter 2, Chapter 3 tested the second hypothesis that the NAcc is necessary for the expression of rapid fear scaling. To inhibit NAcc activity during post-acquisition expression, the NAcc was reversibly inhibited using optogenetics. Rats were NAcc-transducted with an inhibitory opsin, halorhodopsin, or a control fluorophore, and bilaterally implanted with ferrules above the NAcc. Following recovery, rats received ten sessions of fear discrimination to danger, uncertainty, and safety. Next, rats received eight sessions in which the NAcc was green-light illuminated during cue presentation or a control period, optogenetically inhibiting activity in halorhodopsin rats. This within-subjects design controlled for general effects of illumination by allowing for behavioral comparisons of cue and control illumination periods in the same rat. Light illumination during the cue period impaired rapid uncertainty-safety discrimination in NAcc-halorhodopsin rats, but not NAcc-YFP rats. By contrast, light illumination during a control period produced equivalent and modest reductions in nose poking for both groups. Thus, optogenetic inhibition of the NAcc was insufficient to reduce rewarded nose poking.

The failure of NAcc inhibition to suppress nose poking may seem odd. Mice will readily perform actions that channelrhodopsin-excite D1 and D2 cell types (Cole et al., 2018), and rats will perform actions that channelrhodopsin-excite NAcc glutamatergic inputs (Stuber et al., 2011; Britt et al., 2012). However, these studies demonstrate that NAcc activity is sufficient, but not necessary, to

support reward-seeking. Prominent theories posit that reward-seeking initially depends on medial striatal structures, such as the NAcc. With further training, lateral striatal regions (e.g., dorsolateral striatum) control reward-seeking (Gerdeman et al., 2003; Belin and Everitt, 2008; Corbit et al., 2012; Burton et al., 2015). In this experiment, rats had extensive experience with nose poking by the time the NAcc was inhibited. By this time, reward-seeking may not have been under NAcc control, yet the NAcc continued to contribute to rapid fear scaling. In another intriguing reward tie-in, dopamine bursts, “blips” onto D1-NAcc neurons promote cue-reward generalization while dopamine pauses, “dips”, onto D2-NAcc neurons promote cue-reward discrimination (Iino et al., 2020). Receptor and cell type specific dopamine shaping of NAcc threat responding would be an appealing future research direction and is perhaps likely to occur (Badrinarayan et al., 2012; Jo et al., 2018). The current results demonstrate that NAcc activity is necessary for the expression of rapid uncertainty-safety discrimination. Chapters 2 and 3 together, demonstrate that NAcc activity is necessary for the acquisition of general fear scaling across cue presentation, as well as the acquisition and expression of rapid uncertainty-safety discrimination at cue onset.

Chapter 4 tested the final hypotheses: first, do NAcc single units show firing changes to threat cues and second, what specific patterns of threat responding are observed? To test these hypotheses, I used *in vivo* electrophysiology to record NAcc single-unit activity from female rats undergoing fear discrimination to danger, uncertainty, and safety. Fear discrimination took place over a baseline of reward-seeking, allowing for the recording single-unit

activity during cue presentation, as well as during reward-seeking and reward delivery. This design enabled each event to be analyzed separately, as well as compared. Clustering analyses revealed two primary types of NAcc cue-responsive neurons: units showing phasic activity at cue onset and tonic activity across cue presentation. Both phasic and tonic populations consisted of separate populations of inhibitory and excitatory neurons. Interestingly, all NAcc neurons showed responding to threat cues, but specific threat responding differed between populations. Phasic units showed threat-responsive firing (i.e., greatest changes in firing to danger and uncertainty, lesser changes to safety) while tonic units showed danger-responsive firing (i.e., greatest changes in firing to danger, lesser changes to uncertainty and safety). The current finding of NAcc threat-responsive units extends NAcc threat function beyond IEG upregulation (Beck and Fibiger, 1995; Campeau et al., 1997; Thomas et al., 2002) by demonstrating the most robust threat signals in the NAcc are achieved by firing decreases, which only electrophysiology can detect.

Our analyses revealed distinct response patterns for each population. Tonic Inhibited neurons showed a response pattern that suggests bidirectional valence signaling. This is supported by strong inhibition to danger throughout cue presentation and excitation to reward as well as negative correlations for both danger - safety onset and danger - reward delivery, as well as a positive correlation for safety onset - reward delivery. Phasic Inhibited neurons were threat-selective showing the strongest increases in firing to danger and uncertainty onset and a lesser increase to safety onset and showed a negative

correlation for danger - reward delivery. Tonic Excited neurons exhibited partial valence signaling showing greatest excitation to danger, lesser excitation to uncertainty and safety, as well as a negative correlation between danger and safety onset. Tonic Excited neurons showed trends for a positive correlation between safety onset and reward delivery and a negative correlation between danger and reward delivery. Taken together, the current results reveal complete valence responses by Tonic Inhibited neurons, partial valence responses by Tonic Excited neurons and selective threat responses by Phasic Inhibited neurons. This demonstrates that NAcc neurons are threat responsive and exhibit heterogeneity in the timing and specific nature of threat firing. Taken together with the chapters 2 and 3, this suggests the NAcc is not just necessary for fear scaling but also processes threat cues on both a rapid and enduring timescale.

5.2 Additional Research

My dissertation is focused on the NAcc, however, studies examining the BLA-NAcc pathway would likely be fruitful. It has long been demonstrated that the BLA is essential to fear learning and expression and the BLA sends direct projections to the NAcc. The predominant view suggests the BLA-NAcc pathway preferentially routes positive-valence to the NAcc and negative-valence to the CeA (Beyeler et al., 2016). While considerable research supports this, few studies have examined the routing of negative-valence information from the BLA to the NAcc. One such study found that optogenetic stimulation of the BLA-NAcc pathway decreases long-term fear (Correia et al., 2016). Consistent with the

overwhelming BLA fear literature, our laboratory has found that BLA lesions diminish fear to all three auditory cues. Additionally, the present data from my NAcc-lesioned rats show the NAcc is necessary for general fear scaling while single-unit data demonstrates NAcc activity is threat-responsive. Taken together, the data suggest the BLA-NAcc circuit is essential for adaptive fear, revising the prevailing view this circuit is exclusive to reward.

To test this hypothesis, I propose the following two studies to 1) determine if NAcc single units receiving direct BLA input are threat-selective and 2) determine if the BLA-NAcc pathway is necessary for adaptive fear. Experiment one would utilize single-unit recordings in the NAcc with opto-tagging inputs from the BLA. This viral/recording approach permits 'photo-tagging' with blue-light to determine whether isolated NAcc units receive direct BLA inputs. I would predict that NAcc neurons that receive direct BLA inputs will be threat-selective, increasing or decreasing activity to threatening cues (danger and uncertainty). The second aim will determine if BLA-NAcc projections are necessary for adaptive fear by inhibiting BLA terminals in the NAcc during ongoing fear discrimination, similar to the approach in chapter 3. I would predict that inhibiting BLA terminals in the NAcc will result in impaired scaling of fear, compressing fear to danger and safety. These experiments would reveal routing of negative valence threat information from the BLA to the NAcc and a necessary role for the BLA-NAcc pathway in adaptive fear.

However, it is possible that the BLA is not routing negative-valence information to the NAcc. Therefore, I would hypothesize that either the mPFC or

vHPC is responsible for routing threat-relevant information to the NAcc. In this case, similar electrophysiology and optogenetic approaches, either isolating the mPFC-NAcc or vHPC-NAcc pathways, would prove useful in elucidating the negative-valence routing to the NAcc.

5.3 Biological Sex

One important strength of our findings is generalization of findings to both sexes. Specifically, I found that NAcc activity in females (chapter 4) is directly related to our behavioral findings in males (chapters 2 and 3), it is likely that NAcc neurons in males and females respond in comparable ways during our paradigm. Multiple cued-fear conditioning studies have found no sex differences (Maren et al., 1994; Markus and Zecevic, 1997; Maes, 2002; Fenton et al., 2014; Clark et al., 2019), and our laboratory has found only modest sex differences (Walker et al., 2018, 2019), suggesting akin neural circuits may be used across sexes. However, it is important to recognize that while women are more vulnerable to anxiety disorders (Kessler et al., 1996; Breslau et al., 1999, 2004) and experience worsened symptom severity (Kessler et al., 1996; Breslau et al., 2004; Tolin and Foa, 2006), the overwhelming majority of behavioral neuroscience research has used only males (Beery and Zucker, 2011; Shansky and Woolley, 2016). Given the prevalence of anxiety disorders in women, it is more critical than ever that our field utilizes females in research (Shansky and Woolley, 2016).

For the current studies, I used conditioned suppression of my measure of fear. Though at first glance this may seem confusing given that freezing is a more popular measure, one major drawback of using freezing is the sex differences found in this measure. Females exhibit lower freezing rates than males (Maren et al., 1994; Gupta et al., 2001; Gruene et al., 2015a) and recent investigations have revealed that females display more active fear responses, known as darting, which is reflected as a reduction in freezing (Gruene et al., 2015a, 2015b; Colom-Lapetina et al., 2019; Greiner et al., 2019). Our lab is currently collecting more data on potential behavioral sex differences using more complex behavioral measures and analyses, such as machine learning.

5.4 Where does the NAcc fit in the context of a larger network-level model of aversive learning?

The present work establishes the NAcc as a necessary component for rapid fear scaling. Critically, I am not saying that the NAcc is the region for fear scaling, but rather one component of a larger neural circuit permitting fear scaling (Figure 5.1).

The NAcc is comprised of GABAergic MSNs and FSIs. NAcc MSNs are characterized by their expression of either D1 or D2 receptors, while few (~5%) of MSNs express both (Bertran-Gonzalez et al., 2008; Perreault et al., 2011; Gangarossa et al., 2013; Gagnon et al., 2017). The prevailing view is that D1 MSNs encode positive valence while D2 MSNs encode negative valence (Hikida et al., 2010; Lobo et al., 2010; Kravitz et al., 2012; Tai et al., 2012), however,

more recent studies have revised this theory, proposing that D1 and D2 MSNs control both positive and negative valence (Soares-Cunha et al., 2016, 2018, 2020; Vicente et al., 2016; Natsubori et al., 2017), making it challenging to theorize on the functionality of these cell types. MSNs and FSIs can be distinguished based on differences in waveform width (Roesch et al., 2007; Wright and McDannald, 2019). FSIs have narrower waveforms (Kawaguchi, 1993) and can fire at substantially higher baseline rates while MSNs have wider waveforms and lower baseline firing rates (Plenz and Kitai, 1998; Berke, 2011). Based on these characteristics, the wide waveforms of Phasic Inhibited neurons suggest they are likely MSN projection neurons whereas, the narrow waveforms of Tonic Excited neurons suggest they are FSIs. While these two populations showed distinct waveform widths, Tonic Inhibited neurons showed the greatest variation, suggesting they are likely a mix of MSNs and FSIs (Berke et al., 2004; Gage et al., 2010; Lansink et al., 2010; Ahmad et al., 2017). The waveform characteristics of each population suggest that while Tonic excited neurons are likely non-projection FSIs, Phasic and Tonic Inhibited neurons likely communicate threat information to regions receiving NAcc innervation.

The NAcc may serve as a valence hub, like that typically ascribed to the amygdala. The greatest evidence for this is found in the Tonic Inhibited neurons. Tonic inhibited neurons responded in a pattern consistent with bidirectional valence signaling. Parts of this pattern are also seen in the Tonic Excited neurons, which demonstrated partial valence signaling. Concurrently, the NAcc more uniquely signals threat, as found in the Phasic Inhibited neurons which

selectively responded to threat. The present electrophysiology data in combination with the lesion and optogenetic inhibition data reveal the NAcc is required for adaptive fear behavior and NAcc activity responds to threat value. Continued work delineating the NAcc's position in the threat network is likely to be fruitful.

Before we discuss where the NAcc might be sending threat-information, it's important to discuss where the NAcc might be receiving threat input from. The BLA is the most likely candidate based on its direct glutamatergic projections and role in forming and maintaining cue-shock associations (LeDoux et al., 1990; Maren et al., 1996; Amorapanth et al., 2000; LeDoux, 2000; Goosens and Maren, 2003; Koo et al., 2004). The BLA is a valence hub and the predominant view is that the BLA preferentially routes information regarding negative valence to the CeA while the NAcc receives information regarding positive valence (Beyeler et al., 2016, 2018). However, that view is based on simplistic behavioral paradigms. Given the present data demonstrating a critical role for the NAcc in adaptive fear, it is plausible that the BLA is also routing negative valence to the NAcc, particularly when the fear learning is more complex, as is the case in our paradigm. If this were the case, I would expect that the NAcc threat responsive neurons would receive direct BLA input.

The NAcc also receives direct innervation from the mPFC, which has close anatomical and functional connections with both the NAcc and amygdala (Krettek and Price, 1978; Kita and Kitai, 1990; Garcia et al., 1999; Gabbott et al., 2005; Li et al., 2018). Manipulating the mPFC impairs cued fear learning (Morgan

et al., 1993; Quirk et al., 2000). The mPFC subregions play dissociable roles in the expression and extinction of fear conditioning: IL activity inhibits fear during extinction while PL activity promotes the expression of conditioned fear (Quirk et al., 2000; Corcoran and Quirk, 2007; Burgos-Robles et al., 2009). Given the NAcc innervation by the PL (Brog et al., 1993) and its role in the expression of conditioned fear, it is plausible that the PL routes threat-related information to the NAcc that is necessary for the expression of fear scaling.

Another region of interest for NAcc input is the vHPC, which is classically associated with the regulation of emotional states, including fear and anxiety (Moser and Moser, 1998; Fanselow and Dong, 2010). Some studies have shown a role for the vHPC in the expression of fear and fear memory (Zhang et al., 2001; Kjelstrup et al., 2002; Hobin et al., 2006; Oh and Han, 2020), while others have shown a role for the vHPC in fear acquisition (Bast et al., 2001; Chen et al., 2016). Though the conflicts in vHPC fear literature are dissatisfying, it is clear that future studies utilizing careful behavior and neural activity manipulation is needed, similar to the design of the NAcc experiments in the current dissertation. One notable vHPC finding is that inactivation of the vHPC impairs acquisition of fear learning (Bast et al., 2001; Chen et al., 2016). Specifically, rats who receive muscimol in the vHPC did not freeze to a danger cue, suggesting an inability to acquire fear learning. Thus, it is possible that the vHPC routes threat signals to the NAcc, informing the NAcc and shaping adaptive threat responses. Looking at these three NAcc threat-input candidate regions: BLA, PL, and vHPC, the BLA is the most likely candidate region, followed by the PL and vHPC, respectively.

The waveform duration data from chapter 4 suggests that Phasic and Tonic Inhibited neurons are medium-spiny projection neurons that are broadcasting threat information to regions outside the NAcc. Phasic inhibited neurons are threat-selective showing strongest changes in firing to danger and uncertainty onset. Meanwhile, Tonic Inhibited activity was indicative of bidirectional valence signaling: reward and safety firing increases but danger firing decreases. These two populations likely support rapid and general fear scaling, respectively. So where are these signals being sent?

A likely candidate for receiving NAcc threat activity is the Ventral Pallidum (VP). Similar to the NAcc, the VP is a region classically known for its role in reward processes. However, our lab's postdoctoral fellow Dr. Mahsa Moaddab has developed a pivotal line of work demonstrating that VP neurons dynamically signal relative threat in our behavioral paradigm. Specifically, neural activity in the VP revealed widespread threat-related firing and relative threat signaling with most neurons being maximally responsive to danger. Additionally, one population of neurons increased activity following reward delivery, signaling relative value that spans threat and reward (Moaddab et al., 2021). Unlike the VP, NAcc neurons do not signal relative threat. Thus, NAcc threat representations may shape or guide VP relative threat signals. Interestingly, the VP projects directly to the BLA (Woolf and Butcher, 1982; Carlsen et al., 1985; Root et al., 2015). This anatomical connection suggests that the NAcc may indirectly route threat information to the BLA, via the VP. This indirect pathway would allow for the

NAcc to send threat-relevant activity to the BLA, shaping the cue-shock associations formed and potentially supporting more accurate fear responses.

New neural recording techniques are being developed at a rapid pace and propelling the field forward. One such technique is the development of high-yield electrophysiology recordings, such as Neuropixels. Neuropixels allows researchers to simultaneously record hundreds of neurons along a DV axis. Our lab has recently begun using Neuropixels to record in midbrain regions. Using Neuropixels to record in the striatum would allow for simultaneous recordings of hundreds of neurons in the NAcc, NAcS, and VP, which standard single-unit recordings cannot account for. Neuropixels recordings would potentially delineate neural interactions between the NAcc, NAcS, and VP during adaptive fear behavior.

I propose the following updated neural circuit for adaptive fear: BLA-NAcc-VP-BLA. Supporting this theory, neuroanatomical studies looking at the glutamatergic inputs to the NAcc demonstrated that, although the NAcc receives glutamatergic input from the BLA, vHPC, and mPFC, only the glutamatergic BLA projections synapse directly onto the NAcc MSNs projecting directly to the VP (Papp et al., 2012). This suggests that the glutamatergic inputs from the BLA, and not the vHPC or mPFC, are responsible for the direct flow of information from the NAcc to VP. The VP in turn sends GABAergic, glutamatergic, and cholinergic projections to the BLA, though the cholinergic and GABAergic are most likely to be sending threat signals to the BLA (Woolf and Butcher, 1982; Carlsen et al., 1985; Mascagni and McDonald, 2009; Root et al., 2015; Unal et

al., 2015; Faget et al., 2018; Macpherson et al., 2019; Wulff et al., 2019). Taken together with the current results, it is plausible that the NAcc's role in adaptive fear is part of the BLA-NAcc-VP-BLA circuit in which works together to coordinate accurate threat responses.

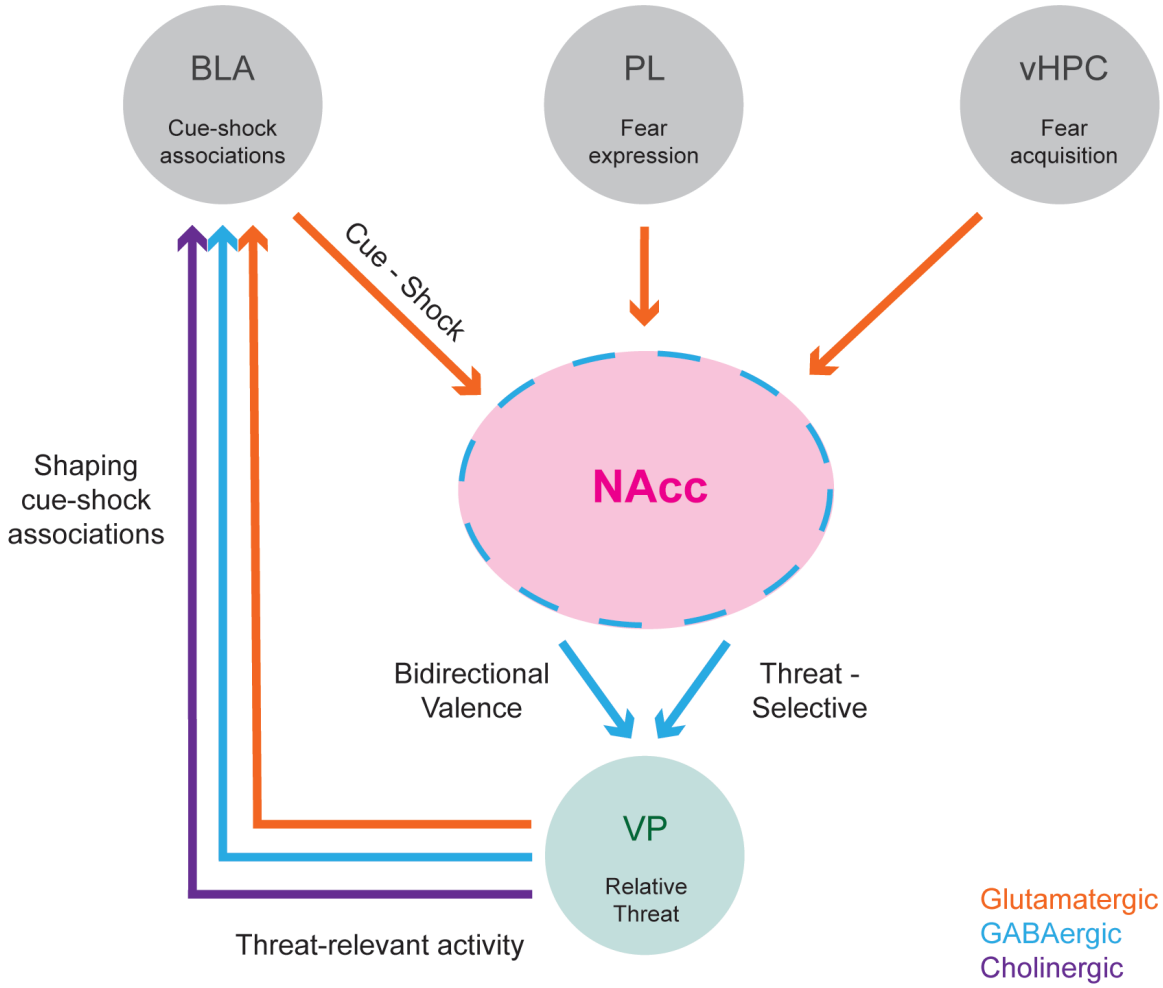

Figure 5.1 Proposed neural network for fear scaling. Based on the present experimental evidence for the NAcc's role in fear scaling, combined with experimental and neuroanatomical findings, I propose the BLA-NAcc-VP-BLA circuit for fear scaling. The BLA, mPFC, and vHPC send projections to the NAcc, however, only the BLA projections synapse directly onto VP projections MSNs. This suggests that the BLA sends cue-shock associations to the NAcc, which sends two signals to the VP: bidirectional valence and threat-selective signals. These signals converge in the VP, where relative threat is signaled. The VP in turn projects this information back to the BLA to shape and guide cue-shock associations. Abbreviations: **BLA**: basolateral amygdala; **PL**: prelimbic cortex; **vHPC**: ventral hippocampus; **NAcc**: nucleus accumbens core; **VP**: ventral pallidum.

5.5 Relevance to Clinical Research

Identifying the neural underpinnings of adaptive fear is fundamental to understanding and developing more effective treatments for anxiety disorders. Adaptive fear requires fear to scale to the level of threat and dysfunction in this capacity is a hallmark of fear-related anxiety disorders, including post-traumatic stress disorder (PTSD). Women are at a higher risk for being diagnosed with PTSD and anxiety-disorders, comorbid disorders, and experience greater symptom severity (Kessler et al., 1996; Breslau et al., 1999, 2004; Tolin and Foa, 2006). While our present data suggest that NAcc function is conserved across sexes, future research into potential sex differences is critical and currently underway in our laboratory.

The current results demonstrate that NAcc activity is necessary for adaptive fear responses and responds to threat and offer a potential mechanism by which maladaptive fear occurs (Ray et al., 2020). These results clarify at least one role for the NAcc in adaptive fear, yet much more work remains. NAcc structure and function is altered in anxiety and stress disorders (Cha et al., 2014; Felmingham et al., 2014; Manning et al., 2015; Morey et al., 2017). Disrupted threat-safety discrimination may be conceptualized as maladaptive fear scaling. Recent work shows that NAcc resting-state functional connectivity is highly conserved across mice, macaques and humans (Balsters et al., 2020). Preclinical research detailing NAcc threat function, and mapping a more complete neural circuit for fear scaling, is likely to inform strategies to promote adaptive fear in anxiety and stress disorders. Identifying novel neural circuits

underlying adaptive fear will reveal neural targets to propel future pharmacological treatments for anxiety disorders.

5.6 Conclusion

My dissertation examined a role for the NAcc in scaling fear to degree of threat. These experiments demonstrate that the NAcc is essential to scale fear to degree of threat and responds to threat cues across both rapid and longer-lasting timescales. Taken together, the results reveal a novel role for the NAcc in scaling fear and identify it as a critical component of a larger fear scaling network. Future research should work to elucidate the larger neural network for fear scaling.

References

Ahmad T, Sun N, Lyons D, Laviolette SR (2017) Bi-directional cannabinoid signaling in the basolateral amygdala controls rewarding and aversive emotional processing via functional regulation of the nucleus accumbens. Addiction Biology 22:1218–1231.

Amadi U, Lim SH, Liu E, Baratta MV, Goosens KA (2017) Hippocampal Processing of Ambiguity Enhances Fear Memory. Psychol Sci 28:143–161.

Ambroggi F, Ghazizadeh A, Nicola SM, Fields HL (2011) Roles of Nucleus Accumbens Core and Shell in Incentive-Cue Responding and Behavioral Inhibition. Journal of Neuroscience 31:6820–6830.

Amorapanth P, LeDoux JE, Nader K (2000) Different lateral amygdala outputs mediate reactions and actions elicited by a fear-arousing stimulus. Nature Neuroscience 3:74–79.

Amorapanth P, Nader K, LeDoux JE (1999) Lesions of periaqueductal gray dissociate-conditioned freezing from conditioned suppression behavior in rats. Learning & Memory 6:491–499.

Anglada-Figueroa D, Quirk GJ (2005) Lesions of the basal amygdala block expression of conditioned fear but not extinction. Journal of Neuroscience 25:9680–9685.

Arico C, McNally GP (2014) Opioid receptors regulate blocking and overexpectation of fear learning in conditioned suppression. Behavioral neuroscience 128:199–206.

Badrinarayan A, Wescott SA, Vander Weele CM, Saunders BT, Couturier BE, Maren S, Aragona BJ (2012) Aversive Stimuli Differentially Modulate Real-Time Dopamine Transmission Dynamics within the Nucleus Accumbens Core and Shell. J Neurosci 32:15779–15790.

Baker-Andresen D, Flavell CR, Li X, Bredy TW (2013) Activation of BDNF signaling prevents the return of fear in female mice. Learning & Memory 20:237–240.

Balsters JH, Zerbi V, Sallet J, Wenderoth N, Mars RB (2020) Primate homologs of mouse cortico-striatal circuits. Elife 9 Available at: https://www.ncbi.nlm.nih.gov/pubmed/32298231.

Bast T, Zhang W-N, Feldon J (2001) The ventral hippocampus and fear conditioning in rats. Experimental Brain Research 139:39–52.

Beck CH, Fibiger HC (1995) Conditioned fear-induced changes in behavior and in the expression of the immediate early gene c-fos: with and without diazepam pretreatment. Journal of Neuroscience 15:709–720.

Beery AK, Zucker I (2011) Sex bias in neuroscience and biomedical research. Neuroscience & Biobehavioral Reviews 35:565–572.

Belin D, Everitt BJ (2008) Cocaine seeking habits depend upon dopamine-dependent serial connectivity linking the ventral with the dorsal striatum. Neuron 57:432–441.

Belova MA, Paton JJ, Morrison SE, Salzman CD (2007) Expectation modulates neural responses to pleasant and aversive stimuli in primate amygdala. Neuron 55:970–984.

Berg BA, Schoenbaum G, McDannald MA (2014) The dorsal raphe nucleus is integral to negative prediction errors in Pavlovian fear. European Journal of Neuroscience 40:3096–3101.

Berke JD (2011) Functional Properties of Striatal Fast-Spiking Interneurons. Front Syst Neurosci 5 Available at: https://www.frontiersin.org/articles/10.3389/fnsys.2011.00045/full#B61 [Accessed February 8, 2021].

Berke JD, Okatan M, Skurski J, Eichenbaum HB (2004) Oscillatory Entrainment of Striatal Neurons in Freely Moving Rats. Neuron 43:883–896.

Bertran-Gonzalez J, Bosch C, Maroteaux M, Matamales M, Hervé D, Valjent E, Girault J-A (2008) Opposing Patterns of Signaling Activation in Dopamine D1 and D2 Receptor-Expressing Striatal Neurons in Response to Cocaine and Haloperidol. J Neurosci 28:5671–5685.

Beyeler A, Chang CJ, Silvestre M, Leveque C, Namburi P, Wildes CP, Tye KM (2018) Organization of Valence-Encoding and Projection-Defined Neurons in the Basolateral Amygdala. Cell Rep 22:905–918.

Beyeler A, Namburi P, Glober GF, Simonnet C, Calhoon GG, Conyers GF, Luck R, Wildes CP, Tye KM (2016) Divergent Routing of Positive and Negative Information from the Amygdala during Memory Retrieval. Neuron 90:348–361.

Bissonette GB, Burton AC, Gentry RN, Goldstein BL, Hearn TN, Barnett BR, Kashtelyan V, Roesch MR (2013) Separate Populations of Neurons in Ventral Striatum Encode Value and Motivation. PLOS ONE 8:e64673.

Blaiss CA, Janak PH (2009) The nucleus accumbens core and shell are critical for the expression, but not the consolidation, of Pavlovian conditioned approach. Behav Brain Res 200:22–32.

Blanchard DC (1969) Crouching as an index of fear. Journal of comparative and physiological psychology 67:370–375.

Bolles RC (1970) Species-Specific Defense Reactions and Avoidance Learning. Psychol Rev 77:32–48.

Bolles RC, Collier AC (1976) The effect of predictive cues on freezing in rats. Animal Learning & Behavior 4:6–8.

Bouton ME, Bolles RC (1980) Conditioned fear assessed by freezing and by the suppression of three different baselines. Animal Learning & Behavior 8:429–434.

Breslau N, Chilcoat HD, Kessler RC, Davis GC (1999) Previous Exposure to Trauma and PTSD Effects of Subsequent Trauma: Results From the Detroit Area Survey of Trauma. AJP 156:902–907.

Breslau N, Peterson EL, Poisson LM, Schultz LR, Lucia VC (2004) Estimating post-traumatic stress disorder in the community: Lifetime perspective and the impact of typical traumatic events. Psychological Medicine 34:889–898.

Britt JP, Benaliouad F, McDevitt RA, Stuber GD, Wise RA, Bonci A (2012) Synaptic and behavioral profile of multiple glutamatergic inputs to the nucleus accumbens. Neuron 76:790–803.

Brog JS, Salyapongse A, Deutch AY, Zahm DS (1993) The patterns of afferent innervation of the core and shell in the “accumbens” part of the rat ventral striatum: immunohistochemical detection of retrogradely transported fluoro-gold. J Comp Neurol 338:255–278.

Bukalo O, Nonaka M, Weinholtz CA, Mendez A, Taylor WW, Holmes A (2021) Effects of optogenetic photoexcitation of infralimbic cortex inputs to the basolateral amygdala on conditioned fear and extinction. Behavioural Brain Research 396:112913.

Bukalo O, Pinard CR, Silverstein S, Brehm C, Hartley ND, Whittle N, Colacicco G, Busch E, Patel S, Singewald N, Holmes A (2015) Prefrontal inputs to the amygdala instruct fear extinction memory formation. Sci Adv 1:e1500251.

Burgos-Robles A, Vidal-Gonzalez I, Quirk GJ (2009) Sustained conditioned responses in prelimbic prefrontal neurons are correlated with fear expression and extinction failure. J Neurosci 29:8474–8482.

Burton AC, Nakamura K, Roesch MR (2015) From ventral-medial to dorsal-lateral striatum: Neural correlates of reward-guided decision-making. Neurobiol Learn Mem 117:51–59.

Campeau S, Falls WA, Cullinan WE, Helmreich DL, Davis M, Watson SJ (1997) Elicitation and reduction of fear: Behavioural and neuroendocrine indices and brain induction of the immediate-early gene c-fos. Neuroscience 78:1087–1104.

Campeau S, Liang KC, Davis M (1990) Long-term retention of fear-potentiated startle following a short training session. Animal Learning & Behavior 18:462–468.

Carlsen J, Záborszky L, Heimer L (1985) Cholinergic projections from the basal forebrain to the basolateral amygdaloid complex: a combined retrograde fluorescent and immunohistochemical study. Journal of Comparative Neurology 234:155–167.

Cha J, Carlson JM, DeDora DJ, Greenberg T, Proudfit GH, Mujica-Parodi LR (2014) Hyper-Reactive Human Ventral Tegmental Area and Aberrant Mesocorticolimbic Connectivity in Overgeneralization of Fear in Generalized Anxiety Disorder. J Neurosci 34:5855–5860.

Chen VM, Foilb AR, Christianson JP (2016) Inactivation of ventral hippocampus interfered with cued-fear acquisition but did not influence later recall or discrimination. Behav Brain Res 296:249–253.

Ciocchi S, Herry C, Grenier F, Wolff SBE, Letzkus JJ, Vlachos I, Ehrlich I, Sprengel R, Deisseroth K, Stadler MB, Müller C, Lüthi A (2010) Encoding of conditioned fear in central amygdala inhibitory circuits. Nature 468:277–282.

Ciocchi S, Passecker J, Malagon-Vina H, Mikus N, Klausberger T (2015) Selective information routing by ventral hippocampal CA1 projection neurons. Science 348:560–563.

Clark JW, Drummond SPA, Hoyer D, Jacobson LH (2019) Sex differences in mouse models of fear inhibition: Fear extinction, safety learning, and fear–safety discrimination. British Journal of Pharmacology 176:4149–4158.

Cole SL, Robinson MJF, Berridge KC (2018) Optogenetic self-stimulation in the nucleus accumbens: D1 reward versus D2 ambivalence. PLoS One 13:e0207694.

Colom-Lapetina J, Li AJ, Pelegrina-Perez TC, Shansky RM (2019) Behavioral Diversity Across Classic Rodent Models Is Sex-Dependent. Front Behav Neurosci 13 Available at: https://www.frontiersin.org/articles/10.3389/fnbeh.2019.00045/full [Accessed February 6, 2021].

Cooch NK, Stalnaker TA, Wied HM, Bali-Chaudhary S, McDannald MA, Liu TL, Schoenbaum G (2015) Orbitofrontal lesions eliminate signalling of biological significance in cue-responsive ventral striatal neurons. Nat Commun 6:7195.

Corbit LH, Balleine BW (2011) The general and outcome-specific forms of pavlovian-instrumental transfer are differentially mediated by the nucleus accumbens core and shell. J Neurosci 31:11786–11794.

Corbit LH, Muir JL, Balleine BW (2001) The role of the nucleus accumbens in instrumental conditioning: Evidence of a functional dissociation between accumbens core and shell. Journal of Neuroscience 21:3251–3260.

Corbit LH, Nie H, Janak PH (2012) Habitual Alcohol Seeking: Time Course and the Contribution of Subregions of the Dorsal Striatum. Biol Psychiat 72:389–395.

Corcoran KA, Quirk GJ (2007) Activity in prelimbic cortex is necessary for the expression of learned, but not innate, fears. J Neurosci 27:840–844.

Correia SS, McGrath AG, Lee A, Graybiel AM, Goosens KA (2016) Amygdala-ventral striatum circuit activation decreases long-term fear. Elife 5 Available at: https://www.ncbi.nlm.nih.gov/pubmed/27671733.

Crameri F (2018) Scientific colour maps (Version 4.0.0).

Cromwell HC, Schultz W (2003) Effects of expectations for different reward magnitudes on neuronal activity in primate striatum. J Neurophysiol 89:2823–2838.

Davis M (1986) Pharmacological and anatomical analysis of fear conditioning using the fear-potentiated startle paradigm. Behavioral Neuroscience 100:814–824.

Davis M (1992) The role of the amygdala in fear-potentiated startle: implications for animal models of anxiety. Trends in Pharmacological Sciences 13:35–41.

Day HLL, Reed MM, Stevenson CW (2016) Sex differences in discriminating between cues predicting threat and safety. Neurobiol Learn Mem 133:196–203.

DiLeo A, Wright KM, McDannald MA (2016) Sub-second fear discrimination in rats: Adult impairment in adolescent heavy alcohol drinkers. Learning & Memory 23:618–622.

Duits P, Cath DC, Lissek S, Hox JJ, Hamm AO, Engelhard IM, van den Hout MA, Baas JM (2015) Updated meta-analysis of classical fear conditioning in the anxiety disorders. Depress Anxiety 32:239–253.

Dunsmoor JE, Bandettini PA, Knight DC (2008) Neural correlates of unconditioned response diminution during Pavlovian conditioning. NeuroImage 40:811–817.

Dutta S, Beaver J, Gilman TL, Jasnow AM (2020) The nucleus accumbens core and shell sub-regions differentially regulate conditioned fear expression and extinction. The FASEB Journal 34:1–1.

Estes KW, Skinner BF (1941) Some Quantitative Properties of Anxiety. Journal of Experimental Psychology 29:390–400.

Fadok JP, Darvas M, Dickerson TMK, Palmiter RD (2010) Long-Term Memory for Pavlovian Fear Conditioning Requires Dopamine in the Nucleus Accumbens and Basolateral Amygdala. Plos One 5 Available at: ://WOS:000281815800018.

Fadok JP, Markovic M, Tovote P, Lüthi A (2018) New perspectives on central amygdala function. Current Opinion in Neurobiology 49:141–147.

Faget L, Zell V, Souter E, McPherson A, Ressler R, Gutierrez-Reed N, Yoo JH, Dulcis D, Hnasko TS (2018) Opponent control of behavioral reinforcement by inhibitory and excitatory projections from the ventral pallidum. Nat Commun 9:849.

Fanselow MS (1980) Conditioned and unconditional components of post-shock freezing. Pavlov J Biol Sci 15:177–182.

Fanselow MS (1993) The Periaqueductal Gray and the Organization of Defensive Behavior. Aggressive Behavior 19:18–19.

Fanselow MS, Dong H-W (2010) Are the dorsal and ventral hippocampus functionally distinct structures? Neuron 65:7–19.

Felix-Ortiz AC, Beyeler A, Seo C, Leppla CA, Wildes CP, Tye KM (2013) BLA to vHPC Inputs Modulate Anxiety-Related Behaviors. Neuron 79:658–664.

Felmingham KL, Falconer EM, Williams L, Kemp AH, Allen A, Peduto A, Bryant RA (2014) Reduced Amygdala and Ventral Striatal Activity to Happy Faces in PTSD Is Associated with Emotional Numbing. Plos One 9 Available at: ://WOS:000341257700007.

Fenton GE, Pollard AK, Halliday DM, Mason R, Bredy TW, Stevenson CW (2014) Persistent prelimbic cortex activity contributes to enhanced learned fear expression in females. Learning & Memory 21:55–60.

Foilb AR, Bals J, Sarlitto MC, Christianson JP (2018) Sex differences in fear discrimination do not manifest as differences in conditioned inhibition. Learn Memory 25:49–53.

Gabbott PLA, Warner TA, Jays PRL, Salway P, Busby SJ (2005) Prefrontal cortex in the rat: Projections to subcortical autonomic, motor, and limbic centers. Journal of Comparative Neurology 492:145–177.

Gage GJ, Stoetzner CR, Wiltschko AB, Berke JD (2010) Selective Activation of Striatal Fast-Spiking Interneurons during Choice Execution. Neuron 67:466–479.

Gagnon D, Petryszyn S, Sanchez MG, Bories C, Beaulieu JM, De Koninck Y, Parent A, Parent M (2017) Striatal Neurons Expressing D 1 and D 2 Receptors are Morphologically Distinct and Differently Affected by Dopamine Denervation in Mice. Scientific Reports 7:41432.

Gale JTPD, Shields DC, Ishizawa Y, Eskandar EN (2014) Reward and reinforcement activity in the nucleus accumbens during learning. Front Behav Neurosci 8 Available at: https://www.frontiersin.org/articles/10.3389/fnbeh.2014.00114/full [Accessed February 13, 2021].

Galtress T, Kirkpatrick K (2010) The Role of the Nucleus Accumbens Core in Impulsive Choice, Timing, and Reward Processing. Behav Neurosci 124:26–43.

Gangarossa G, Espallergues J, De Kerchove D'Exaerde A, El Mestikawy S, Gerfen C, Hervé D, Girault J-A, Valjent E (2013) Distribution and compartmental organization of GABAergic medium-sized spiny neurons in the mouse nucleus accumbens. Front Neural Circuits 7 Available at: https://www.frontiersin.org/articles/10.3389/fncir.2013.00022/full [Accessed February 15, 2021].

Garcia R, Vouimba R-M, Baudry M, Thompson RF (1999) The amygdala modulates prefrontal cortex activity relative to conditioned fear. Nature 402:294–296.

Gerdeman GL, Partridge JG, Lupica CR, Lovinger DM (2003) It could be habit forming: drugs of abuse and striatal synaptic plasticity. Trends Neurosci 26:184–192.

Goldstein BL, Barnett BR, Vasquez G, Tobia SC, Kashtelyan V, Burton AC, Bryden DW, Roesch MR (2012) Ventral Striatum Encodes Past and Predicted Value Independent of Motor Contingencies. J Neurosci 32:2027–2036.

Goosens KA, Maren S (2001) Contextual and auditory fear conditioning are mediated by the lateral, basal, and central amygdaloid nuclei in rats. Learning & Memory 8:148–155.

Goosens KA, Maren S (2003) Pretraining NMDA receptor blockade in the basolateral complex, but not the central nucleus, of the amygdala prevents savings of conditional fear. Behav Neurosci 117:738–750.

Greiner EM, Muller I, Norris MR, Ng KH, Sangha S (2019) Sex differences in fear regulation and reward-seeking behaviors in a fear safety-reward discrimination task. Behav Brain Res 368:131–139.

Grillon C, Davis M (1997) Fear-potentiated startle conditioning in humans: explicit and contextual cue conditioning following paired versus unpaired training. Psychophysiology 34:451–458.

Gruene TM, Flick K, Stefano A, Shea SD, Shansky RM (2015a) Sexually divergent expression of active and passive conditioned fear responses in rats. Elife 4 Available at: ://WOS:000373851900001.

Gruene TM, Roberts E, Thomas V, Ronzio A, Shansky RM (2015b) Sex-Specific Neuroanatomical Correlates of Fear Expression in Prefrontal-Amygdala Circuits. Biol Psychiat 78:186–193.

Gupta RR, Sen S, Diepenhorst LL, Rudick CN, Maren S (2001) Estrogen modulates sexually dimorphic contextual fear conditioning and hippocampal long-term potentiation (LTP) in rats. Brain Res 888:356–365.

Hagenaars MA, Oitzl M, Roelofs K (2014) Updating freeze: Aligning animal and human research. Neuroscience & Biobehavioral Reviews 47:165–176.

Hall J, Parkinson JA, Connor TM, Dickinson A, Everitt BJ (2001) Involvement of the central nucleus of the amygdala and nucleus accumbens core in mediating Pavlovian influences on instrumental behaviour. European Journal of Neuroscience 13:1984–1992.

Haralambous T, Westbrook RF (1999) An infusion of bupivacaine into the nucleus accumbens disrupts the acquisition but not the expression of contextual fear conditioning. Behav Neurosci 113:925–940.

Hikida T, Kimura K, Wada N, Funabiki K, Nakanishi S (2010) Distinct Roles of Synaptic Transmission in Direct and Indirect Striatal Pathways to Reward and Aversive Behavior. Neuron 66:896–907.

Hirsch SM (1977) Of rats and cats. A laboratory study of rats' defensive postures. In: meeting of the Western Psychological Association, Seattle, Washington.

Hobin JA, Ji J, Maren S (2006) Ventral hippocampal muscimol disrupts context-specific fear memory retrieval after extinction in rats. Hippocampus 16:174–182.

Hunsaker MR, Kesner RP (2008) Dissociations across the dorsal–ventral axis of CA3 and CA1 for encoding and retrieval of contextual and auditory-cued fear. Neurobiology of Learning and Memory 89:61–69.

Iino Y, Sawada T, Yamaguchi K, Tajiri M, Ishii S, Kasai H, Yagishita S (2020) Dopamine D2 receptors in discrimination learning and spine enlargement. Nature 579:555-+.

Iordanova MD (2009) Dopaminergic Modulation of Appetitive and Aversive Predictive Learning. Rev Neuroscience 20:383–404.

Iordanova MD, McNally GP, Westbrook RF (2006a) Opioid receptors in the nucleus accumbens regulate attentional learning in the blocking paradigm. J Neurosci 26:4036–4045.

Iordanova MD, Westbrook RF, Killcross AS (2006b) Dopamine activity in the nucleus accumbens modulates blocking in fear conditioning. Eur J Neurosci 24:3265–3270.

Ito R, Robbins TW, Everitt BJ (2004) Differential control over cocaine-seeking behavior by nucleus accumbens core and shell. Nature Neuroscience 7:389–397.

Jimenez SA, Maren S (2009) Nuclear disconnection within the amygdala reveals a direct pathway to fear. Learning & Memory 16:766–768.

Jo YS, Heymann G, Zweifel LS (2018) Dopamine neurons reflect the uncertainty in fear generalization. Neuron 100:916–925.

Josselyn SA, Falls WA, Gewirtz JC, Pistell P, Davis M (2005) The nucleus accumbens is not critically involved in mediating the effects of a safety signal on behavior. Neuropsychopharmacology 30:17–26.

Jovanovic T, Kazama A, Bachevalier J, Davis M (2012) Impaired safety signal learning may be a biomarker of PTSD. Neuropharmacology 62:695–704.

Jovanovic T, Norrholm SD, Blanding NQ, Davis M, Duncan E, Bradley B, Ressler KJ (2010) Impaired fear inhibition is a biomarker of PTSD but not depression. Depression and anxiety 27:244–251.

Kamin LJ, Brimer CJ, Black AH (1963) Conditioned suppression as a monitor of fear of the CS in the course of avoidance training. Journal of Comparative and Physiological Psychology 56:497–501.

Kawaguchi Y (1993) Physiological, morphological, and histochemical characterization of three classes of interneurons in rat neostriatum. J Neurosci 13:4908–4923.

Kessler R, Sonnega S, Bromet E, Hughes M, Nelson C (1996) Posttraumatic Stress Disorder in the National Comorbidity Survey. Archives of general psychiatry 52:1048–1060.

Killcross S, Robbins TW, Everitt BJ (1997) Different types of fear-conditioned behaviour mediated by separate nuclei within amygdala. Nature 388:377–380.

Kita H, Kitai ST (1990) Amygdaloid projections to the frontal cortex and the striatum in the rat. Journal of Comparative Neurology 298:40–49.

Kjelstrup KG, Tuvnes FA, Steffenach H-A, Murison R, Moser EI, Moser M-B (2002) Reduced fear expression after lesions of the ventral hippocampus. Proceedings of the National Academy of Sciences 99:10825–10830.

Koo JW, Han JS, Kim JJ (2004) Selective neurotoxic lesions of basolateral and central nuclei of the amygdala produce differential effects on fear conditioning. Journal of Neuroscience 24:7654–7662.

Kravitz AV, Tye LD, Kreitzer AC (2012) Distinct roles for direct and indirect pathway striatal neurons in reinforcement. Nat Neurosci 15:816–818.

Krettek JE, Price JL (1977) Projections from the amygdaloid complex to the cerebral cortex and thalamus in the rat and cat. Journal of Comparative Neurology 172:687–722.

Krettek JE, Price JL (1978) Amygdaloid projections to subcortical structures within the basal forebrain and brainstem in the rat and cat. Journal of Comparative Neurology 178:225–254.

Lansink CS, Goltstein PM, Lankelma JV, Pennartz CMA (2010) Fast-spiking interneurons of the rat ventral striatum: temporal coordination of activity with principal cells and responsiveness to reward. European Journal of Neuroscience 32:494–508.

Lebron-Milad K, Milad MR (2012) Sex differences, gonadal hormones and the fear extinction network: implications for anxiety disorders. Biol Mood Anxiety Disord 2:3.

LeDoux JE (2000) Emotion circuits in the brain. Annu Rev Neurosci 23:155–184.

LeDoux JE, Cicchetti P, Xagoraris A, Romanski LM (1990) The lateral amygdaloid nucleus: sensory interface of the amygdala in fear conditioning. Journal of Neuroscience 10:1062–1069.

LeDoux JE, Iwata J, Cicchetti P, Reis DJ (1988) Different projections of the central amygdaloid nucleus mediate autonomic and behavioral correlates of conditioned fear. Journal of Neuroscience 8:2517–2529.

Lee JLC, Dickinson A, Everitt BJ (2005) Conditioned suppression and freezing as measures of aversive Pavlovian conditioning: effects of discrete amygdala lesions and overtraining. Behavioural Brain Research 159:221–233.

Levita L, Dalley JW, Robbins TW (2002) Disruption of Pavlovian contextual conditioning by excitotoxic lesions of the nucleus accumbens core. Behavioral Neuroscience 116:539–552.

Li SSY, McNally GP (2015) A Role of Nucleus Accumbens Dopamine Receptors in the Nucleus Accumbens Core, but Not Shell, in Fear Prediction Error. Behav Neurosci 129:450–456.

Li Z, Chen Z, Fan G, Li A, Yuan J, Xu T (2018) Cell-Type-Specific Afferent Innervation of the Nucleus Accumbens Core and Shell. Front Neuroanat 12 Available at: https://www.frontiersin.org/articles/10.3389/fnana.2018.00084/full [Accessed February 13, 2021].

Lissek S, Kaczkurkin AN, Rabin S, Geraci M, Pine DS, Grillon C (2014) Generalized Anxiety Disorder Is Associated With Overgeneralization of Classically Conditioned Fear. Biol Psychiat 75:909–915.

Lobo MK, Covington HE, Chaudhury D, Friedman AK, Sun H, Damez-Werno D, Dietz DM, Zaman S, Koo JW, Kennedy PJ, Mouzon E, Mogri M, Neve RL, Deisseroth K, Han M-H, Nestler EJ (2010) Cell Type-Specific Loss of BDNF Signaling Mimics Optogenetic Control of Cocaine Reward. Science 330:385–390.

Macpherson T, Mizoguchi H, Yamanaka A, Hikida T (2019) Preproenkephalin-expressing ventral pallidal neurons control inhibitory avoidance learning. Neurochemistry international 126:11–18.

Maes JHR (2002) No Sex Difference in Contextual Control over the Expression of Latent Inhibition and Extinction in Pavlovian Fear Conditioning in Rats. Neurobiology of Learning and Memory 78:258–278.

Manning J, Reynolds G, Saygin ZM, Hofmann SG, Pollack M, Gabrieli JD, Whitfield-Gabrieli S (2015) Altered resting-state functional connectivity of the frontal-striatal reward system in social anxiety disorder. PLoS One 10:e0125286.

Marek R, Sah P (2018) Neural Circuits Mediating Fear Learning and Extinction. In: Advances in Neurobiology, pp 35–48.

Maren S (2001) Neurobiology of Pavlovian fear conditioning. Annu Rev Neurosci 24:897–931.

Maren S, Aharonov G, Stote DL, Fanselow MS (1996) N-methyl-D-aspartate receptors in the basolateral amygdala are required for both acquisition and expression of conditional fear in rats. Behav Neurosci 110:1365–1374.

Maren S, De Oca B, Fanselow MS (1994) Sex differences in hippocampal long-term potentiation (LTP) and Pavlovian fear conditioning in rats: positive correlation between LTP and contextual learning. Brain Research 661:25–34.

Maren S, Quirk GJ (2004) Neuronal signaling of fear memory. Nature Reviews Neuroscience 5:844–852.

Markus EJ, Zecevic M (1997) Sex differences and estrous cycle changes in hippocampus-dependent fear conditioning. Psychobiology 25:246–252.

Mascagni F, McDonald AJ (2009) Parvalbumin-immunoreactive neurons and GABAergic neurons of the basal forebrain project to the rat basolateral amygdala. Neuroscience 160:805–812.

McDannald MA (2009) The behavioral and neural mechanisms underlying conditioned suppression: A model of human anxiety. Available at: https://search.proquest.com/docview/304916166/abstract/F3F6AAAA4D194A6FPQ/1 [Accessed February 18, 2021].

McDannald MA (2010) Contributions of the amygdala central nucleus and ventrolateral periaqueductal grey to freezing and instrumental suppression in Pavlovian fear conditioning. Behavioural Brain Research 211:111–117.

McDannald MA, Galarce EM (2011) Measuring Pavlovian fear with conditioned freezing and conditioned suppression reveals different roles for the basolateral amygdala. Brain Research 1374:82–89.

McDannald MA, Lucantonio F, Burke KA, Niv Y, Schoenbaum G (2011) Ventral Striatum and Orbitofrontal Cortex Are Both Required for Model-Based, But Not Model-Free, Reinforcement Learning. J Neurosci 31:2700–2705.

McDannald MA, Setlow B, Holland PC (2013) Effects of ventral striatal lesions on first- and second-order appetitive conditioning. European Journal of Neuroscience 38:2589–2599.

McDonald AJ (1982) Neurons of the lateral and basolateral amygdaloid nuclei: a Golgi study in the rat. Journal of Comparative Neurology 212:293–312.

McDonald AJ (1992) Projection neurons of the basolateral amygdala: a correlative Golgi and retrograde tract tracing study. Brain research bulletin 28:179–185.

McDonald AJ, Mascagni F (2001) Colocalization of calcium-binding proteins and GABA in neurons of the rat basolateral amygdala. Neuroscience 105:681–693.

McGinty VB, Lardeux S, Taha SA, Kim JJ, Nicola SM (2013) Invigoration of reward seeking by cue and proximity encoding in the nucleus accumbens. Neuron 78:910–922.

Moaddab M, Ray MH, McDannald MA (2021) Ventral pallidum neurons dynamically signal relative threat. Communications Biology 4:1–14.

Moita MAP (2004) Putting Fear in Its Place: Remapping of Hippocampal Place Cells during Fear Conditioning. Journal of Neuroscience 24:7015–7023.

Moita MAP, Rosis S, Zhou Y, LeDoux JE, Blair HT (2003) Hippocampal Place Cells Acquire Location-Specific Responses to the Conditioned Stimulus during Auditory Fear Conditioning. Neuron 37:485–497.

Morey RA, Davis SL, Garrett ME, Haswell CC, Marx CE, Beckham JC, McCarthy G, Hauser MA, Ashley-Koch AE, Workgrp M-AM (2017) Genome-wide association study of subcortical brain volume in PTSD cases and trauma-exposed controls. Transl Psychiat 7 Available at: ://WOS:000417257200006.

Morgan MA, Romanski LM, LeDoux JE (1993) Extinction of emotional learning: contribution of medial prefrontal cortex. Neurosci Lett 163:109–113.

Moser M-B, Moser EI (1998) Functional differentiation in the hippocampus. Hippocampus 8:608–619.

Natsubori A, Tsutsui-Kimura I, Nishida H, Bouchekioua Y, Sekiya H, Uchigashima M, Watanabe M, de Kerchove d'Exaerde A, Mimura M, Takata N, Tanaka KF (2017) Ventrolateral Striatal Medium Spiny Neurons Positively Regulate Food-Incentive, Goal-Directed Behavior Independently of D1 and D2 Selectivity. J Neurosci 37:2723–2733.

Oh J-P, Han J-H (2020) A critical role of hippocampus for formation of remote cued fear memory. Molecular Brain 13:112.

Ottenheimer D, Richard JM, Janak PH (2018) Ventral pallidum encodes relative reward value earlier and more robustly than nucleus accumbens. Nat Commun 9 Available at: ://WOS:000447697100008.

Papp E, Borhegyi Z, Tomioka R, Rockland KS, Mody I, Freund TF (2012) Glutamatergic input from specific sources influences the nucleus accumbens-ventral pallidum information flow. Brain Structure and Function 217:37–48.

Parkinson JA, Olmstead MC, Burns LH, Robbins TW, Everitt BJ (1999) Dissociation in effects of lesions of the nucleus accumbens core and shell on appetitive pavlovian approach behavior and the potentiation of conditioned reinforcement and locomotor activity by D-amphetamine. Journal of Neuroscience 19:2401–2411.

Pavlov IP (1928) Lectures on conditioned reflexes: Twenty-five years of objective study of the higher nervous activity (behaviour) of animals. New York, NY, US: Liverwright Publishing Corporation.

Perreault ML, Hasbi A, O'Dowd BF, George SR (2011) The Dopamine D1–D2 Receptor Heteromer in Striatal Medium Spiny Neurons: Evidence for a Third Distinct Neuronal Pathway in Basal Ganglia. Front Neuroanat 5 Available at: https://www.frontiersin.org/articles/10.3389/fnana.2011.00031/full [Accessed February 15, 2021].

Petrovich GD, Risold PY, Swanson LW (1996) Organization of projections from the basomedial nucleus of the amygdala: a PHAL study in the rat. J Comp Neurol 374:387–420.

Piantadosi PT (2017) Contributions of nucleus accumbens circuitry to aspects of aversively-motivated behaviors. Psychology Ph.D.

Piantadosi PT, Yeates DCM, Floresco SB (2020) Prefrontal cortical and nucleus accumbens contributions to discriminative conditioned suppression of reward-seeking. Learn Mem 27:429–440.

Pickens CL, Golden SA, Adams-Deutsch T, Nair SG, Shaham Y (2009) Long-lasting incubation of conditioned fear in rats. Biological Psychiatry 65:881–886.

Pisansky MT, Lefevre EM, Retzlaff CL, Trieu BH, Leipold DW, Rothwell PE (2019) Nucleus Accumbens Fast-Spiking Interneurons Constrain Impulsive Action. Biological Psychiatry 86:836–847.

Plenz D, Kitai ST (1998) Up and Down States in Striatal Medium Spiny Neurons Simultaneously Recorded with Spontaneous Activity in Fast-Spiking Interneurons Studied in Cortex–Striatum–Substantia Nigra Organotypic Cultures. J Neurosci 18:266–283.

Quirk GJ, Armony JL, LeDoux JE (1997) Fear conditioning enhances different temporal components of tone-evoked spike trains in auditory cortex and lateral amygdala. Neuron 19:613–624.

Quirk GJ, Repa C, LeDoux JE (1995) Fear conditioning enhances short-latency auditory responses of lateral amygdala neurons: parallel recordings in the freely behaving rat. Neuron 15:1029–1039.

Quirk GJ, Russo GK, Barron JL, Lebron K (2000) The role of ventromedial prefrontal cortex in the recovery of extinguished fear. J Neurosci 20:6225–6231.

Ramirez DR, Savage LM (2007) Differential Involvement of the Basolateral Amygdala, Orbitofrontal Cortex, and Nucleus Accumbens Core in the Acquisition and Use of Reward Expectancies. Behav Neurosci 121:896–906.

Ray MH, Hanlon E, McDannald MA (2018) Lateral orbitofrontal cortex partitions mechanisms for fear regulation and alcohol consumption. PLOS ONE 13:e0198043.

Ray MH, Russ AN, Walker RA, McDannald MA (2020) The Nucleus Accumbens Core is Necessary to Scale Fear to Degree of Threat. J Neurosci 40:4750–4760.

Repa JC, Muller J, Apergis J, Desrochers TM, Zhou Y, LeDoux JE (2001) Two different lateral amygdala cell populations contribute to the initiation and storage of memory. Nat Neurosci 4:724–731.

Rescorla RA (1968) Probability of shock in the presence and absence of CS in fear conditioning. Journal of Comparative and Physiological Psychology 66:1–5.

Rescorla RA, Wagner AR (1972) A theory of Pavlovian conditioning: Variations in the effectiveness of reinforcement and nonreinforcement. In: Classical Conditioning II: Current Research and Theory (AH B, WF P, eds), pp 64–99. New York: Appleton Century Crofts.

Roesch MR, Calu DJ, Schoenbaum G (2007) Dopamine neurons encode the better option in rats deciding between differently delayed or sized rewards. Nature Neuroscience 10:1615–1624.

Roesch MR, Singh T, Brown PL, Mullins SE, Schoenbaum G (2009) Ventral striatal neurons encode the value of the chosen action in rats deciding between differently delayed or sized rewards. J Neurosci 29:13365–13376.

Rogan MT, Staubli UV, LeDoux JE (1997) Fear conditioning induces associative long-term potentiation in the amygdala. Nature 390:604–607.

Roitman MF, Wheeler RA, Carelli RM (2005) Nucleus accumbens neurons are innately tuned for rewarding and aversive taste stimuli, encode their predictors, and are linked to motor output. Neuron 45:587–597.

Root DH, Melendez RI, Zaborszky L, Napier TC (2015) The ventral pallidum: Subregion-specific functional anatomy and roles in motivated behaviors. Prog Neurobiol 130:29–70.

Saddoris MP, Carelli RM (2014) Cocaine self-administration abolishes associative neural encoding in the nucleus accumbens necessary for higher-order learning. Biol Psychiatry 75:156–164.

Schwienbacher I, Fendt M, Richardson R, Schnitzler H-U (2004) Temporary inactivation of the nucleus accumbens disrupts acquisition and expression of fear-potentiated startle in rats. Brain Research 1027:87–93.

Setlow B, Schoenbaum G, Gallagher M (2003) Neural encoding in ventral striatum during olfactory discrimination learning. Neuron 38:625–636.

Shansky RM, Woolley CS (2016) Considering Sex as a Biological Variable Will Be Valuable for Neuroscience Research. J Neurosci 36:11817–11822.

Shumake J, Monfils MH (2015) Assessing Fear Following Retrieval + Extinction Through Suppression of Baseline Reward Seeking vs. Freezing. Front Behav Neurosci 9 Available at: https://www.frontiersin.org/articles/10.3389/fnbeh.2015.00355/full [Accessed February 15, 2021].

Sierra-Mercado D, Padilla-Coreano N, Quirk GJ (2011) Dissociable Roles of Prelimbic and Infralimbic Cortices, Ventral Hippocampus, and Basolateral Amygdala in the Expression and Extinction of Conditioned Fear. Neuropsychopharmacol 36:529–538.

Soares-Cunha C, Coimbra B, David-Pereira A, Borges S, Pinto L, Costa P, Sousa N, Rodrigues AJ (2016) Activation of D2 dopamine receptor-expressing neurons in the nucleus accumbens increases motivation. Nature Communications 7:11829.

Soares-Cunha C, Coimbra B, Domingues AV, Vasconcelos N, Sousa N, Rodrigues AJ (2018) Nucleus Accumbens Microcircuit Underlying D2-MSN-Driven Increase in Motivation. eNeuro 5 Available at: https://www.ncbi.nlm.nih.gov/pmc/articles/PMC5957524/ [Accessed February 10, 2021].

Soares-Cunha C, de Vasconcelos NAP, Coimbra B, Domingues AV, Silva JM, Loureiro-Campos E, Gaspar R, Sotiropoulos I, Sousa N, Rodrigues AJ (2020) Nucleus accumbens medium spiny neurons subtypes signal both reward and aversion. Molecular Psychiatry 25:3241–3255.

Steele CC, Peterson JR, Marshall AT, Stuebing SL, Kirkpatrick K (2018) Nucleus accumbens core lesions induce sub-optimal choice and reduce sensitivity to magnitude and delay in impulsive choice tasks. Behavioural Brain Research 339:28–38.

Stuber GD, Sparta DR, Stamatakis AM, van Leeuwen WA, Hardjoprajitno JE, Cho S, Tye KM, Kempadoo KA, Zhang F, Deisseroth K, Bonci A (2011) Excitatory transmission from the amygdala to nucleus accumbens facilitates reward seeking. Nature 475:377–380.

Sugam JA, Saddoris MP, Carelli RM (2014) Nucleus accumbens neurons track behavioral preferences and reward outcomes during risky decision making. Biol Psychiatry 75:807–816.

Taha SA (2005) Encoding of Palatability and Appetitive Behaviors by Distinct Neuronal Populations in the Nucleus Accumbens. Journal of Neuroscience 25:1193–1202.

Tai L-H, Lee AM, Benavidez N, Bonci A, Wilbrecht L (2012) Transient stimulation of distinct subpopulations of striatal neurons mimics changes in action value. Nat Neurosci 15:1281–1289.

Thomas KL, Hall J, Everitt BJ (2002) Cellular imaging with zif268 expression in the rat nucleus accumbens and frontal cortex further dissociates the neural pathways activated following the retrieval of contextual and cued fear memory. European Journal of Neuroscience 16:1789–1796.

Tolin DF, Foa EB (2006) Sex differences in trauma and posttraumatic stress disorder: A quantitative review of 25 years of research. Psychol Bull 132:959–992.

Uchida N, Kepecs A, Mainen ZF (2006) Seeing at a glance, smelling in a whiff: rapid forms of perceptual decision making. Nat Rev Neurosci 7:485–491.

Unal CT, Pare D, Zaborszky L (2015) Impact of basal forebrain cholinergic inputs on basolateral amygdala neurons. Journal of Neuroscience 35:853–863.

van Dongen YC, Deniau J-M, Pennartz CMA, Galis-de Graaf Y, Voorn P, Thierry A-M, Groenewegen HJ (2005) Anatomical evidence for direct connections between the shell and core subregions of the rat nucleus accumbens. Neuroscience 136:1049–1071.

Vicente AM, Galvão-Ferreira P, Tecuapetla F, Costa RM (2016) Direct and indirect dorsolateral striatum pathways reinforce different action strategies. Current Biology 26:R267–R269.

Vidal-Gonzalez I, Vidal-Gonzalez B, Rauch SL, Quirk GJ (2006) Microstimulation reveals opposing influences of prelimbic and infralimbic cortex on the expression of conditioned fear. Learn Mem 13:728–733.

Villavicencio M, Moreno MG, Simon SA, Gutierrez R (2018) Encoding of Sucrose's Palatability in the Nucleus Accumbens Shell and Its Modulation by Exteroceptive Auditory Cues. Front Neurosci 12 Available at: https://www.frontiersin.org/articles/10.3389/fnins.2018.00265/full [Accessed February 13, 2021].

Walker DL, Davis M (2002) The role of amygdala glutamate receptors in fear learning, fear-potentiated startle, and extinction. Pharmacol Biochem Behav 71:379–392.

Walker RA, Andreansky C, Ray MH, McDannald MA (2018) Early adolescent adversity inflates threat estimation in females and promotes alcohol use initiation in both sexes. Behav Neurosci 132:171–182.

Walker RA, Wright KM, Jhou TC, McDannald MA (2019) The ventrolateral periaqueductal gray updates fear via positive prediction error. Eur J Neurosci Available at: https://www.ncbi.nlm.nih.gov/pubmed/31376295.

Weiskrantz L (1956) Behavioral changes associated with ablation of the amygdaloid complex in monkeys. Journal of Comparative and Physiological Psychology 49:381–391.

Wheeler RA, Roitman MF, Grigson PS, Carelli RM (2005) Single Neurons in the Nucleus Accumbens Track Relative Reward. :14.

Wilensky AE, Schafe GE, Kristensen MP, LeDoux JE (2006) Rethinking the fear circuit: The central nucleus of the amygdala is required for the acquisition, consolidation, and expression of pavlovian fear conditioning. Journal of Neuroscience 26:12387–12396.

Woolf NJ, Butcher LL (1982) Cholinergic projections to the basolateral amygdala: a combined Evans Blue and acetylcholinesterase analysis. Brain research bulletin 8:751–763.

Wright CI, Groenewegen HJ (1996) Patterns of overlap and segregation between insular cortical, intermediodorsal thalamic and basal amygdaloid afferents in the nucleus accumbens of the rat. Neuroscience 73:359–373.

Wright KM, McDannald MA (2019) Ventrolateral periaqueductal gray neurons prioritize threat probability over fear output. Elife 8 Available at: https://www.ncbi.nlm.nih.gov/pubmed/30843787.

Wulff AB, Tooley J, Marconi LJ, Creed MC (2019) Ventral pallidal modulation of aversion processing. Brain research 1713:62–69.

Zhang W-N, Bast T, Feldon J (2001) The ventral hippocampus and fear conditioning in rats: different anterograde amnesias of fear after infusion of N-methyl-d-aspartate or its noncompetitive antagonist MK-801 into the ventral hippocampus. Behavioural Brain Research 126:159–174.